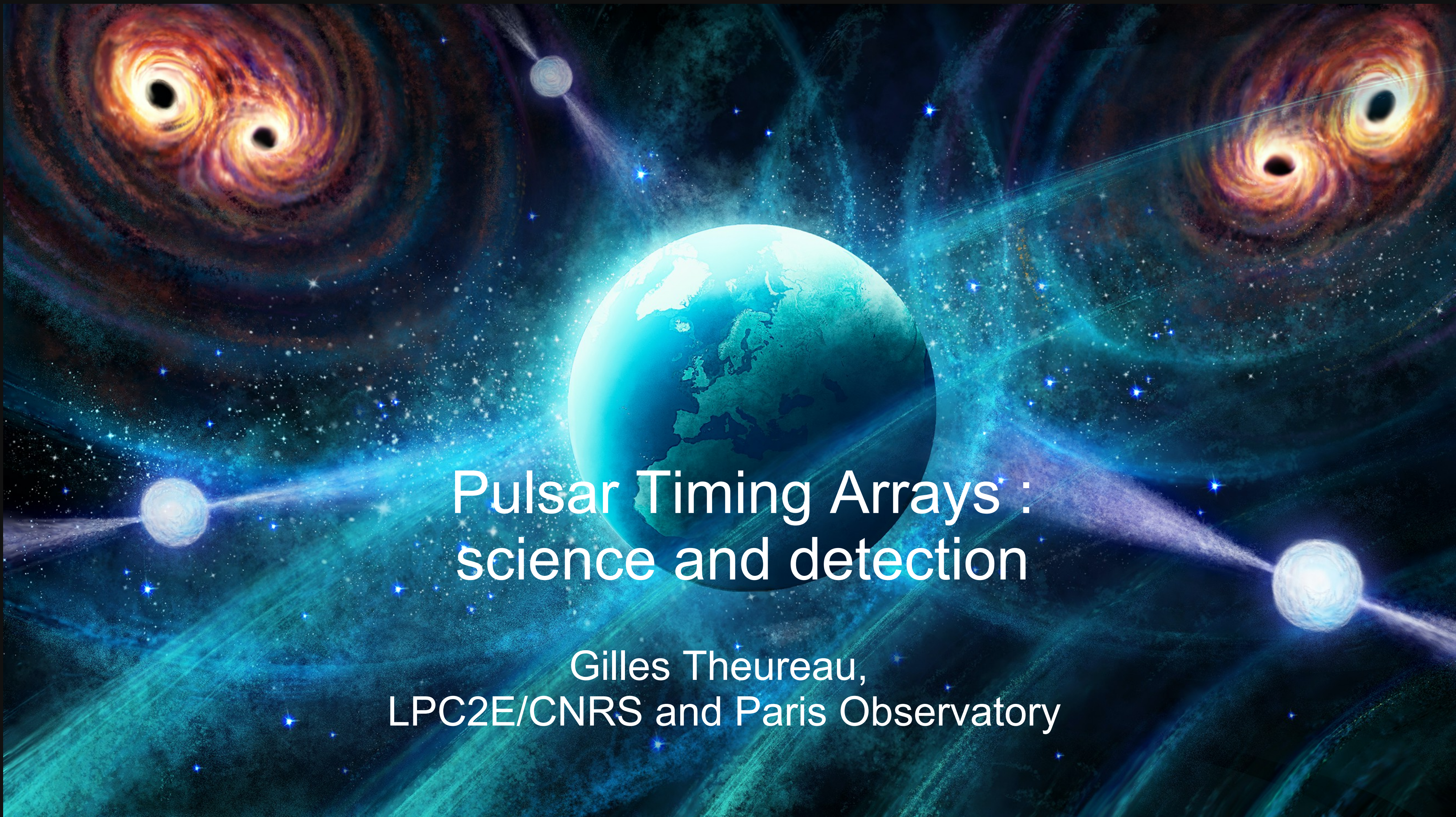

Pulsar Timing Arrays : science and detection

Gilles Theureau,
LPC2E/CNRS and Paris Observatory

AGENCE NATIONALE DE LA RECHERCHE ANR

PNHE Programme national hautes énergies

PNCG Programme National de Cosmologie et Galaxies

LPC2E

SRN l'Observatoire de Paris | PSL Station de Radioastronomie de Nançay

APC, CNRS, FRANCE

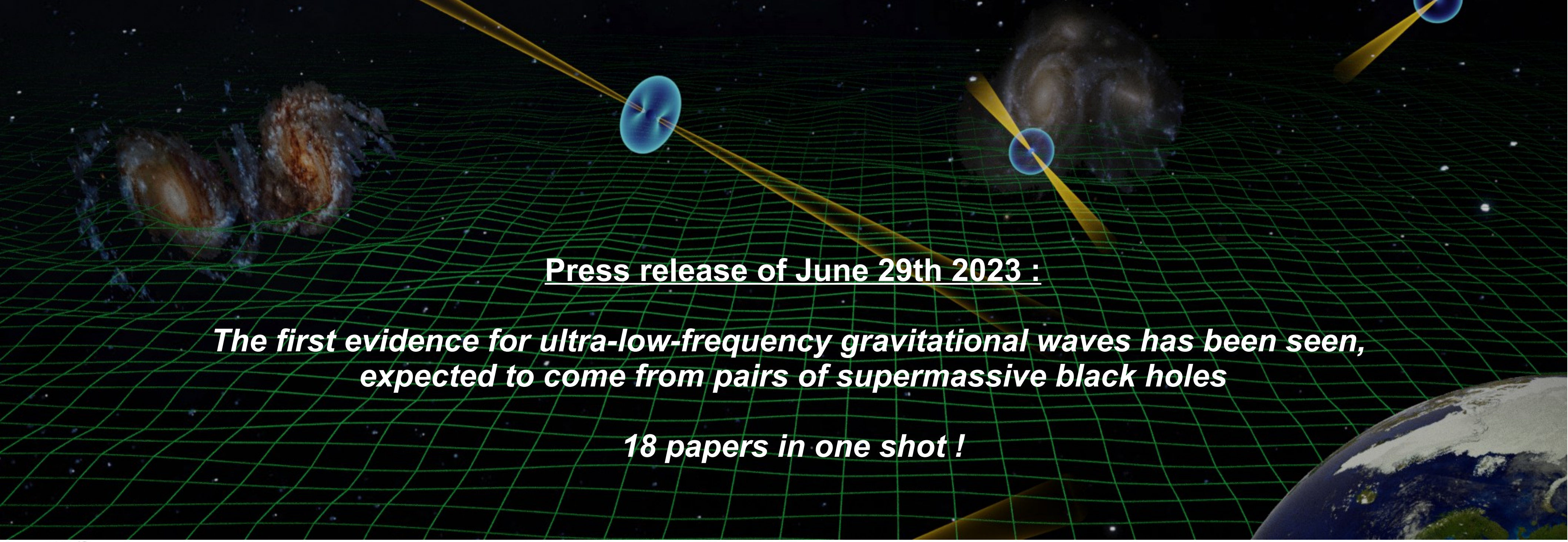

Press release of June 29th 2023 :

The first evidence for ultra-low-frequency gravitational waves has been seen, expected to come from pairs of supermassive black holes

18 papers in one shot !

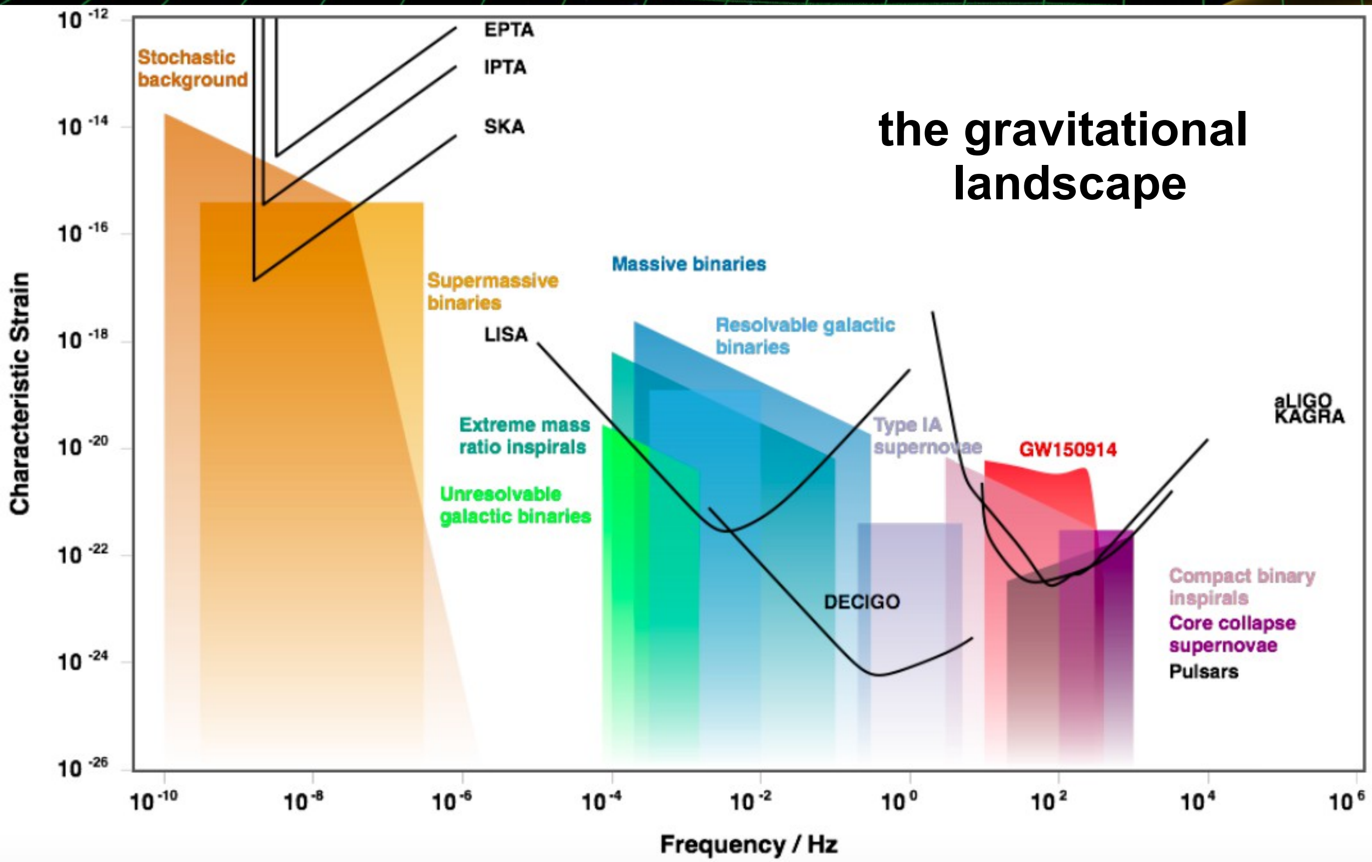

The nanoHertz domain

- Super Massive Black Hole Binaries (SMBHB)

- Cosmic string loops

- Relics of inflation
(e.g. quantum fluctuations of the gravitational field in the early universe, amplified by an inflationary phase

- (M)HD turbulence during QCD
induced by 1st-order phase transition or due to primordial magnetic field

The International Pulsar Timing Array

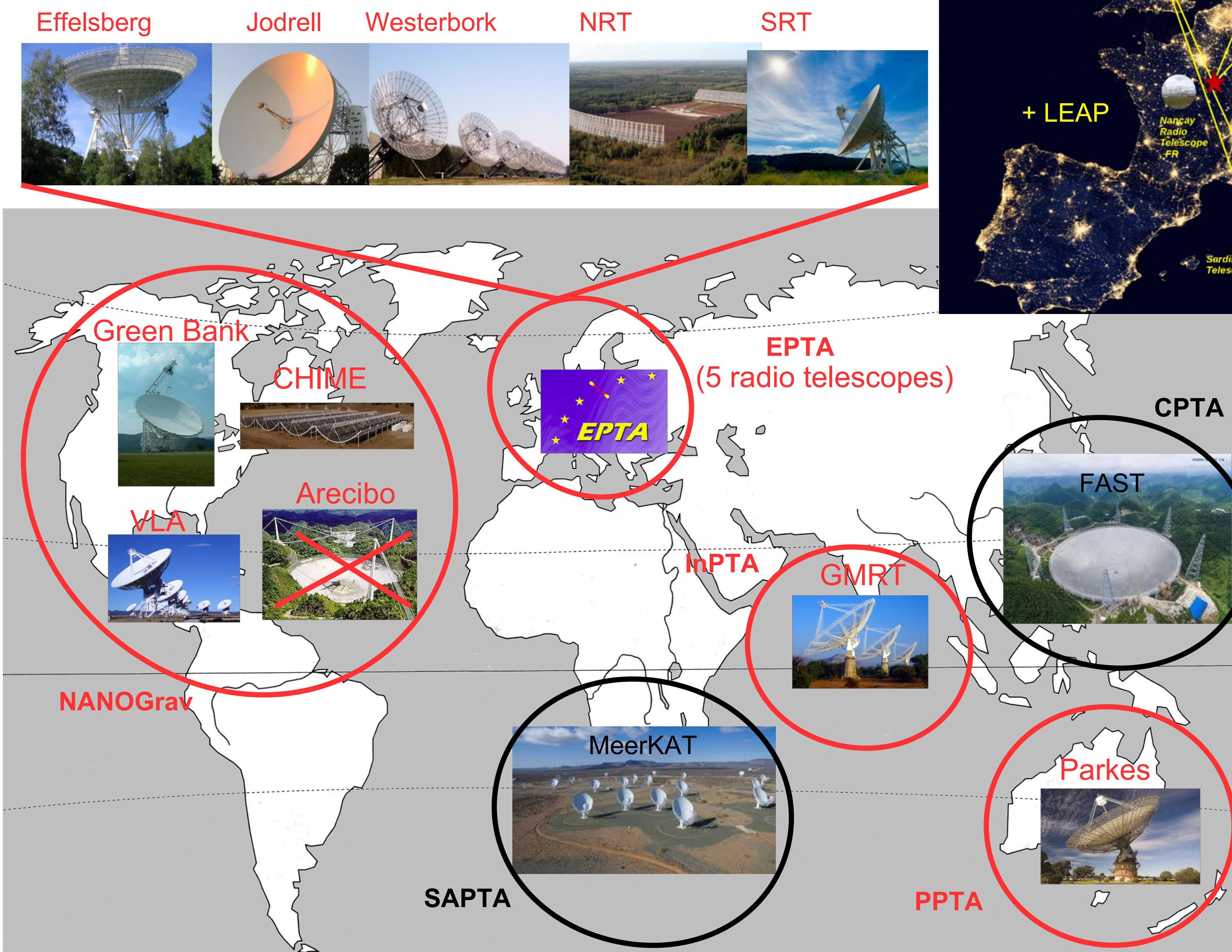

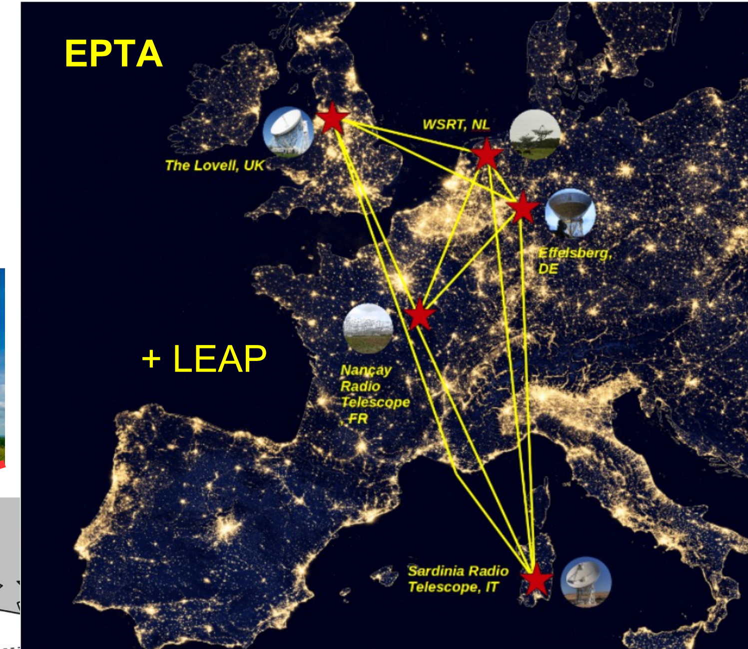

EPTA/InPTA, PPTA and NANOGrav

publish coherent results !

« a low-frequency quadrupolar signal common to all pulsars »

Opportunities for detecting ultralong gravitational waves

Pulsar Timing Arrays : precursors

M. V. Sazhin

Shternberg Astronomical Institute, Moscow

1 (Submitted June 14, 1977)

Astron. Zh. **55**, 65–68 (January–February 1978)

The influence of ultralong gravitational waves on the propagation of electromagnetic pulses is examined. Conditions are set forth whereby it might be possible to detect gravitational waves arriving from binary stars. There are some prospects for detecting gravitational radiation from double superstars with masses $\mathfrak{M}_1 \approx \mathfrak{M}_2 \approx 10^{10} \mathfrak{M}_\odot$.

PULSAR TIMING MEASUREMENTS AND THE SEARCH FOR GRAVITATIONAL WAVES

STEVEN DETWEILER

Department of Physics, Yale University

2 *Received 1979 June 4; accepted 1979 July 6*

ABSTRACT

Pulse arrival time measurements of pulsars may be used to search for gravitational waves with periods on the order of 1 to 10 years and dimensionless amplitudes $\sim 10^{-11}$. The analysis of published data on pulsar regularity sets an upper limit to the energy density of a stochastic background of gravitational waves, with periods ~ 1 year, which is comparable to the closure density of the universe.

UPPER LIMITS ON THE ISOTROPIC GRAVITATIONAL RADIATION BACKGROUND FROM PULSAR TIMING ANALYSIS[1]

3 R. W. HELLINGS AND G. S. DOWNS

Jet Propulsion Laboratory, California Institute of Technology

Received 1982 October 1; accepted 1982 October 20

ABSTRACT

A pulsar and the Earth may be thought of as end masses of a free-mass gravitational wave antenna in which the relative motion of the masses is monitored by observing the Doppler shift of the pulse arrival times. Using timing residuals from PSR 1133+16, 1237+25, 1604−00, and 2045−16, an upper limit to the spectrum of the isotropic gravitational radiation background has been derived in the frequency band 4×10^{-9} to 10^{-7} Hz. This limit is found to be $S_E = 10^{21} f^3$ ergs cm^{-3} Hz^{-1}, where S_E is the energy density spectrum and f is the frequency in Hz. This would limit the energy density at frequencies below 10^{-8} Hz to be 1.4×10^{-4} times the critical density.

+ spatial quadrupolar signature

Pulsars = fastly rotating neutron stars

Supernova explosion of a massive star (**> 9 M_{sun}**)

Core collapse in a neutron star of **1.3-2.2 M_{sun}**

Huge magnetic field: **10^{8} - 10^{14} Gauss**

Rotation periods: **0.001-10 seconds**

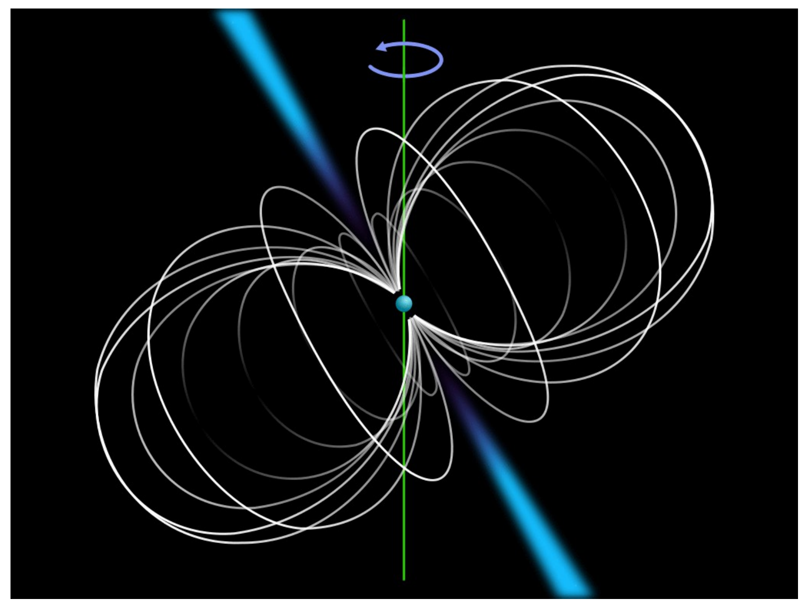

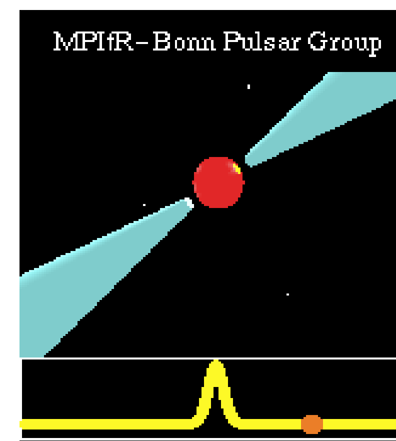

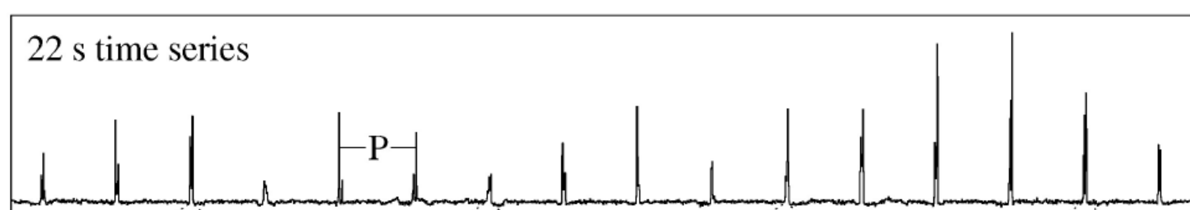

Pulsars = fastly rotating neutron stars

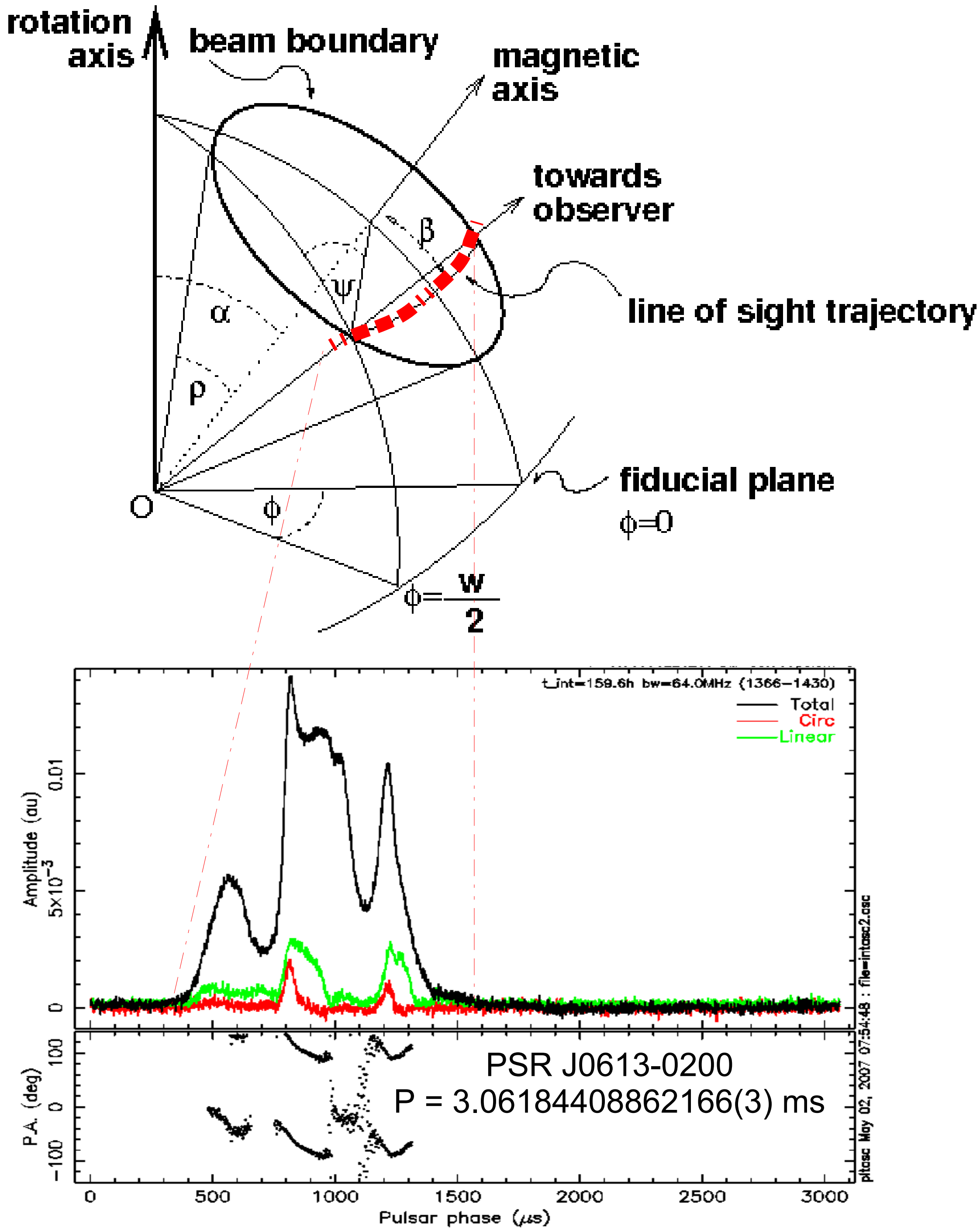

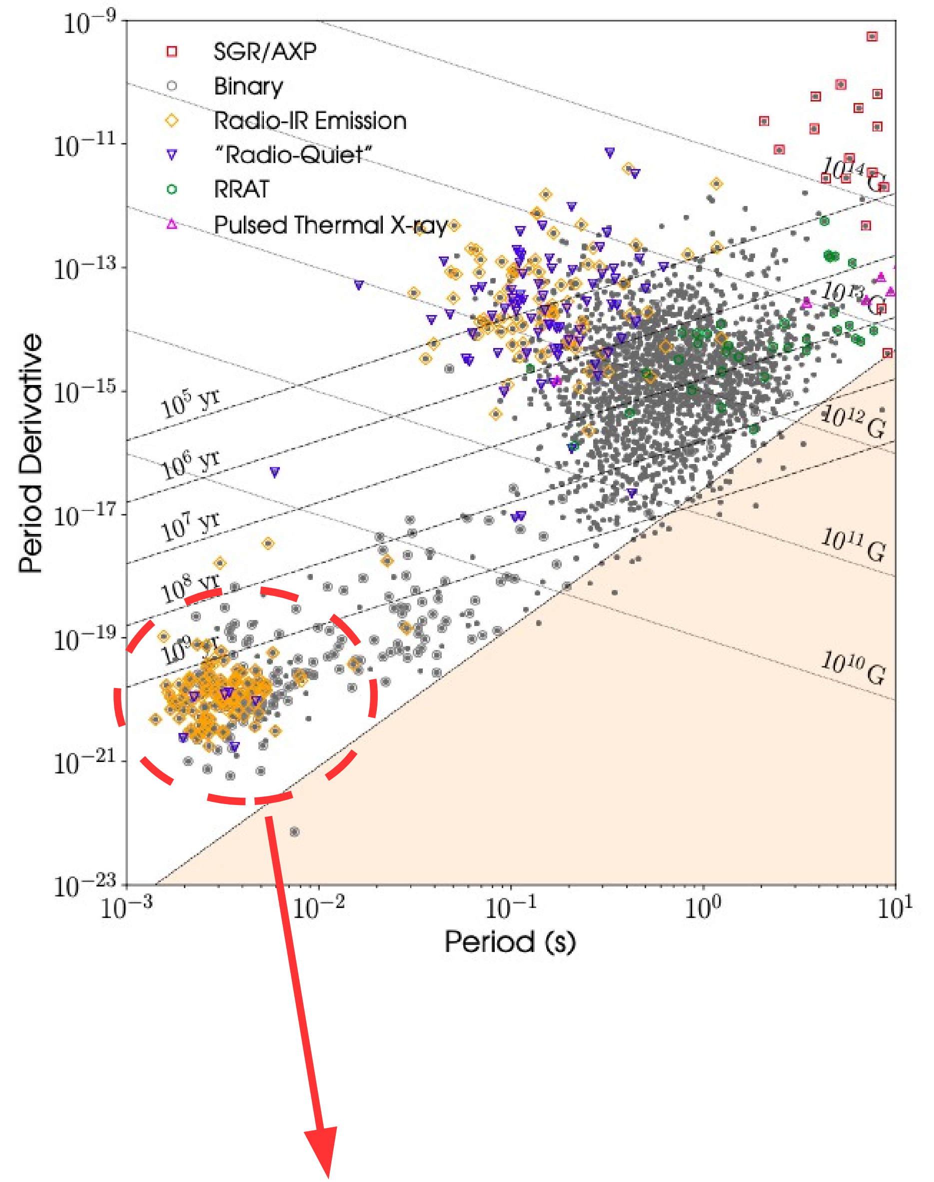

Millisecond pulsar population

very stable rotation < 1μs rms over years

The art of timing

I – the de-dispersion problem

The lowest frequencies are delayed

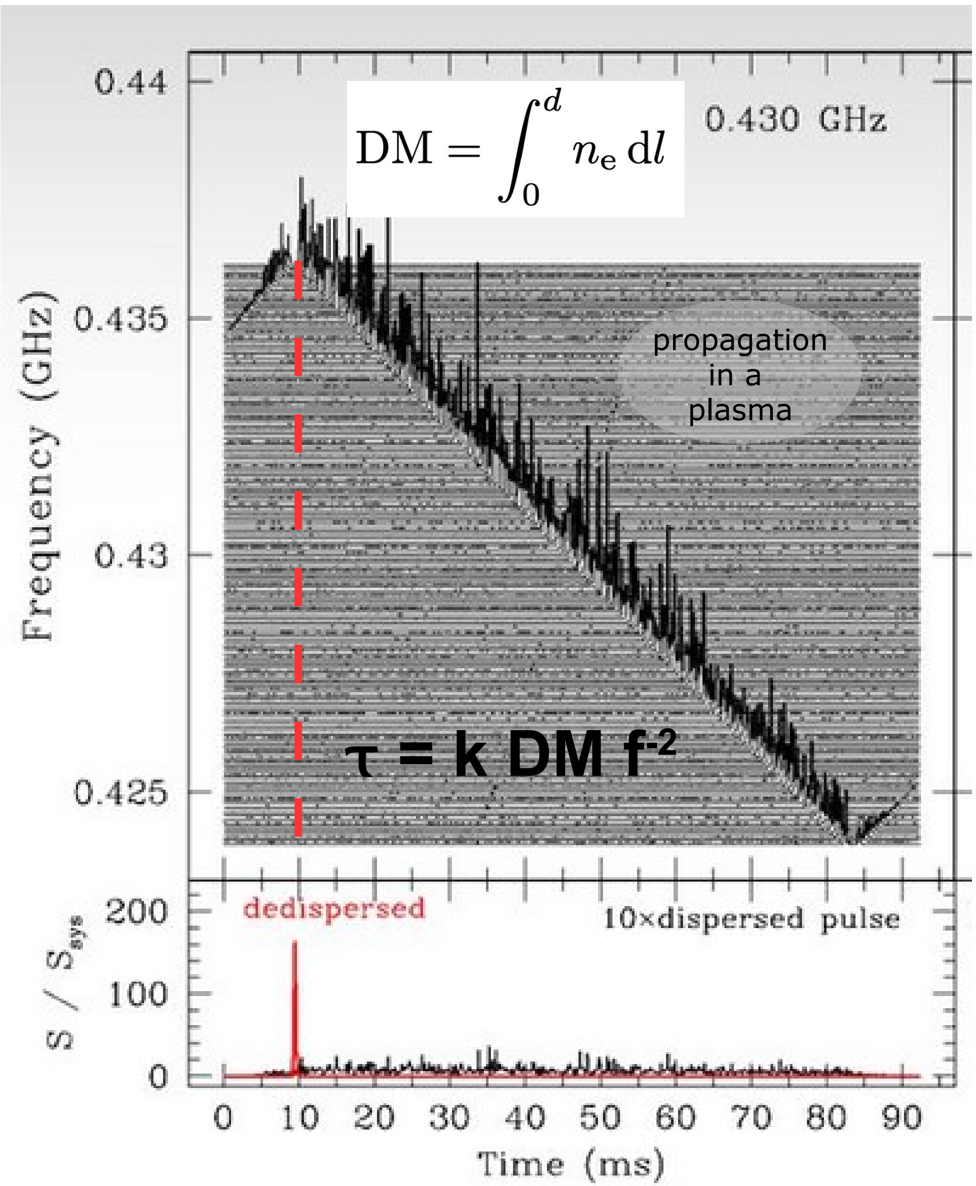

II- phase folding with rotation

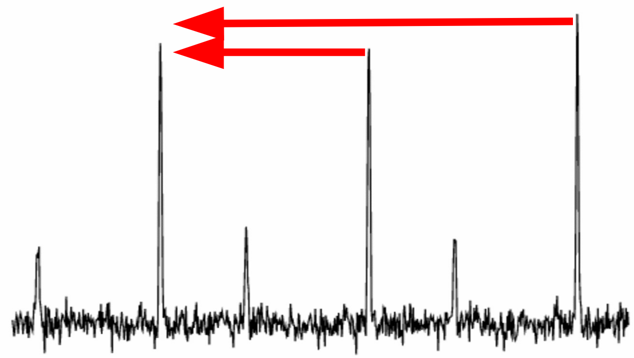

According to a model :

slow down,
orbital motion,
proper motion
planetary ephem.

III – Time stamping

(Time of arrival computation)

« TOA »

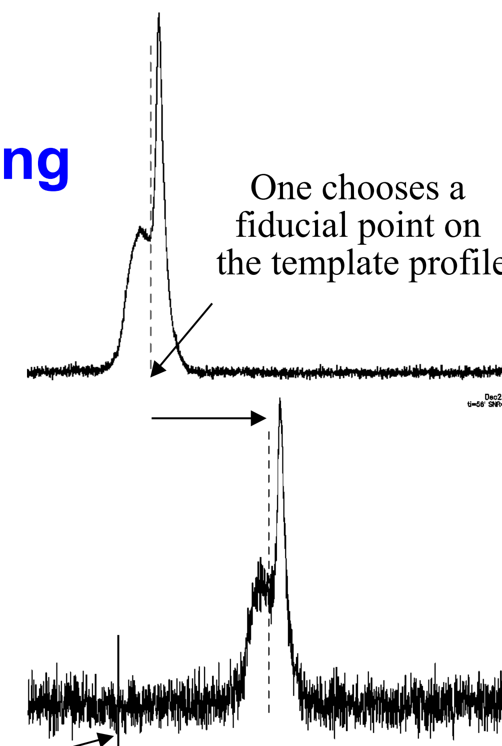

The art of timing

I – the de-dispersion problem

The lowest frequencies are delayed

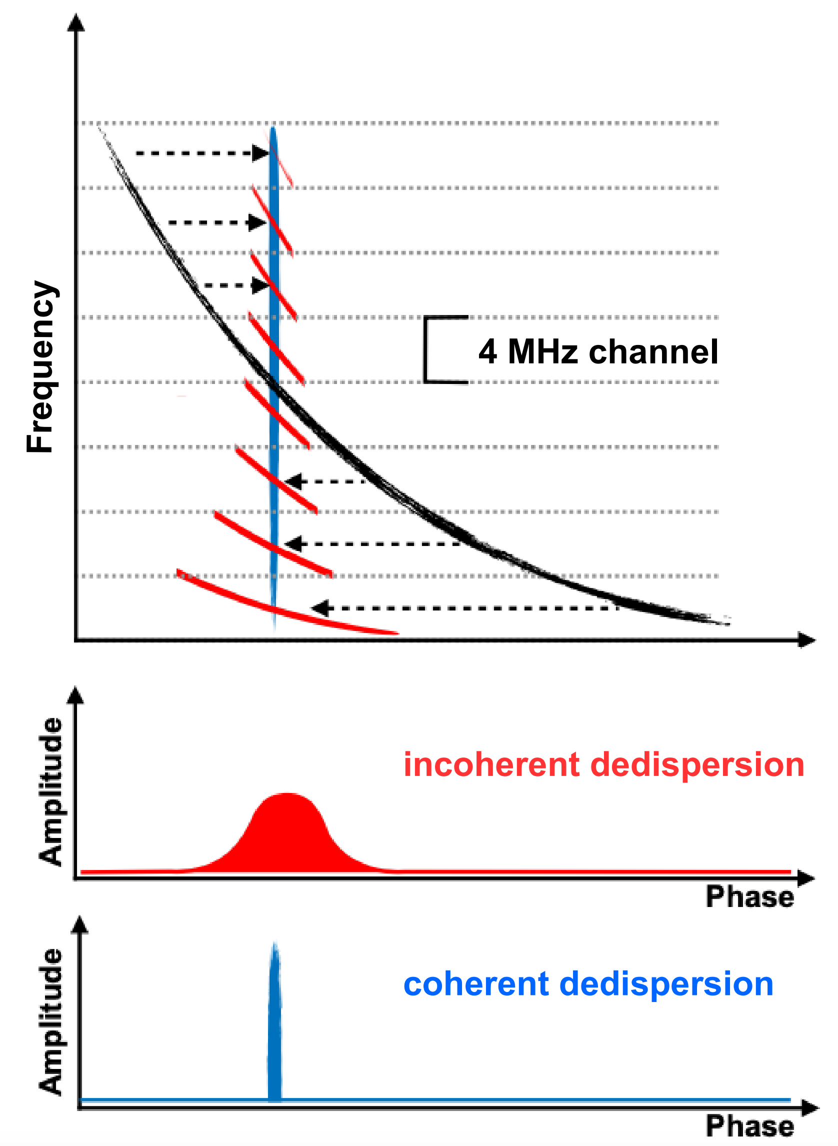

II- phase folding with rotation

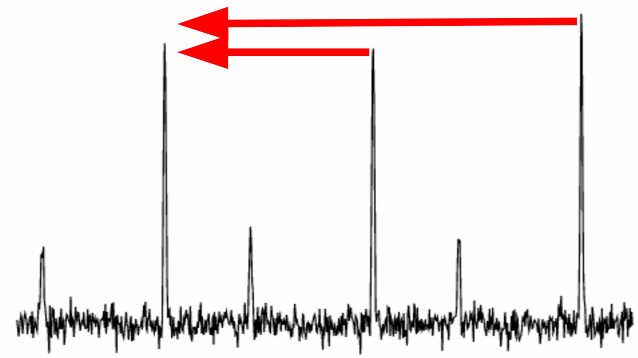

According to a model :
slow down,
orbital motion,
proper motion
planetary ephem.

III – Time stamping

(Time of arrival computation)

« TOA »

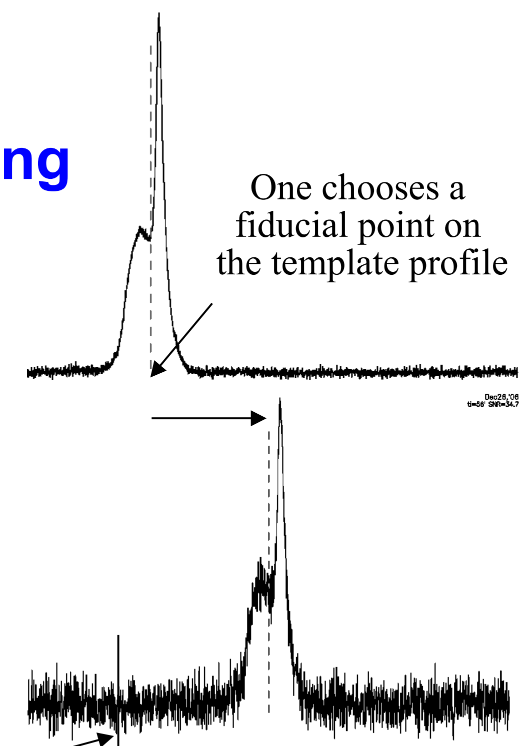

One chooses a fiducial point on the template profile

Position of the first data sample, corresponding to start of observation

Looking for extreme timing precision

the timing uncertainty can go down to 10-20 ns for some pulsars.

$$\sigma_{\mathrm{TOA}} \propto \frac{w}{S_{\mathrm{PSR}}} \frac{T_{\mathrm{sys}}}{A} \frac{1}{\sqrt{BT}}$$

Weak fluxes ~mJy (1 Jy = 10^{-26} W/m^2)

→ requires wide band pass in frequency

→ requires a large radio telescope

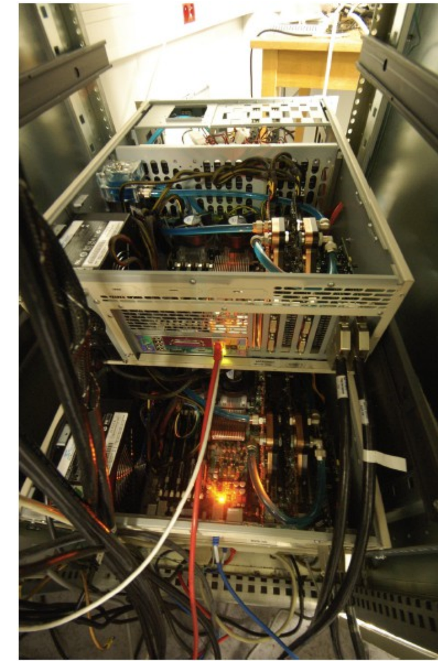

Current instrumentation in Nançay:
Coherent dedispersion over 512 MHz
1 FPGA / 4 PCs / 8 GPUs (16 Gb / s flux)

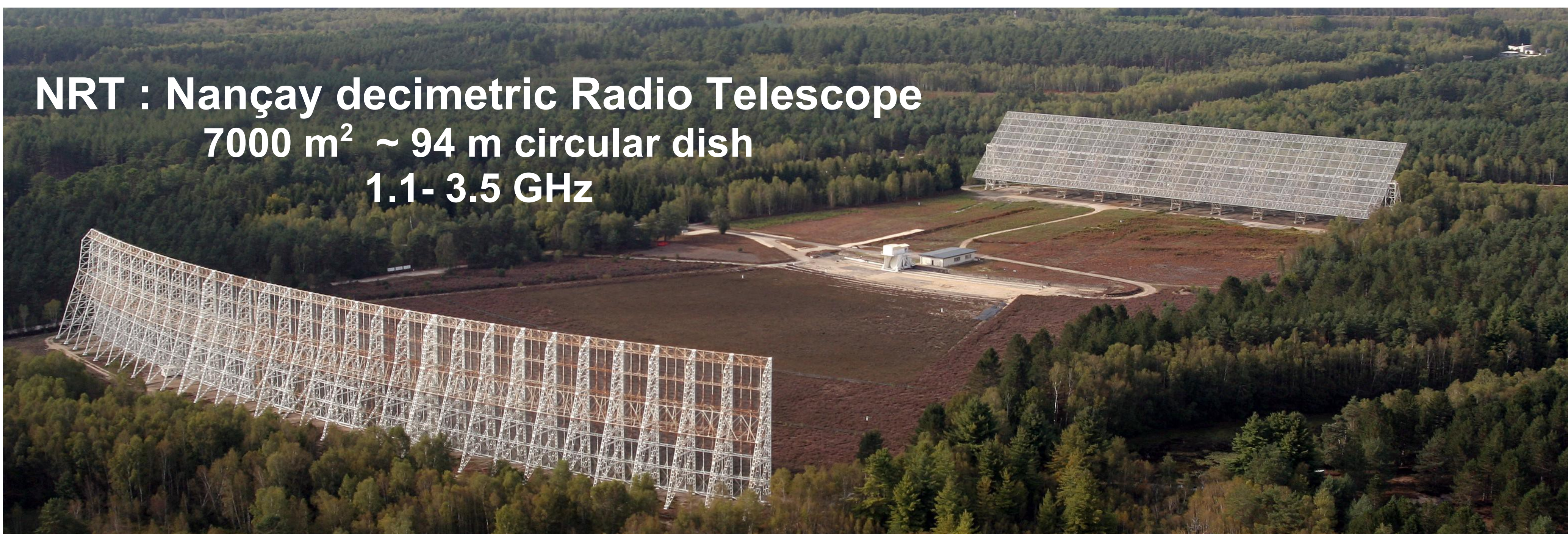

Pulsar Timing Arrays : principles

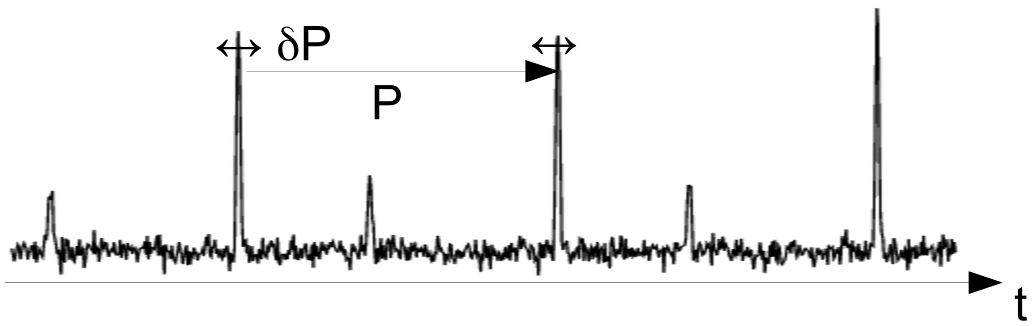

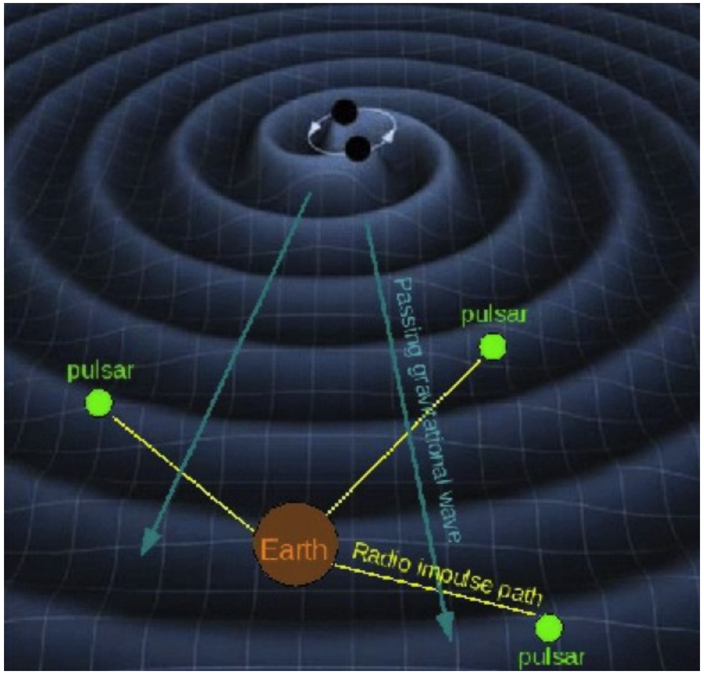

The Earth and the distant pulsar are considered as free masses whose position responds to changes in the metric of space-time

→ *The passage of a gravitational wave disturbs the metric and produces fluctuations in the arrival times of the pulses*

Pulsar Timing Arrays : principles

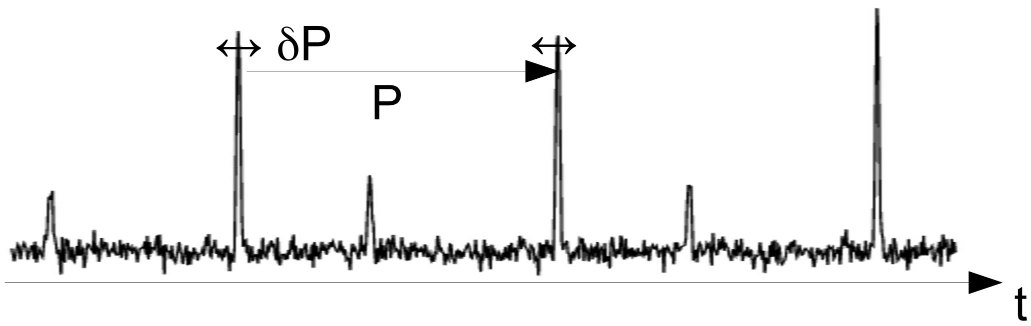

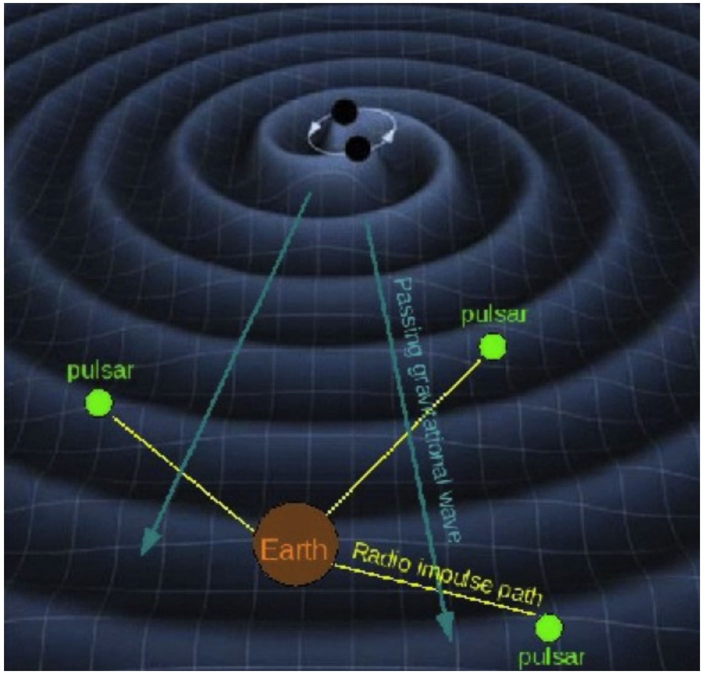

Analysis of time residuals

$$r(t) = \int_0^t \frac{\delta\nu}{\nu}(t')dt'$$

$$\frac{\delta\nu}{\nu}(t) = \frac{1}{2}\frac{\hat{n}^i\hat{n}^j}{1+\hat{n}.\hat{k}}\left(h_{ij}(t - L(1+\hat{k}.\hat{n})) - h_{ij}(t)\right)$$

pulsar-Earth distance

dir pulsar

dir GW source

wave amplitude at the pulsar

wave amplitude at the Earth

The Earth and the distant pulsar are considered as free masses whose position responds to changes in the metric of space-time

→ *The passage of a gravitational wave disturbs the metric and produces fluctuations in the arrival times of the pulses*

Pulsar Timing Arrays : principles

With timing uncertainties dt (~100 ns) and observation time spans T (~25 years)

→ PTA are sensitive to *amplitudes ~ dt/T*
and to frequencies f ~ 1/T

Sensitivity ~ 100 10^{-9} / 25 x 3 10^{7} → A ~ 1.3 10^{-16}

Frequency domain (25 years - 1 week) → 10^{-9} – 10^{-6} Hz

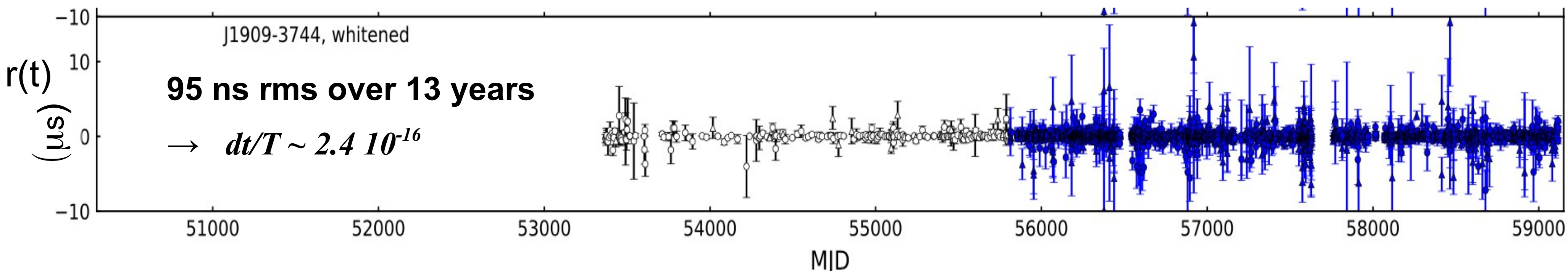

Pulsar Timing Arrays : principles

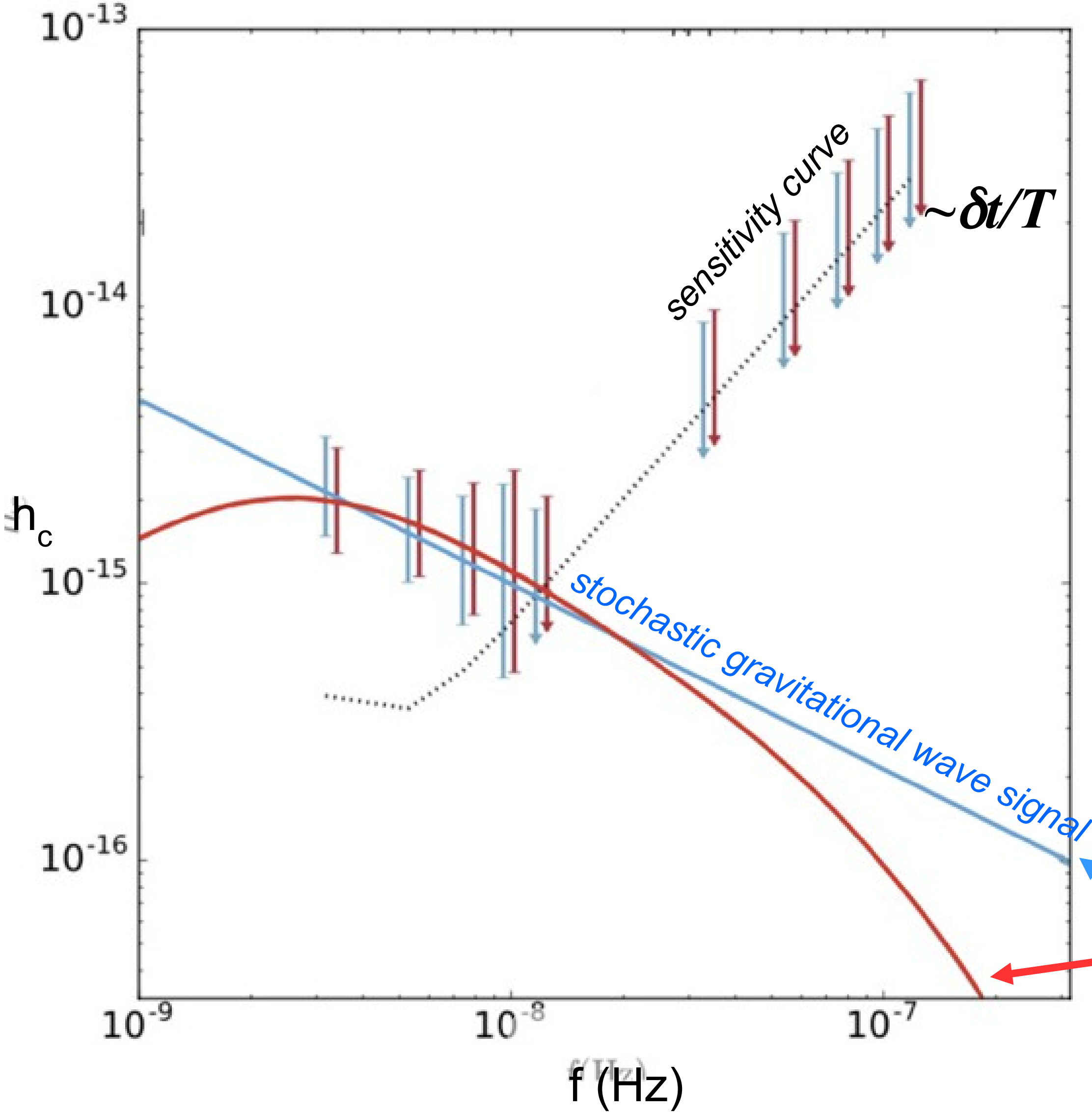

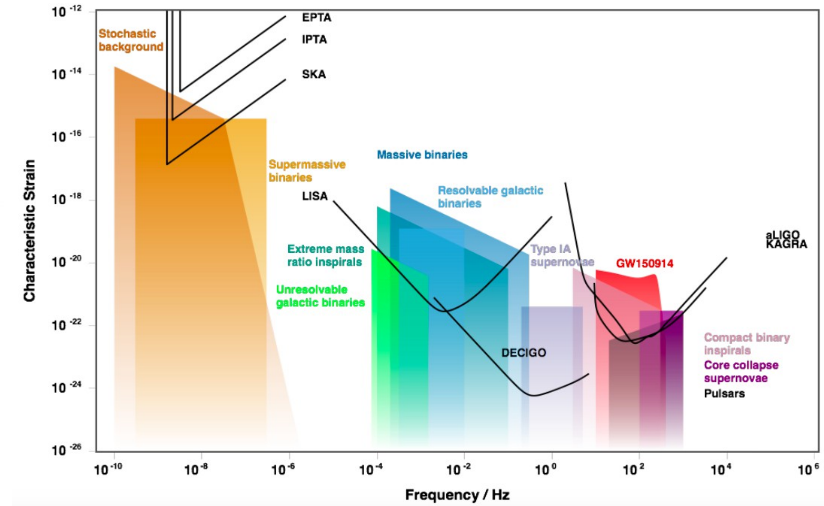

$$h_c(f) = A \left(\frac{f}{\mathrm{yr}^{-1}} \right)^{-2/3}$$

Expected spectrum for a population of super massive black hole binaries

Pulsar Timing Arrays : principles

1) Describe the pulsar rotation in a reference frame co-moving with the pulsar

$$\nu(t) = \nu_0 + \dot{\nu}_0(t - t_0) + \frac{1}{2}\ddot{\nu}_0(t - t_0)^2 + \cdots$$

The observed parameters ν and ν are associated
with the physical processes causing pulsars to spin down

Pulsar Timing Arrays : principles

1) Describe the pulsar rotation in a reference frame co-moving with the pulsar

$$\nu(t) = \nu_0 + \dot{\nu}_0(t - t_0) + \frac{1}{2}\ddot{\nu}_0(t - t_0)^2 + \cdots$$

The observed parameters ν and ν are associated with the physical processes causing pulsars to spin down

2) Timing model (transfer from topocentric to inertial reference frame)

$$t_{SSB} = t_{topo} + \overbrace{t_{corr} - \delta D/f_{obs}^2 + \Delta_{R\odot} + \Delta_{\pi} + \Delta_{S\odot} + \Delta_{E\odot} + \Delta_{R} + \Delta_{S} + \Delta_{E} + \Delta_{A}}^{\boldsymbol{\tau}^{\mathrm{TM}}}$$

- clock (t_{corr})
- dispersion ($\delta D/f_{obs}^2$)
- Solar System: Römer, parallax, Shapiro and Einstein delays ($\Delta_{R\odot} + \Delta_{\pi} + \Delta_{S\odot} + \Delta_{E\odot}$)
- binary system: Römer, Shapiro, Einstein and Aberration delays ($\Delta_{R} + \Delta_{S} + \Delta_{E} + \Delta_{A}$)

Pulsar Timing Arrays : principles

2) Timing model (examples)

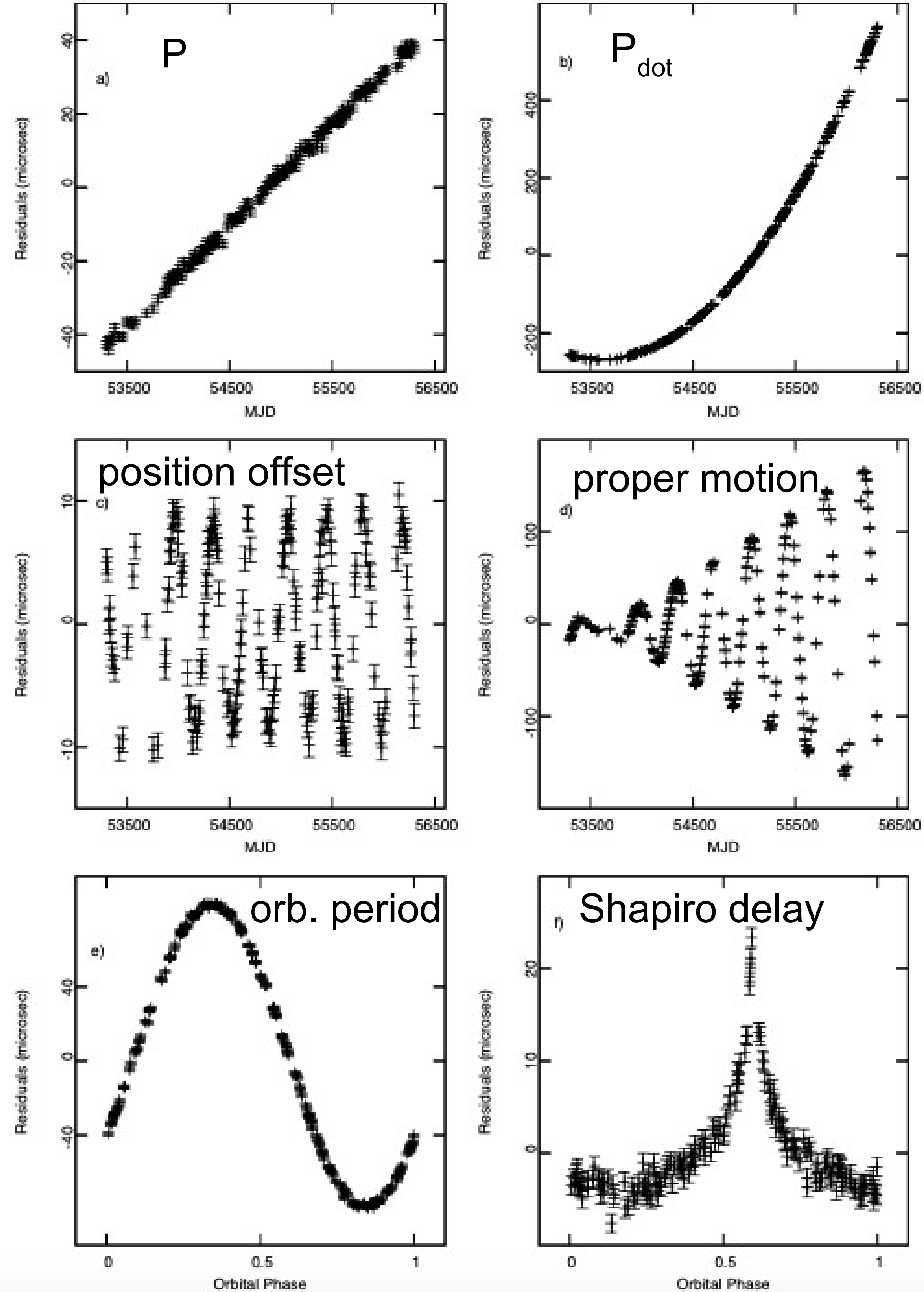

The NANOGrav 67-pulsars dataset

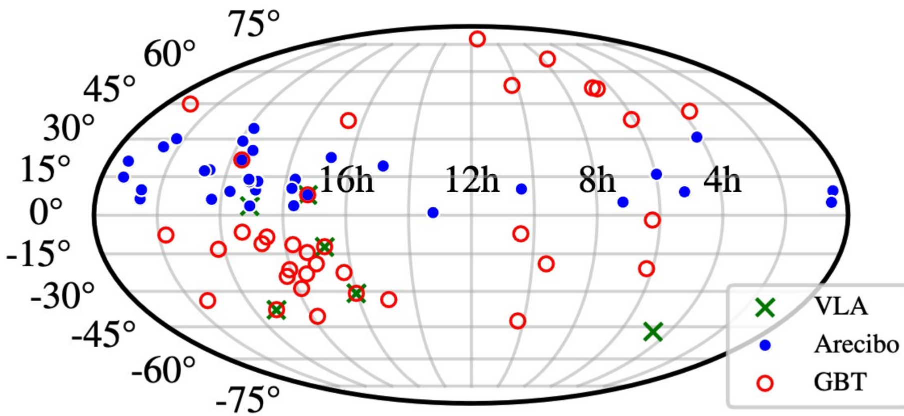

15 years data span Agazie et al 2023a

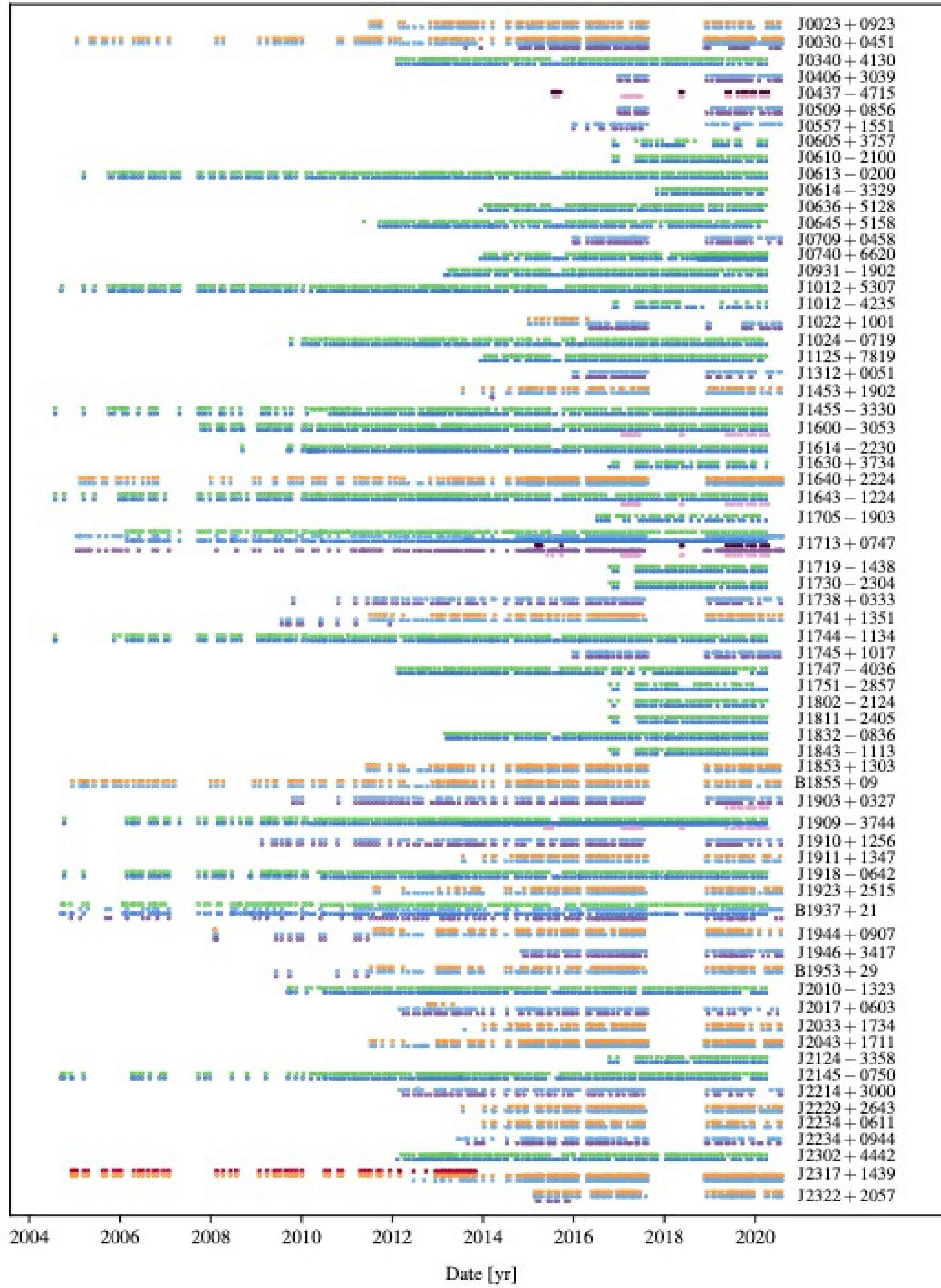

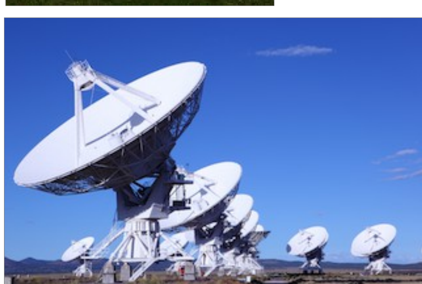

The PPTA 32-pulsars dataset

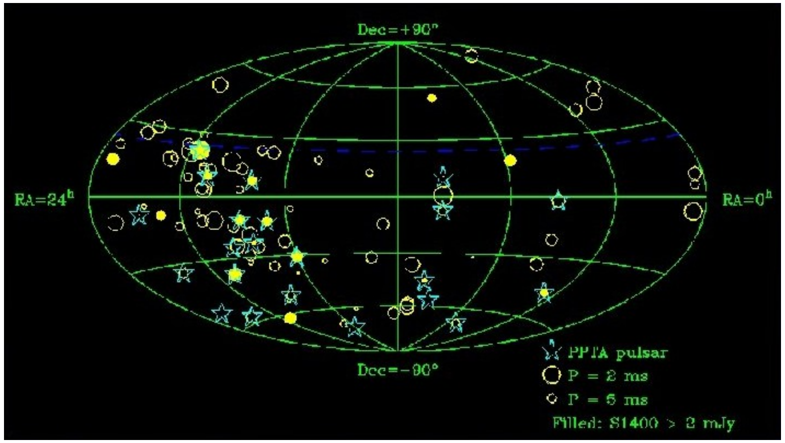

18 years data span Zic et al 2023

The EPTA 25-pulsars dataset

(paper I)

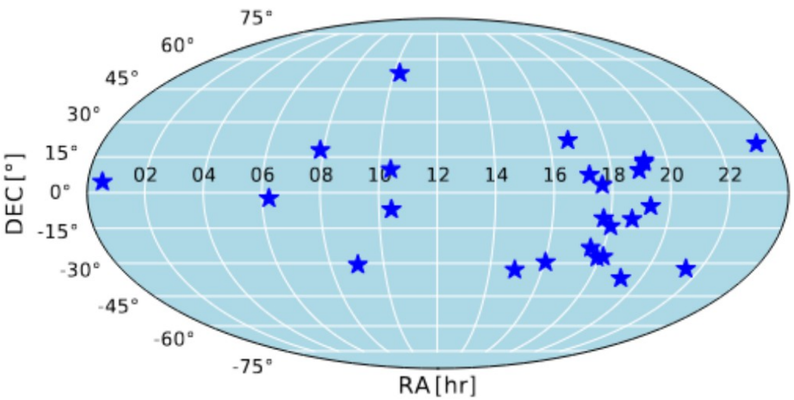

24.5/10.3 years data span

Antoniadis et al 2023a

e.g. 50 millisecond pulsars monitored at Nançay with timing precision better than 1.5 μs and cadence better than 30 days

NRT contribution
~60% of European data

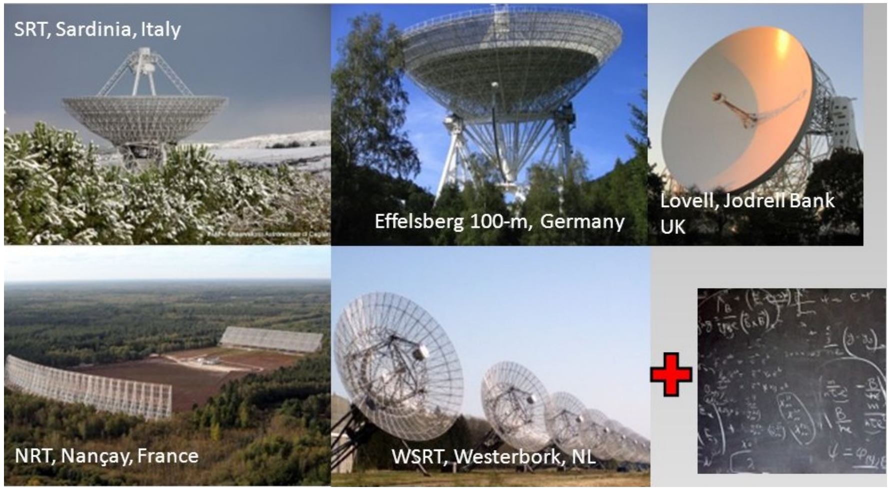

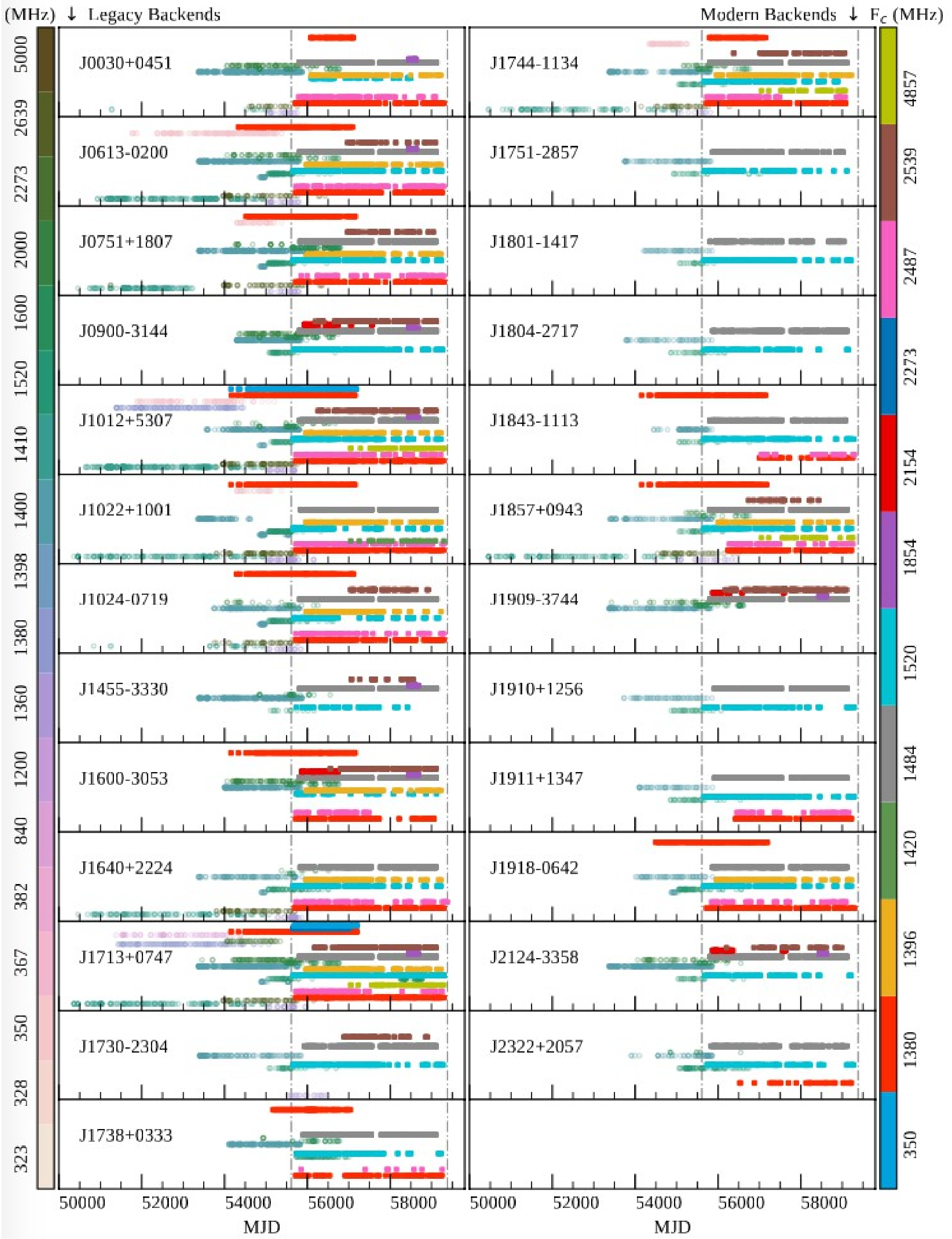

The EPTA 25-pulsars dataset

(paper I)

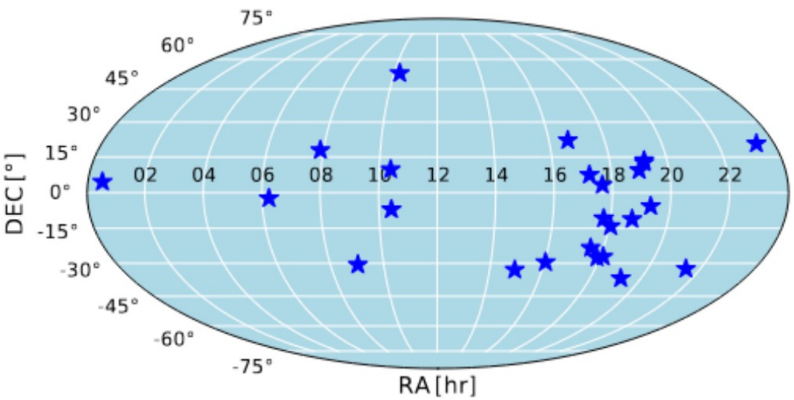

24.5/10.3 years data span

Antoniadis et al 2023a

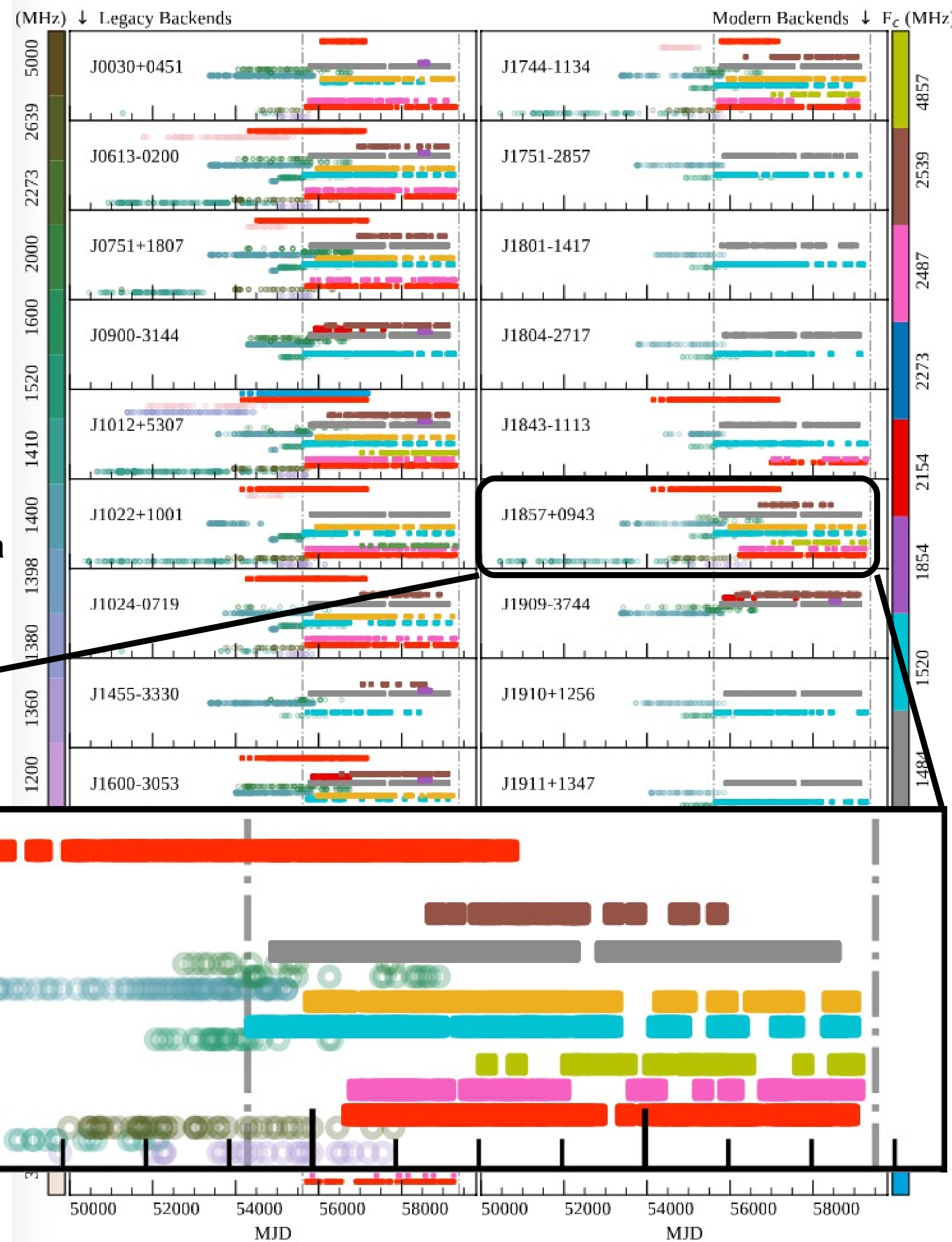

e.g. 50 millisecond pulsars monitored at Nançay with timing precision better than 1.5 μs and cadence better than 30 days

NRT contribution

The EPTA 25-pulsars dataset

(paper I)

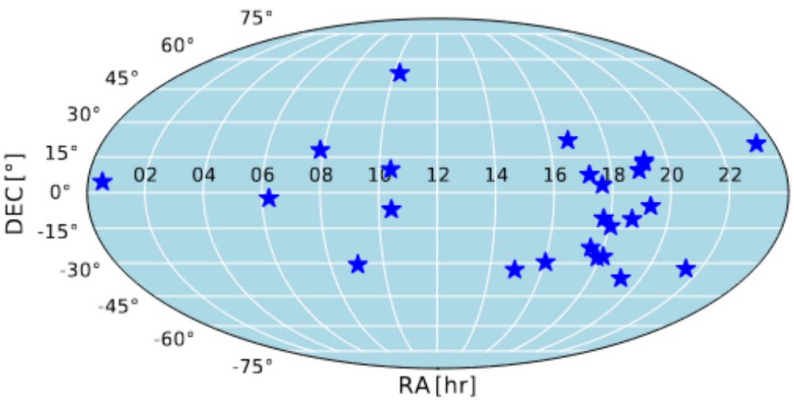

24.5/10.3 years data span

Antoniadis et al 2023a

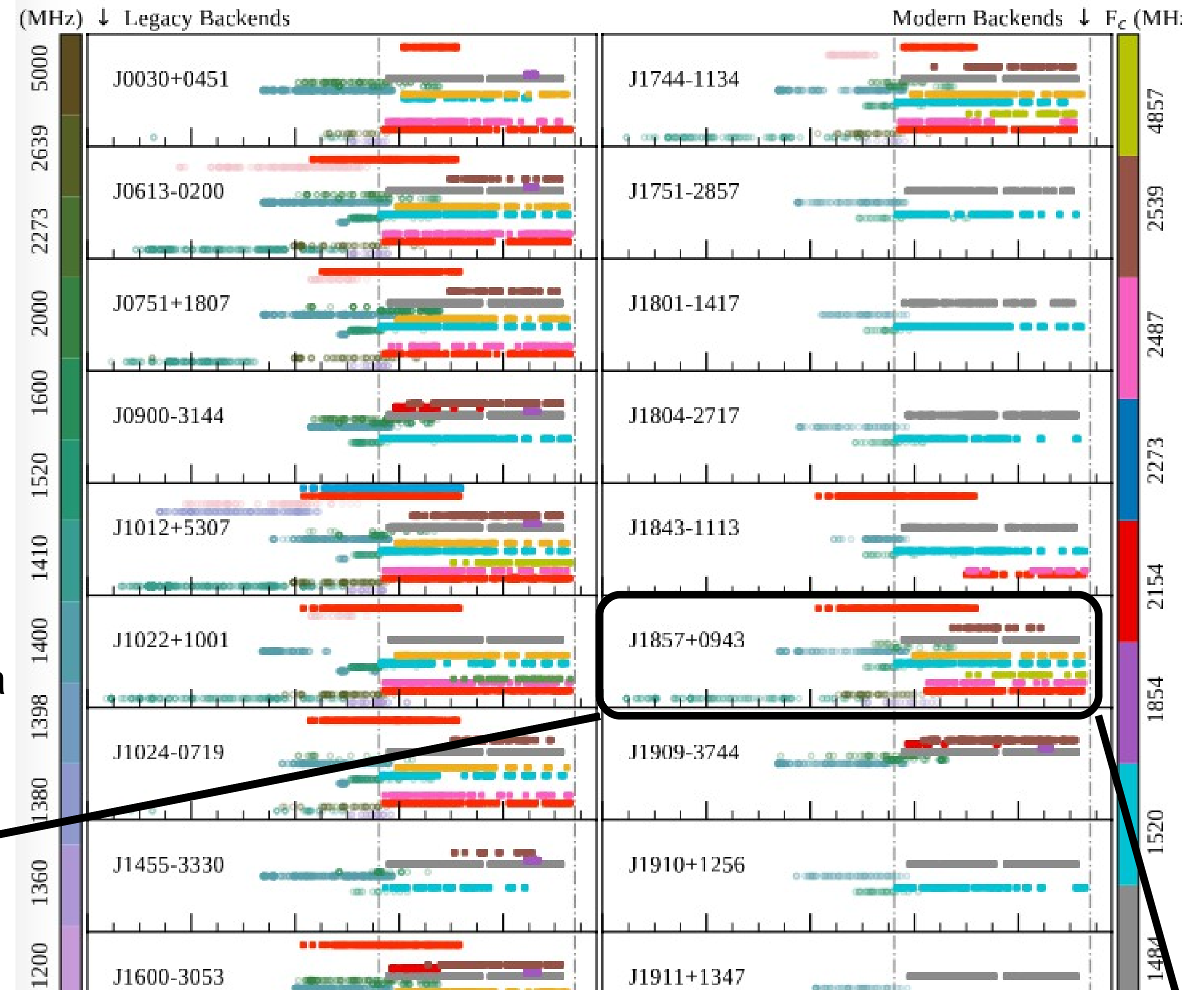

e.g. 50 millisecond pulsars monitored at Nançay with timing precision better than 1.5 μs and cadence better than 30 days

NRT contribution

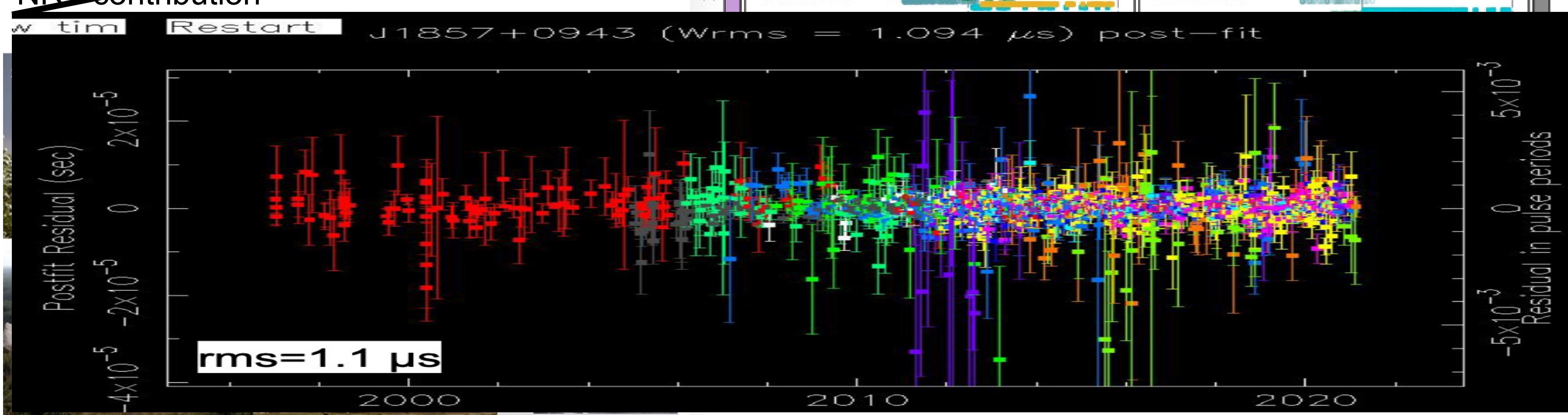

<u>Pulsar's parameters</u> **(paper I)**

Pulsar Jname	J1804−2717	J1843−1113	J1857+0943
Right ascension, α (J2000)	18:04:21.13307(1)	18:43:41.261937(7)	18:57:36.390620(1)
Declination, δ (J2000)	−27:17:31.337(3)	−11:13:31.0684(5)	09:43:17.20712(4)
Spin frequency, ν (Hz)	107.031649219533(4)	541.809745036152(5)	186.4940783779890(9)
Spin frequency derivative, $\dot{\nu}$	$-4.6812(2) \times 10^{-16}$	$-2.80559(3) \times 10^{-15}$	$-6.20522(4) \times 10^{-16}$
DM (cm^{-3} pc)	24.688(4)	59.962(2)	13.2957(9)
DM1 (cm^{-3} pc yr^{-1})	0.0005(7)	−0.0009(3)	0.00082(7)
DM2 (cm^{-3} pc yr^{-2})	−0.00012(9)	$5(8)\times10^{-5}$	−0.00012(2)
Proper motion in α, μ_α (mas yr^{-1})	2.46(2)	−1.99(2)	−2.670(3)
Proper motion in δ, μ_δ (mas yr^{-1})	−16.9(4)	−3.00(7)	−5.428(6)
Parallax, ϖ (mas)	1.1(3)	—	0.89(6)
Binary model	T2	—	T2
Orbital period, P_b (d)	11.1287119652(3)	—	12.32717138285(5)
Projected semi-major axis, x (s)	7.2814511(1)	—	9.23078029(8)
Epoch of ascending node (MJD), T_{asc}	49610.1749842(2)	—	46423.31409197(5)
$\hat{x}$ component of the eccentricity, κ	$1.219(3)\times10^{-5}$	—	$-2.1565(9) \times 10^{-5}$
$\hat{y}$ component of the eccentricity, η	$-3.177(4) \times 10^{-5}$	—	$2.454(5)\times10^{-6}$
Orbital period derivative, $\dot{P}_b$	—	—	$2.6(7)\times10^{-13}$
Derivative of x, $\dot{x}$	—	—	—
Sine of inclination angle, sin i	—	—	0.9989(2)
Companion mass, M_c ($M_\odot$)	—	—	0.258(5)

Pulsar Timing Arrays : principles

1) Describe the pulsar rotation in a reference frame co- moving with the pulsar

$$\nu(t) = \nu_0 + \dot{\nu}_0(t - t_0) + \frac{1}{2}\ddot{\nu}_0(t - t_0)^2 + \cdots$$

The observed parameters ν and ν are associated with the physical processes causing pulsars to spin down

2) Timing model

$$t_{SSB} = \overbrace{t_{topo} + t_{corr} - \delta D/f_{obs}^2 + \Delta_{R\odot} + \Delta_{\pi} + \Delta_{S\odot} + \Delta_{E\odot} + \Delta_R + \Delta_S + \Delta_E + \Delta_A}^{\boldsymbol{\tau}^{\mathrm{TM}}}$$

- clock: t_{corr}
- dispersion: $\delta D/f_{obs}^2$
- Solar System Römer, parallax, Shapiro and Einstein delays: $\Delta_{R\odot} + \Delta_{\pi} + \Delta_{S\odot} + \Delta_{E\odot}$
- binary system Römer, Shapiro, Einstein and Aberration delays: $\Delta_R + \Delta_S + \Delta_E + \Delta_A$

3) Full noise model

$$\text{observed TOA} = \boldsymbol{\tau}^{\mathrm{TM}} + \overbrace{\boldsymbol{\tau}^{\mathrm{WN}} + \boldsymbol{\tau}^{\mathrm{SN}} + \boldsymbol{\tau}^{\mathrm{DM}} + \boldsymbol{\tau}^{\mathrm{CN}}}^{\text{Noise model}} + \boldsymbol{\tau}^{\mathrm{GW}}$$

- $\boldsymbol{\tau}^{\mathrm{TM}}$: Timing Model (deterministic)
- $\boldsymbol{\tau}^{\mathrm{WN}}$: meas. (white) noise
- $\boldsymbol{\tau}^{\mathrm{SN}}$: pulsar spin (red) noise
- $\boldsymbol{\tau}^{\mathrm{DM}}$: DM + scatter (red) noise
- $\boldsymbol{\tau}^{\mathrm{CN}}$: clock + ephem. (red) noise
- $\boldsymbol{\tau}^{\mathrm{GW}}$: GWB (red) noise

Analysis of foregrounds: characterisation and separation of the noise components

« White noises » (un-correlated noise) $\hat{\sigma}^2 = (\sigma \cdot \mathrm{EFAC})^2 + \mathrm{EQUAD}^2$

τ^{WN} Instrumental → telescope gain stability, pass band, backend used

Astrophysical → 'pulse jitter' (pulse stochasticity, variations in pulsar magnetosphere)

« Red noises » (correlated noise) $S \propto A^2 f^{-\gamma}$

τ^{DM} Variations in the Dispersion Measure → changes « e- » content along line of sight (chromatic : multi-frequency measurements)

τ^{Sv} Variations in the scattering → multi-path propagation

τ^{SN} Intrinsic rotation noise → perturbation from small bodies disc ?

Variations in radiated energy ? series of micro-glitches ?

τ^{CN} Clock variations → clock-telescope link → TAI → TT-BIPM

τ^{SSE} Solar System ephemerides → position of SS barycentre → links to INPOP, JPL

Galactic motion of the Sun → LSR

τ^{GW} Gravitational waves → indiv. sources, stochastic background, « bursts » events

Pulsar Timing Arrays : principles

Pulse jitter

EQUAD

PSR B1919+21
P = 1.3 s

Pulsar Timing Arrays : principles

Pulse jitter EQUAD

PSRJ1713+0747
P = 4.57 ms
LEAP Observations
'pulse to pulse' variations
(Bassa et al 2015)
1% in phase ↔ ~100 ns over 1 h

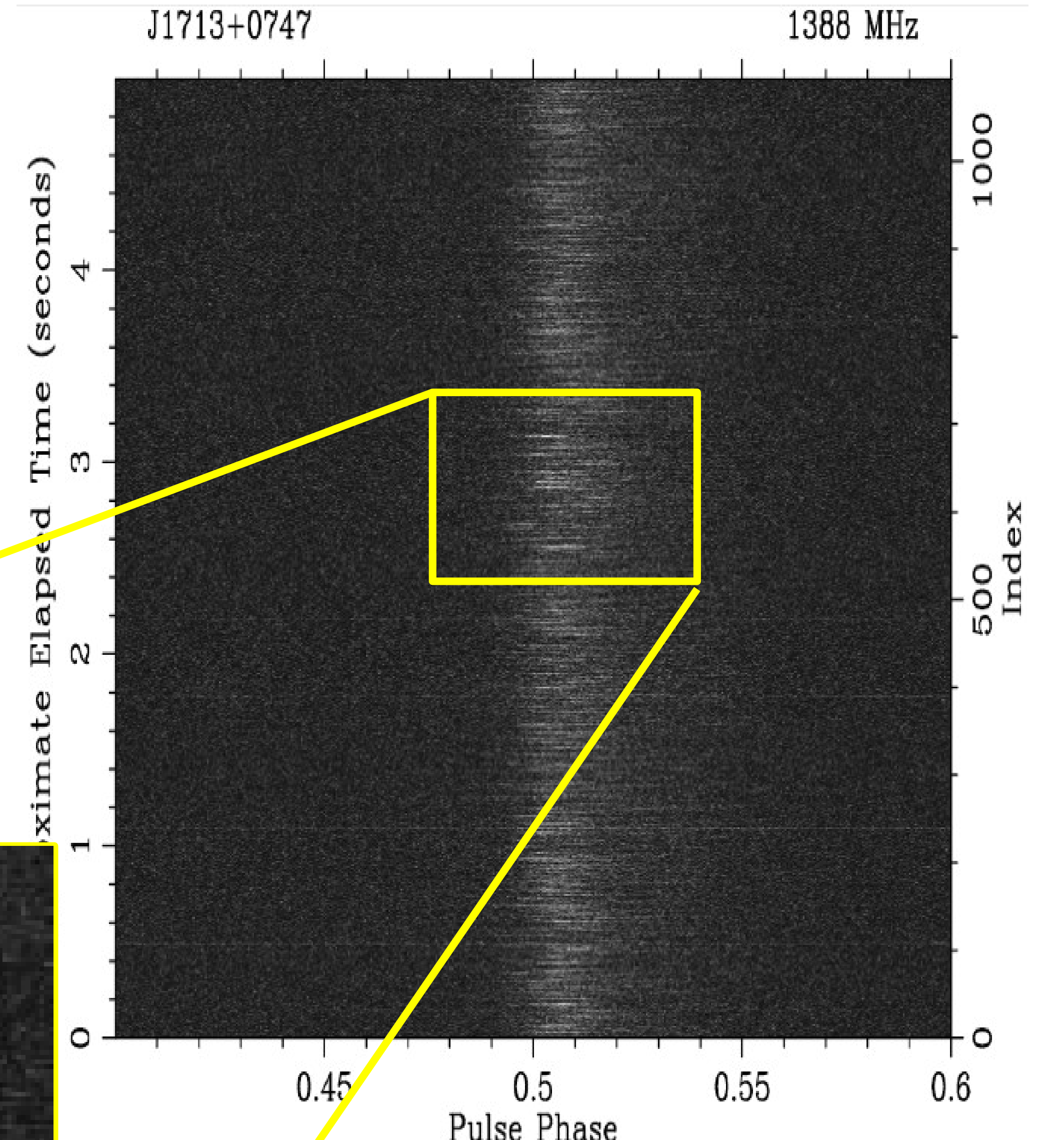

Red noise : dispersion noise or chromatic noise

= effects of interstellar medium

requires multi-wavelength observations
e.g. 500 MHz, 1400 MHz, 2.5 GHz

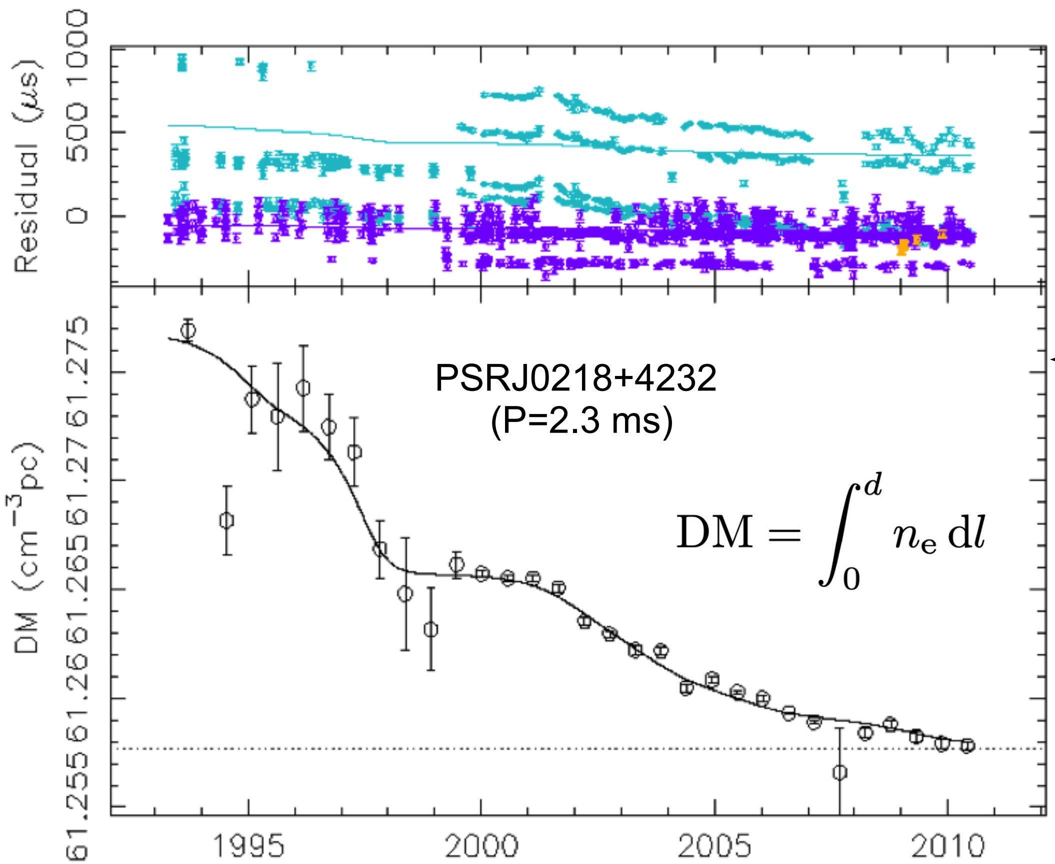

Janssen 2015

Secular variation of the Dispersion Measure
(due to relative proper motion)

$$\tau^{\mathrm{DM}}$$

Red noise : dispersion noise or chromatic noise

= effects of interstellar medium

requires multi-wavelength observations
e.g. 500 MHz, 1400 MHz, 2.5 GHz

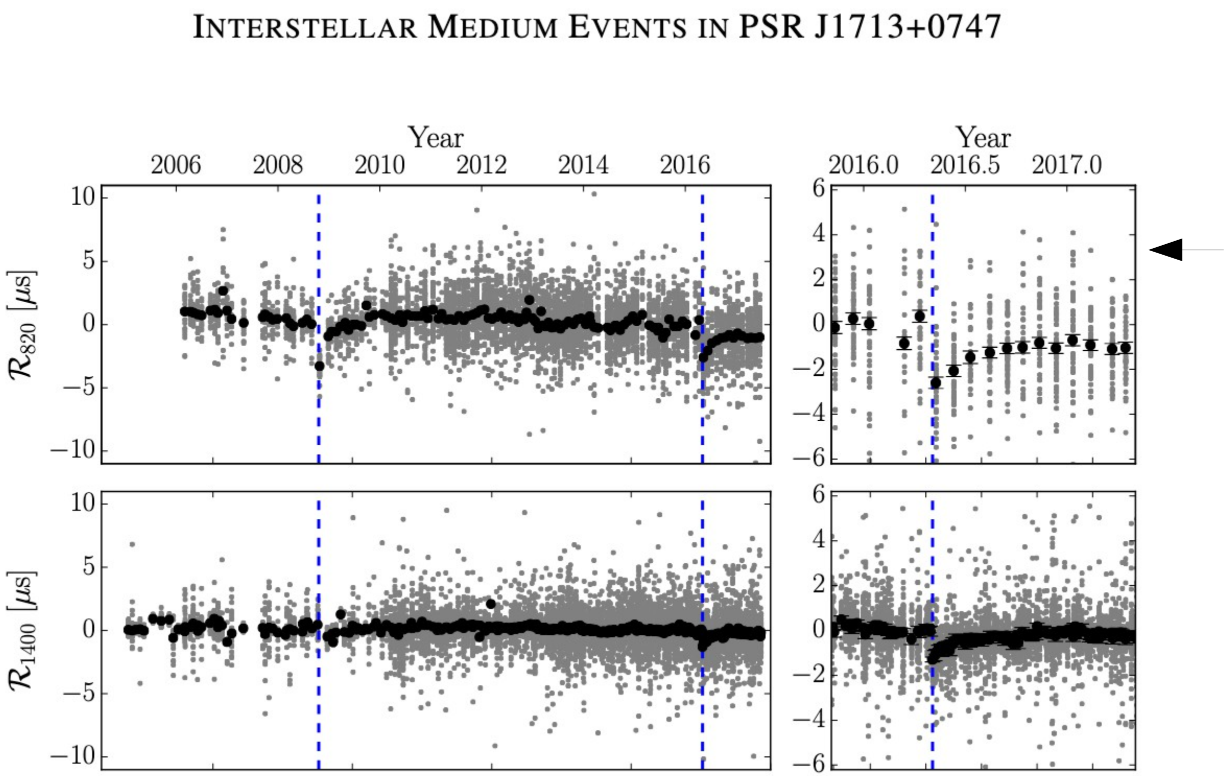

Lam et al 2018

DM events:

1) lense effect due to a plasma bubble along the line of sight

2) local process in the pulsar magnetosphere (pulse shape change)

Red noise : dispersion noise or chromatic noise

= effects of interstellar medium

requires multi-wavelength observations
e.g. 500 MHz, 1400 MHz, 2.5 GHz

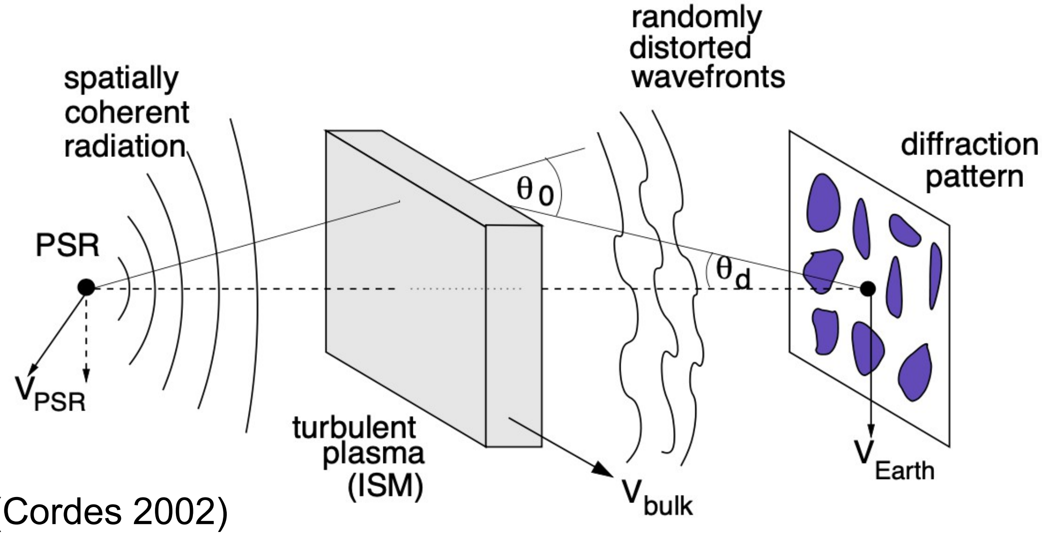

(Cordes 2002)

multi-path propagation through turbulent plasma + scattering variations

τ^{Sv}

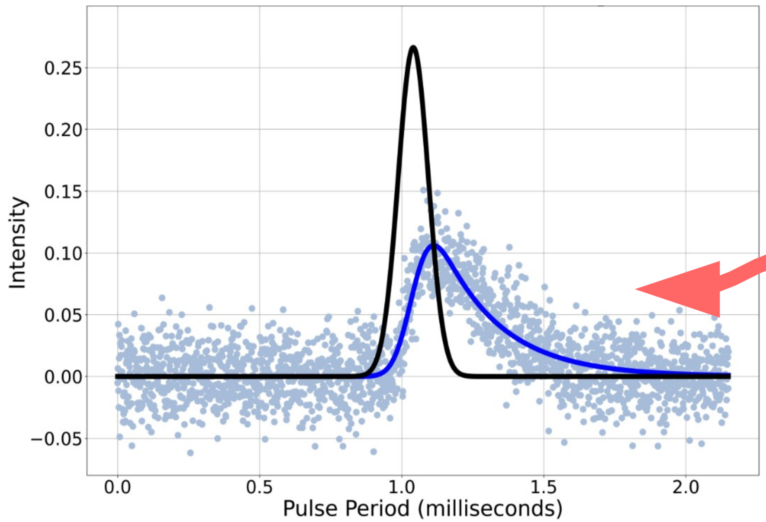

pulse broadening

Geiger&Lam 2022

Red noise : dispersion noise or chromatic noise

= effects of interstellar medium

requires multi-wavelength observations
e.g. 500 MHz, 1400 MHz, 2.5 GHz

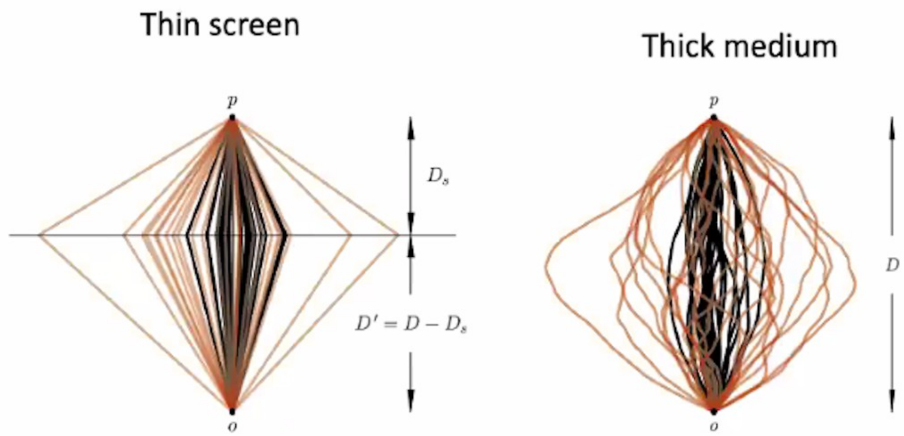

Cordes, Shannon & Stinebring (2016)
Orange: low frequency
Black: high frequency

multi-path propagation
through turbulent plasma
+ scattering variations

τ^{Sv}

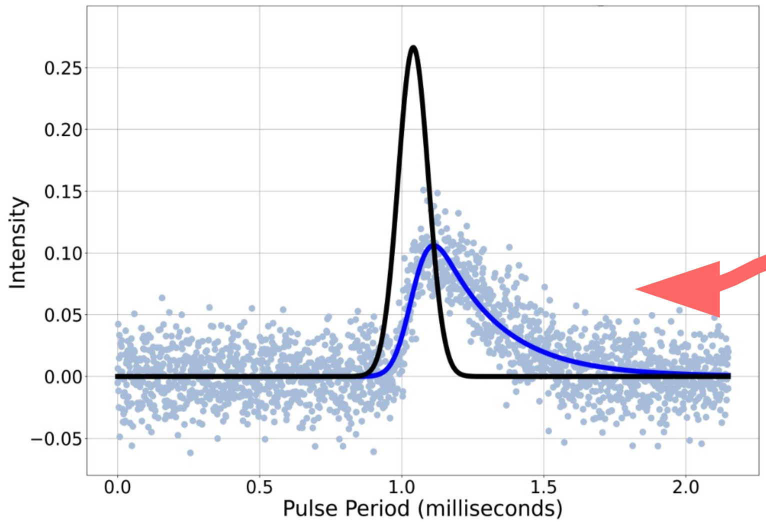

pulse
broadening

Geiger&Lam 2022

Red noise : spin noise

P=1.55 ms rms ~ 34 .5 μs <unc.> ~ 60 ns

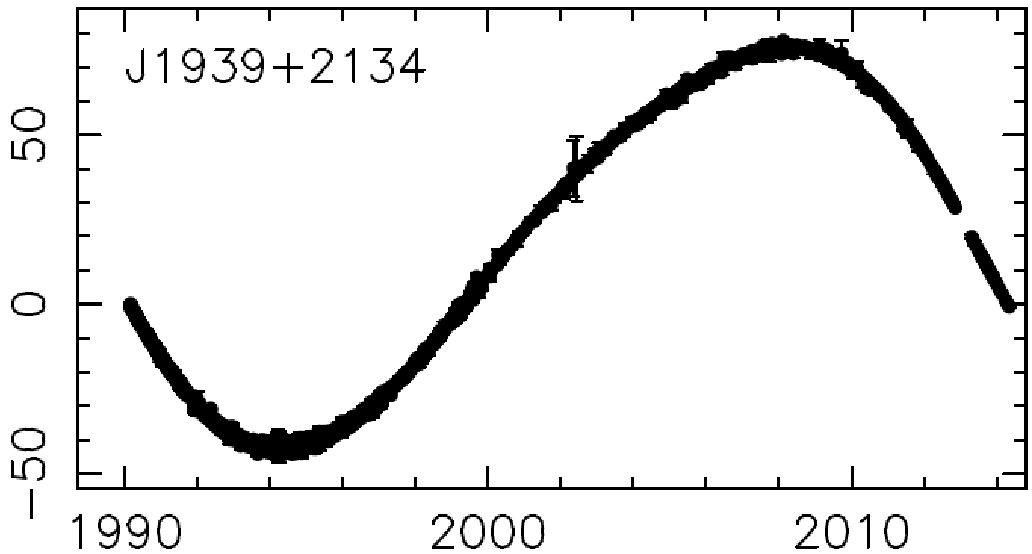

τ^{SN}

P=2.9 ms rms ~ 0.092 μs <INC‰> ~ 60 ns

Small bodies disc perturbation ?

E_{dot} variations?

Series of micro-glitches ?

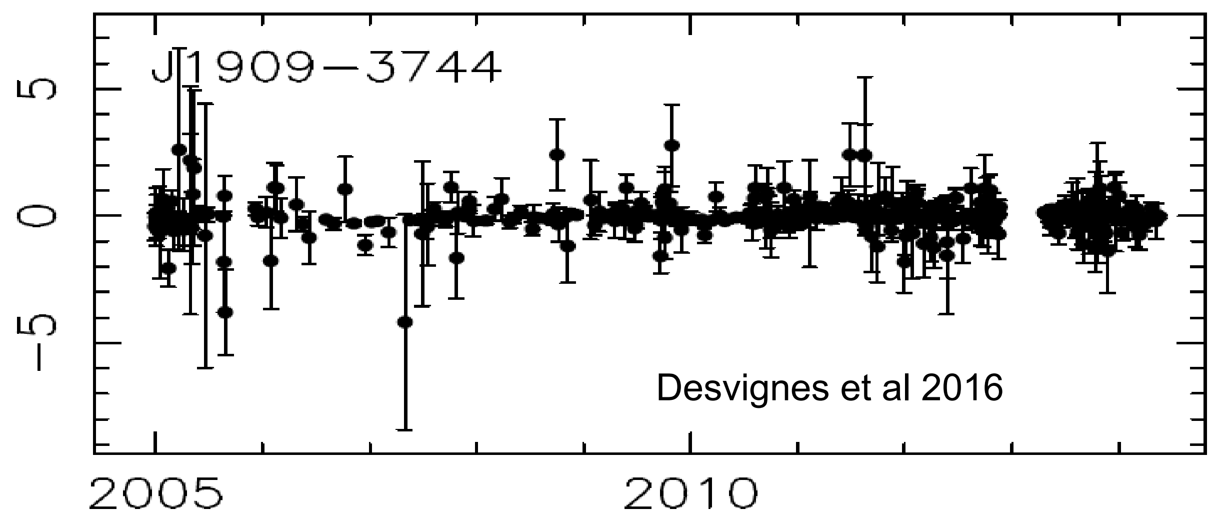

Red noise : Impact of planetary ephemerides

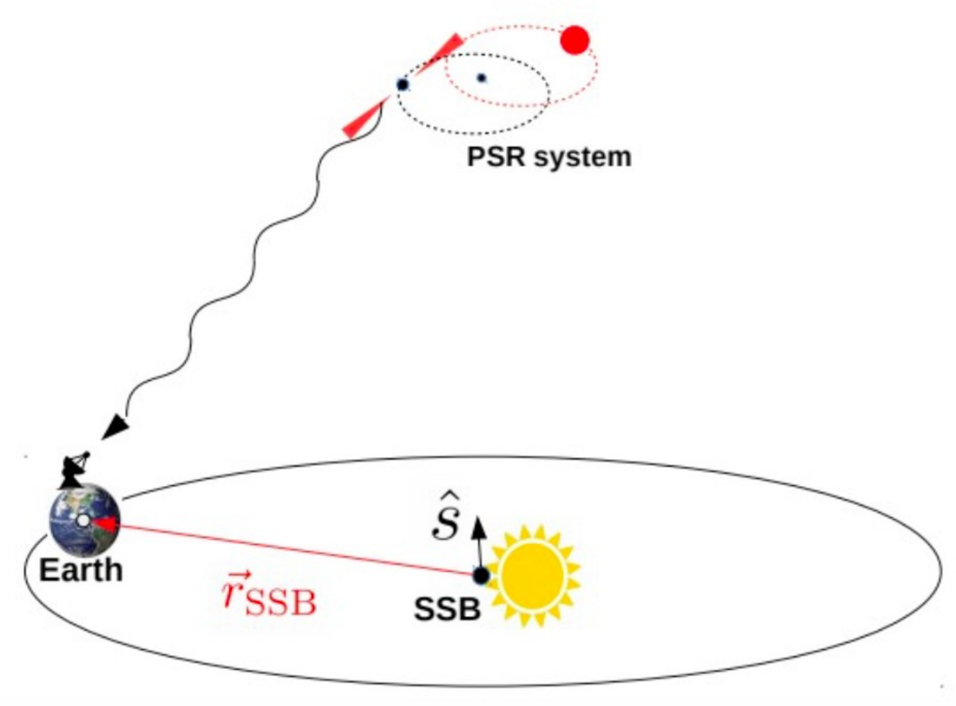

Uncertainties in the Römer delay when transposing to the Solar System barycentre induce a correlated signal with a dipole signature.

Conversely, we are sensitive to the orbital parameters of the planets!

Red noise : Impact of planetary ephemerides

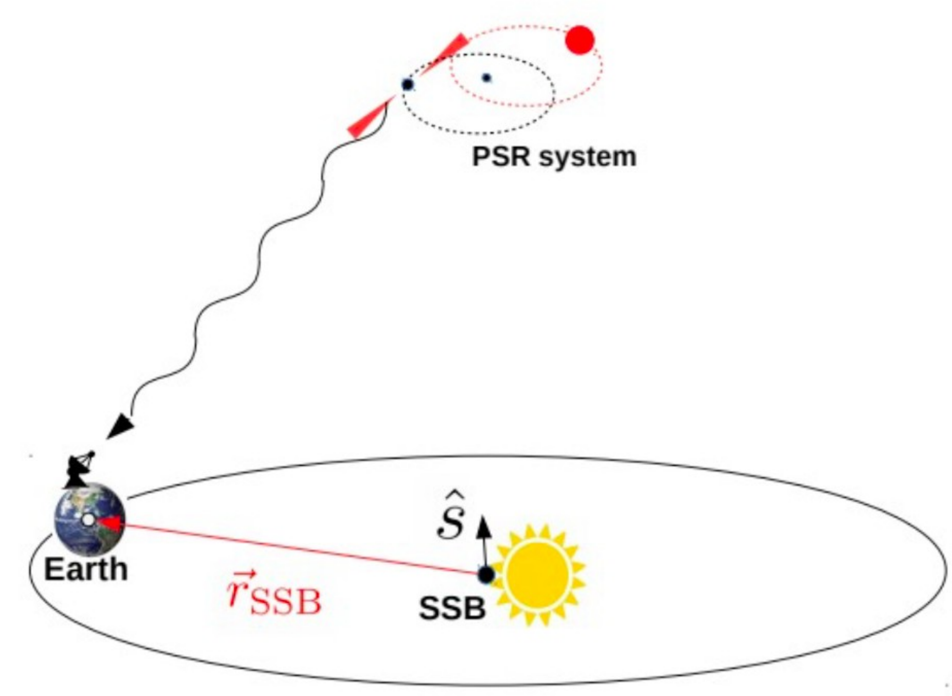

false detection of a common signal when uncertainties are not taken into account in the model

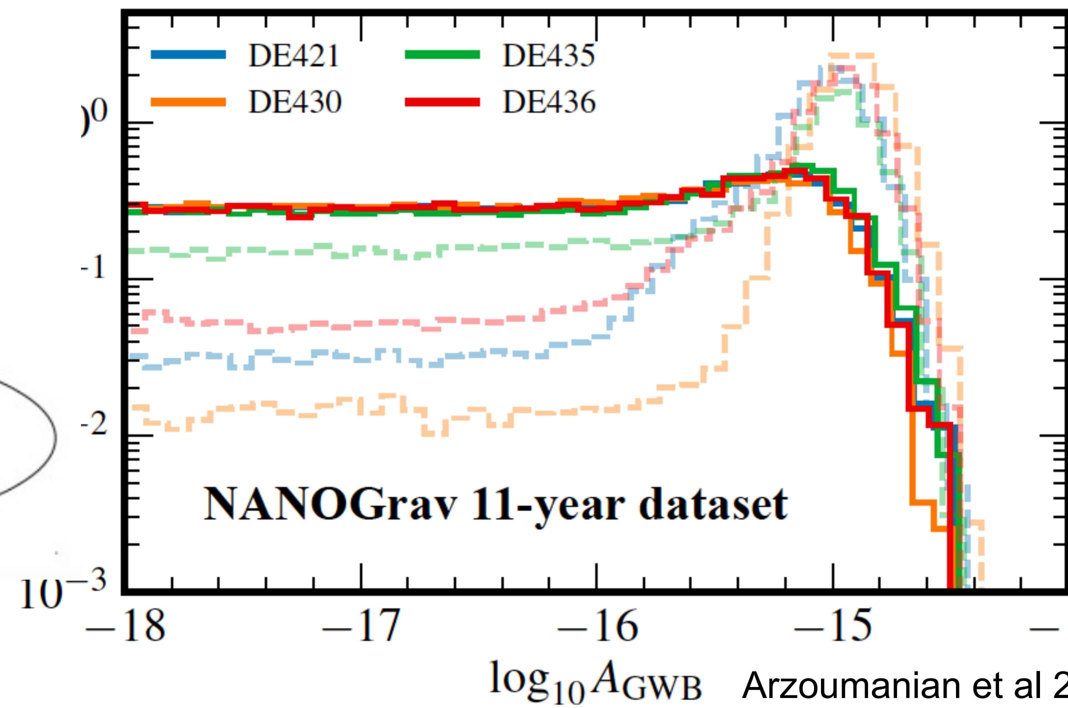

Arzoumanian et al 2018

Uncertainties in the Römer delay when transposing to the Solar System barycentre induce a correlated signal with a dipole signature.

Conversely, we are sensitive to the orbital parameters of the planets!

Red noise : Impact of planetary ephemerides

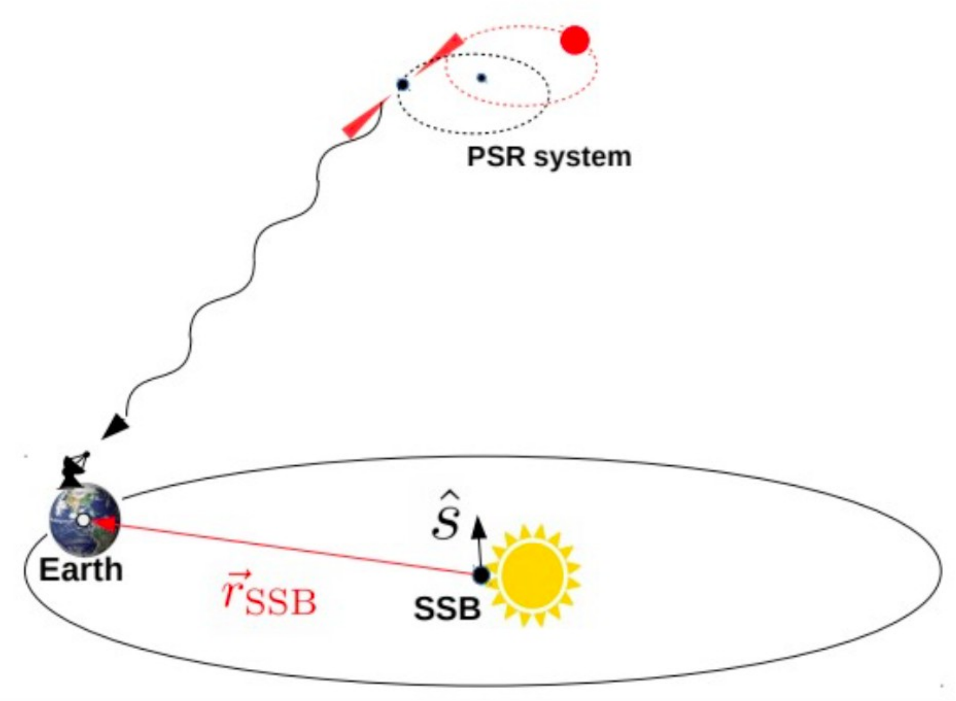

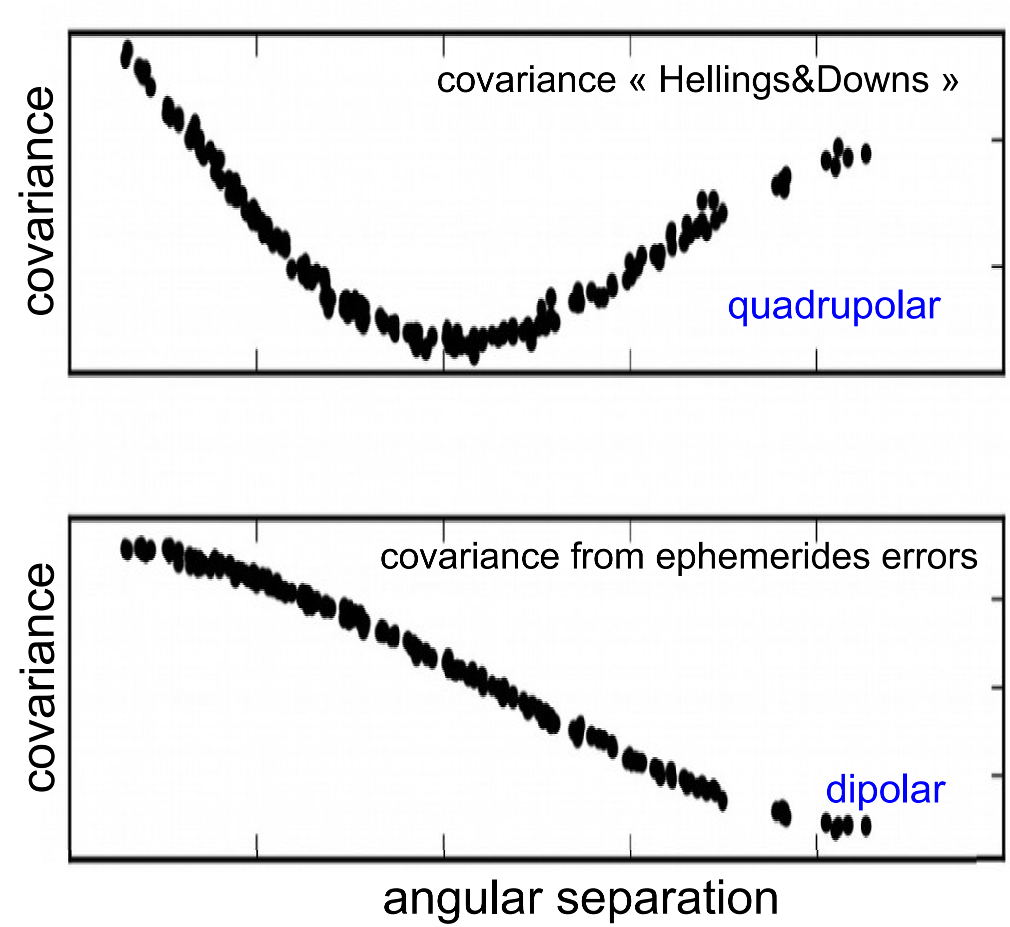

Tiburzi et al 2016

Uncertainties in the Römer delay when transposing to the Solar System barycentre induce a correlated signal with a dipole signature.

Conversely, we are sensitive to the orbital parameters of the planets!

Red noise : individual pulsar models

PSR J1600-3053

Chalumeau et al 2021 (EPTA)

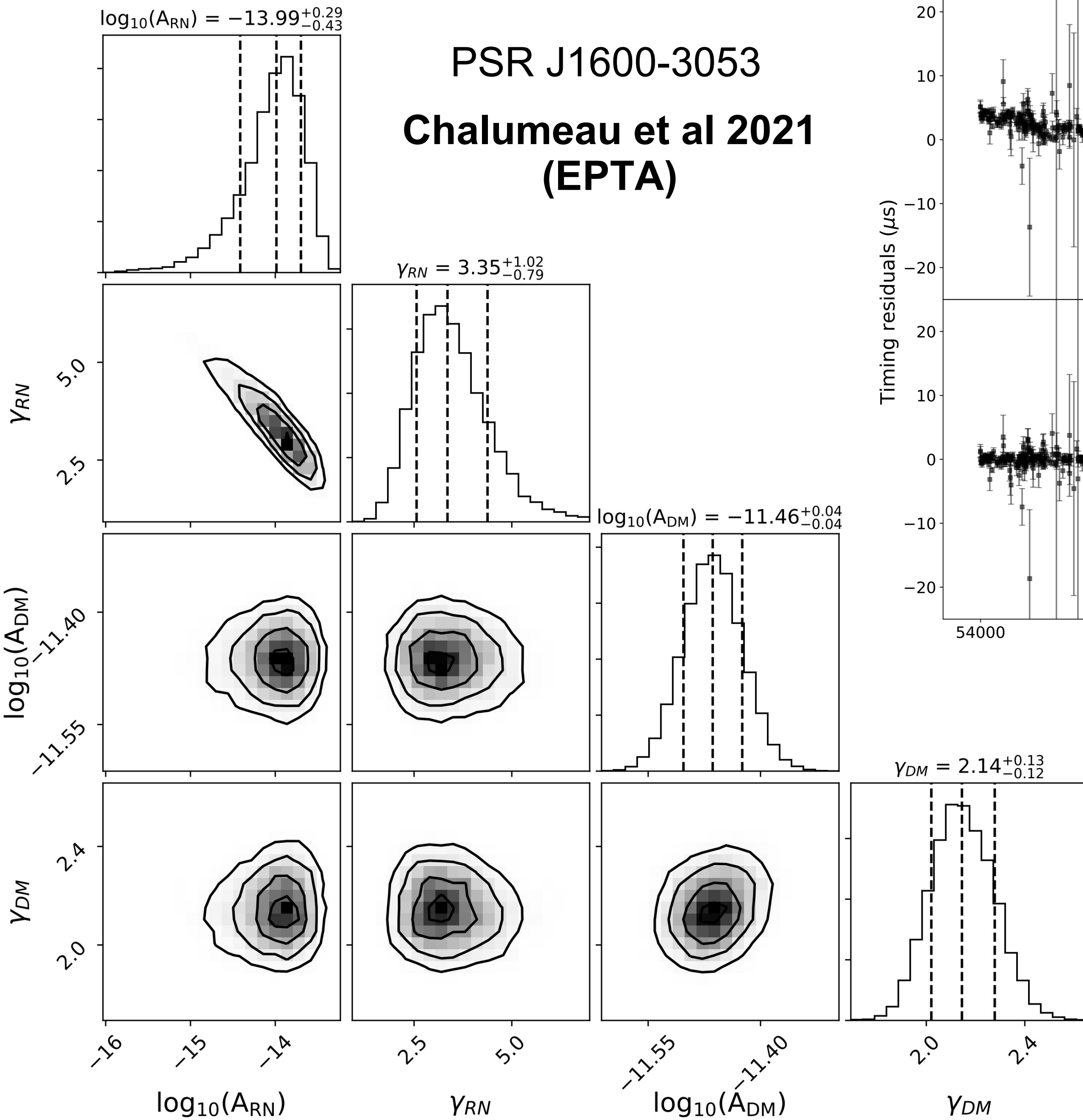

including timing model

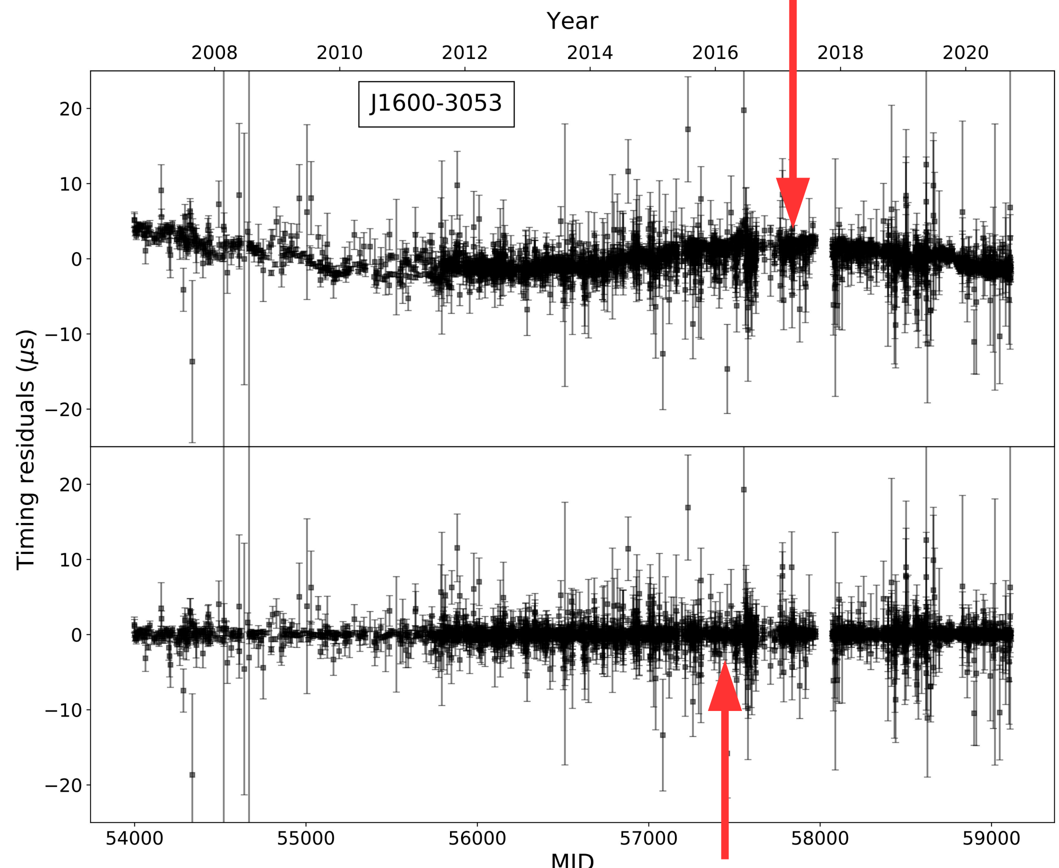

including timing model + noise model

- **Spin noise**
- **DM chromatic noise**
- Scaterring noise
- Band noise
- System noise

\+

Nb of freq bins
to characterise each

Pulsar Timing Arrays : principles

1) Describe the pulsar rotation in a reference frame co- moving with the pulsar

$$\nu(t) = \nu_0 + \dot{\nu}_0(t - t_0) + \frac{1}{2}\ddot{\nu}_0(t - t_0)^2 + \cdots$$

The observed parameters ν and ν are associated with the physical processes causing pulsars to spin down

2) Timing model

$$t_{SSB} = t_{topo} + \overbrace{t_{corr} - \delta D/f_{obs}^2 + \Delta_{R\odot} + \Delta_{\pi} + \Delta_{S\odot} + \Delta_{E\odot} + \Delta_R + \Delta_S + \Delta_E + \Delta_A}^{\boldsymbol{\tau}^{\mathrm{TM}}}$$

- clock (t_{corr})
- dispersion ($\delta D/f_{obs}^2$)
- Solar System Römer, parallax, Shapiro and Einstein delays ($\Delta_{R\odot} + \Delta_{\pi} + \Delta_{S\odot} + \Delta_{E\odot}$)
- binary system Römer, Shapiro, Einstein and Aberration delays ($\Delta_R + \Delta_S + \Delta_E + \Delta_A$)

3) Full noise model

observed TOA $= \boldsymbol{\tau}^{\mathrm{TM}} + \overbrace{\boldsymbol{\tau}^{\mathrm{WN}} + \boldsymbol{\tau}^{\mathrm{SN}} + \boldsymbol{\tau}^{\mathrm{DM}} + \boldsymbol{\tau}^{\mathrm{CN}}}^{\text{Noise model}} + \boldsymbol{\tau}^{\mathrm{GW}}$

- $\boldsymbol{\tau}^{\mathrm{TM}}$: Timing Model (deterministic)
- $\boldsymbol{\tau}^{\mathrm{WN}}$: meas. (white) noise
- $\boldsymbol{\tau}^{\mathrm{SN}}$: pulsar spin (red) noise
- $\boldsymbol{\tau}^{\mathrm{DM}}$: DM (red) noise
- $\boldsymbol{\tau}^{\mathrm{CN}}$: Clock Ephem. Astroph. (red) noise
- $\boldsymbol{\tau}^{\mathrm{GW}}$: GWB (red) noise

Pulsar Timing Arrays : principles

we write the PTA likelihood as $$p(\boldsymbol{\delta t}|\boldsymbol{\eta}) = \frac{\exp\left(-\frac{1}{2}\boldsymbol{\delta t}^T C^{-1}\boldsymbol{\delta t}\right)}{\sqrt{\det(2\pi C)}}$$

The covariance matrix is decomposed into a sum of « noises » whose spectrum is described by a power law

$$C \sim \underbrace{\Gamma_{ab}\rho_i\delta_{ij}}_{\text{GW}} + \underbrace{\epsilon_i\delta_{ij}}_{\text{clock/eph.}} + \underbrace{\eta_i\delta_{ab}\delta_{ij}}_{\text{astro}\varphi} + \underbrace{\kappa_{ai}\delta_{ab}\delta_{ij}}_{\text{indiv. rot./disp.}}$$

GW clock/eph. astroφ indiv. rot./disp.

The GW term depends both on the amplitude of the signal as a function of its sky position and on the «antenna pattern »

$$\Gamma_{ab} = \frac{3}{8\pi}(1+\delta_{ab})\int_{S^2} d\hat{\Omega}\; P(\hat{\Omega}) \sum_q F_a^q(\hat{\Omega}) F_b^q(\hat{\Omega})$$

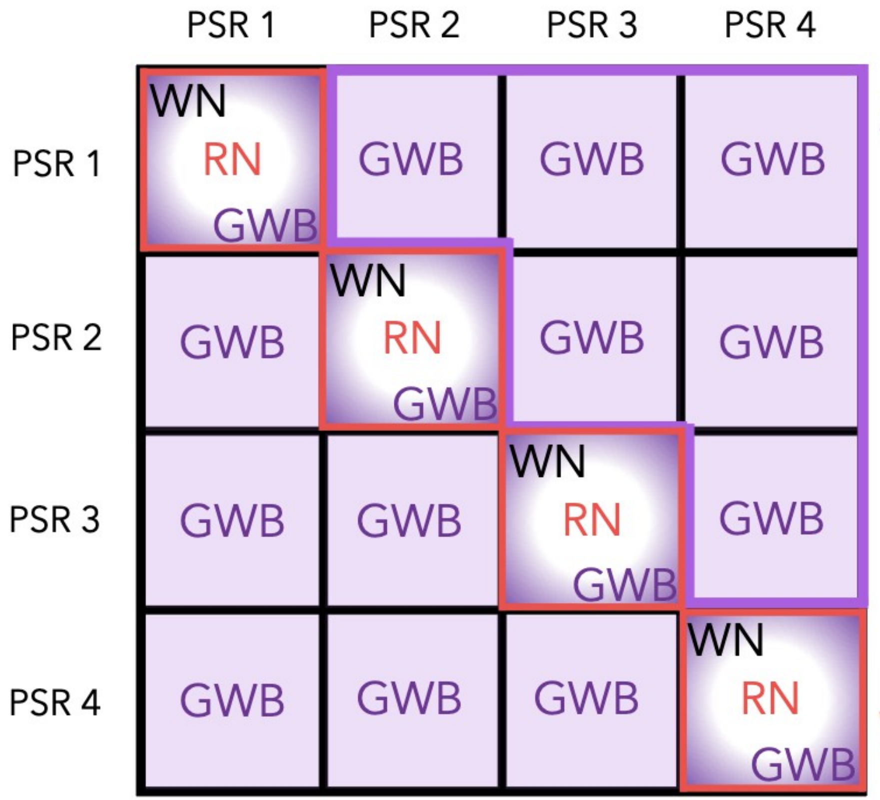

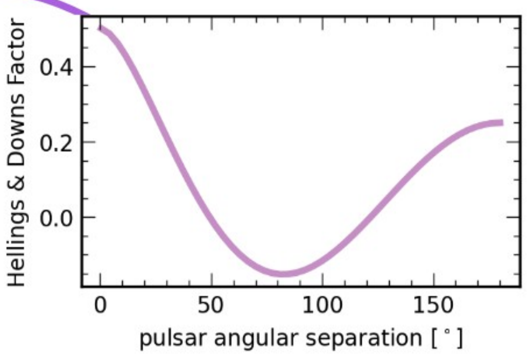

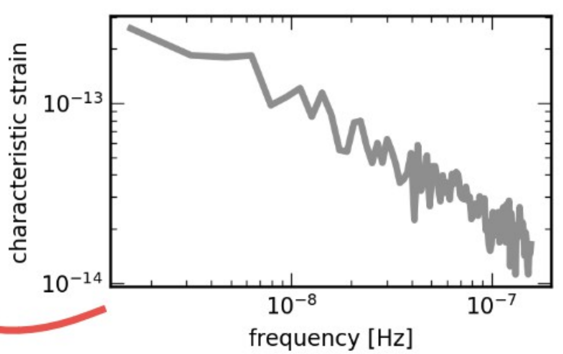

Taylor et al 2022

Pulsar Timing Arrays : principles

we write the PTA likelihood as $$p(\boldsymbol{\delta t}|\boldsymbol{\eta}) = \frac{\exp\left(-\frac{1}{2}\boldsymbol{\delta t}^T C^{-1}\boldsymbol{\delta t}\right)}{\sqrt{\det(2\pi C)}}$$

The covariance matrix is decomposed into a sum of « noises » whose spectrum is described by a power law

$$C \sim \Gamma_{ab}\rho_i\delta_{ij} + \epsilon_i\delta_{ij} + \eta_i\delta_{ab}\delta_{ij} + \kappa_{ai}\delta_{ab}\delta_{ij}$$

GW clock/eph. astroφ indiv. rot./disp.

the covariance matrix C depends both on the amplitude of the signal as a function of its sky position and on the «antenna pattern »

$$\Gamma_{ab} = \frac{3}{8\pi}(1+\delta_{ab})\int_{S^2} d\hat{\Omega}\ P(\hat{\Omega}) \sum_q F_a^q(\hat{\Omega}) F_b^q(\hat{\Omega})$$

Earth term: the stochastic signal is spatially correlated between all pulsars as a function of their angular separation

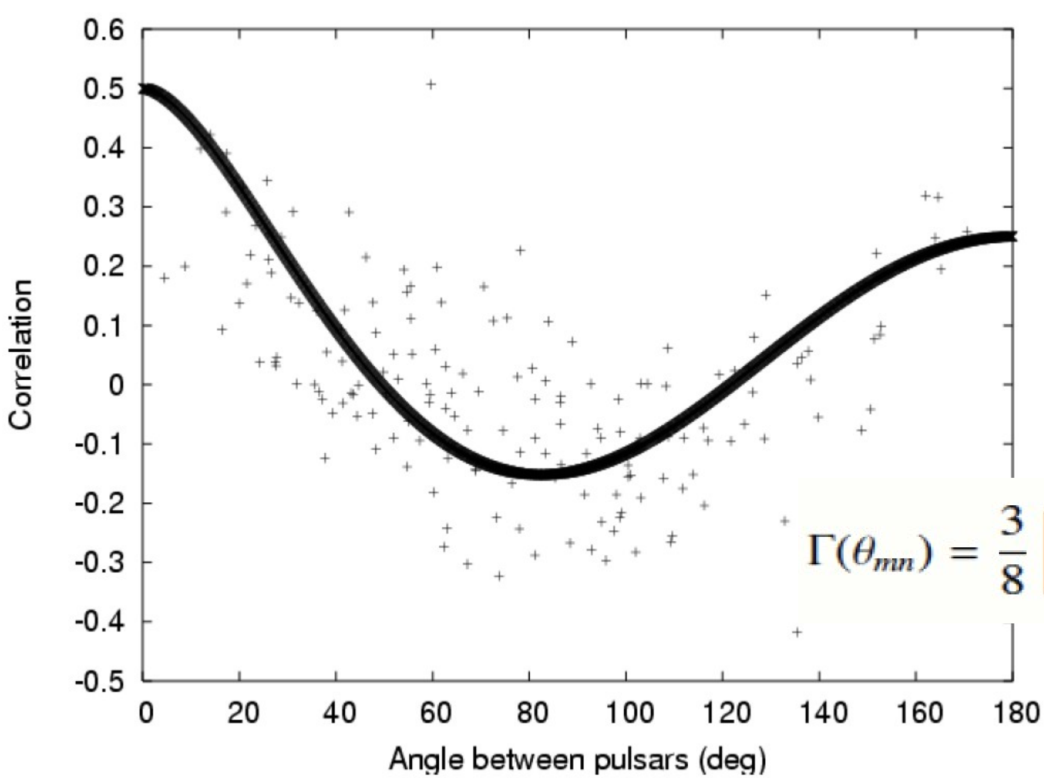

Cf Hellings & Downs 1983

solution for an isotropic background :

$$\Gamma(\theta_{mn}) = \frac{3}{8}\left[1 + \frac{\cos\theta_{mn}}{3} + 4(1-\cos\theta_{mn})\ln\left(\sin\frac{\theta_{mn}}{2}\right)\right](1+\delta_{mn})$$

Observed spectrum

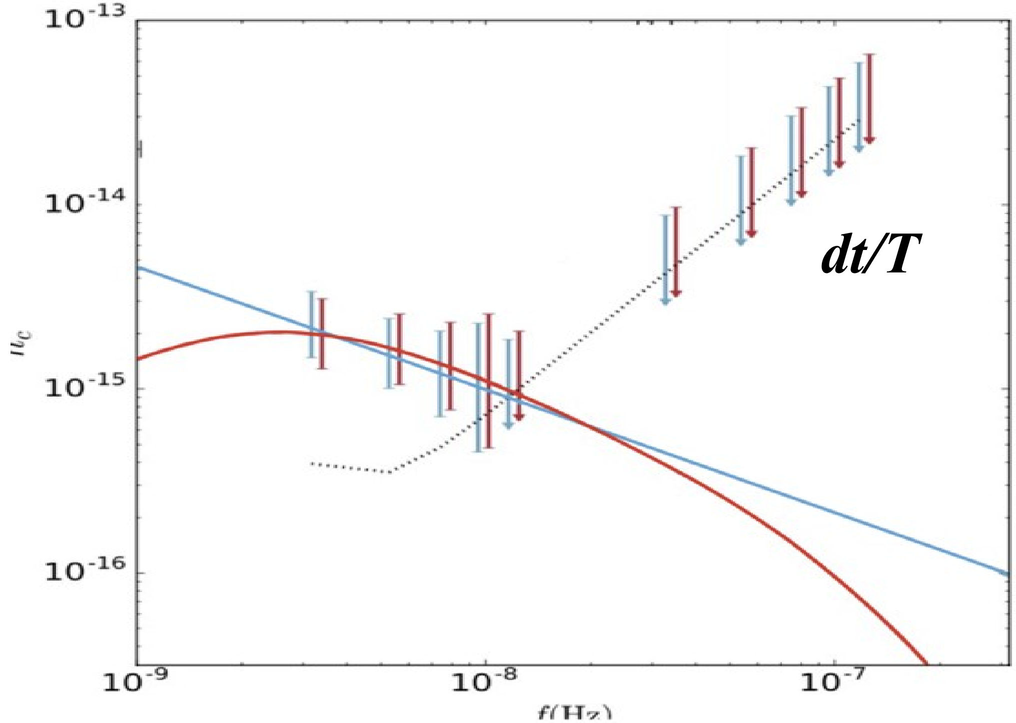

29th June 2023
EPTA, NANOGrav and PPTA show coherent results

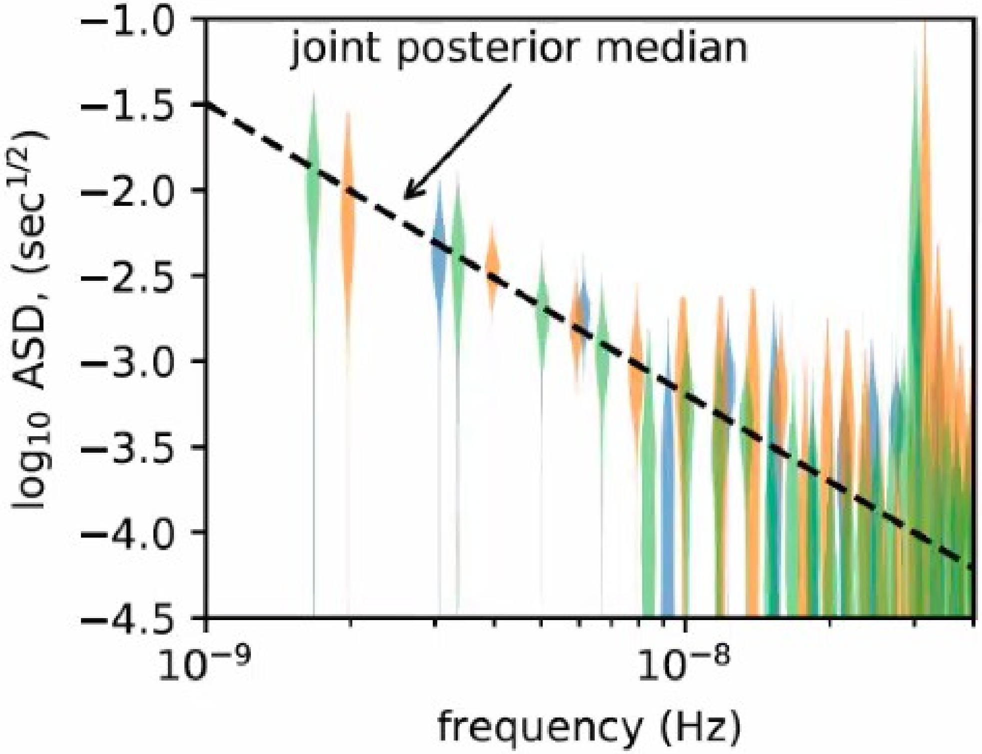

Courtesy of Paul Baker IPTA GWA WG

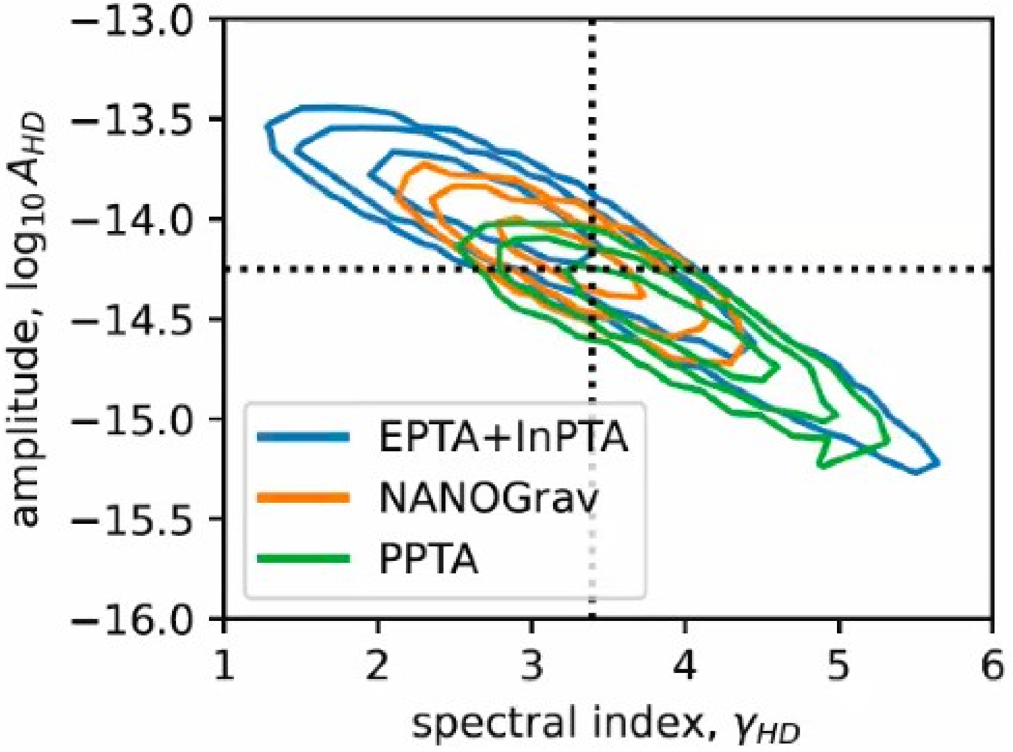

Spatial correlation of the signal

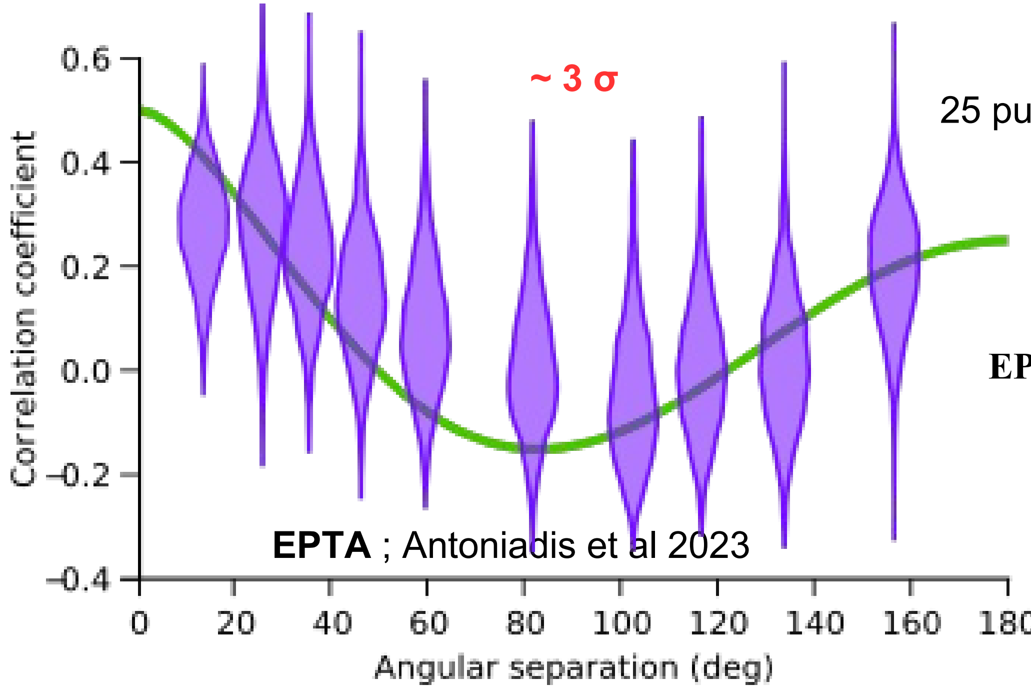

25 pulsars

29th June 2023
EPTA, NANOGrav and PPTA show coherent results

30 pulsars

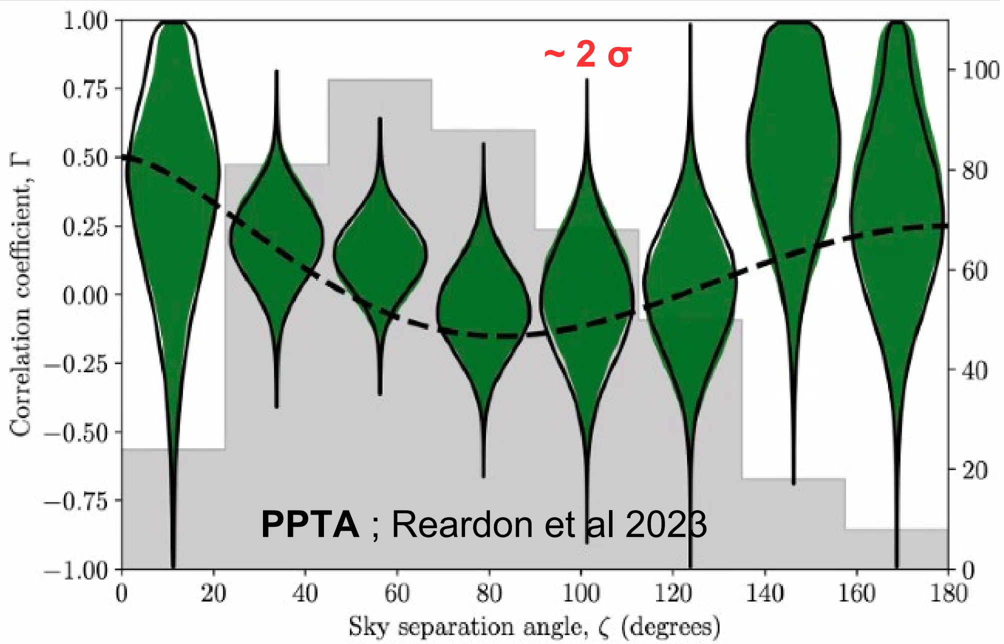

67 pulsars

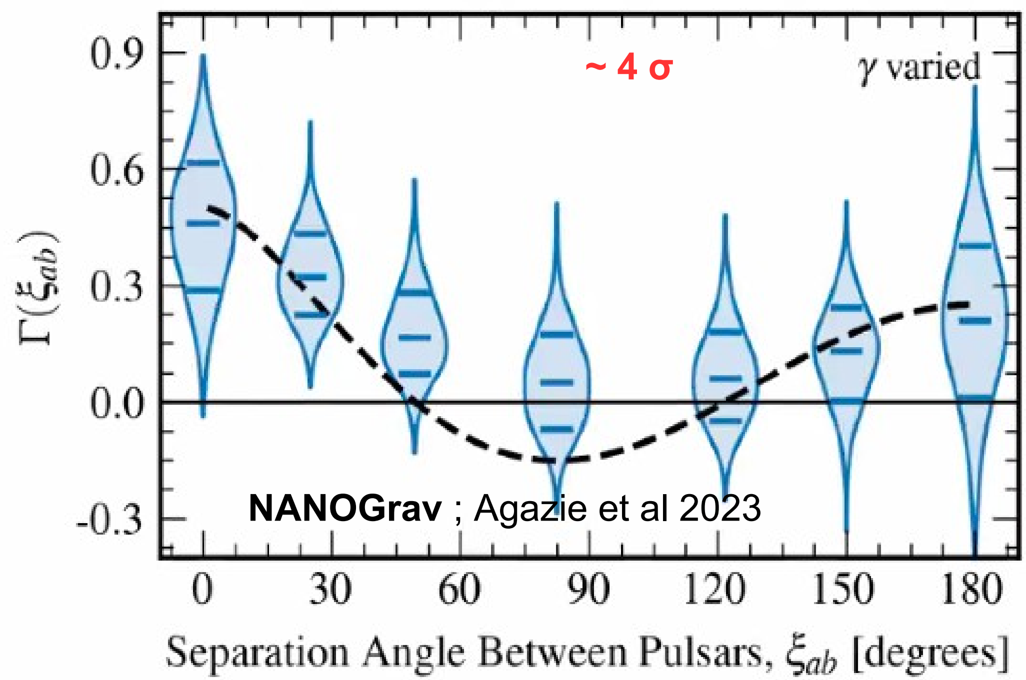

Spatial correlation of the signal

See Joe Romano's presentation on Friday about mathematical formulation, cosmic variance, significance of the results

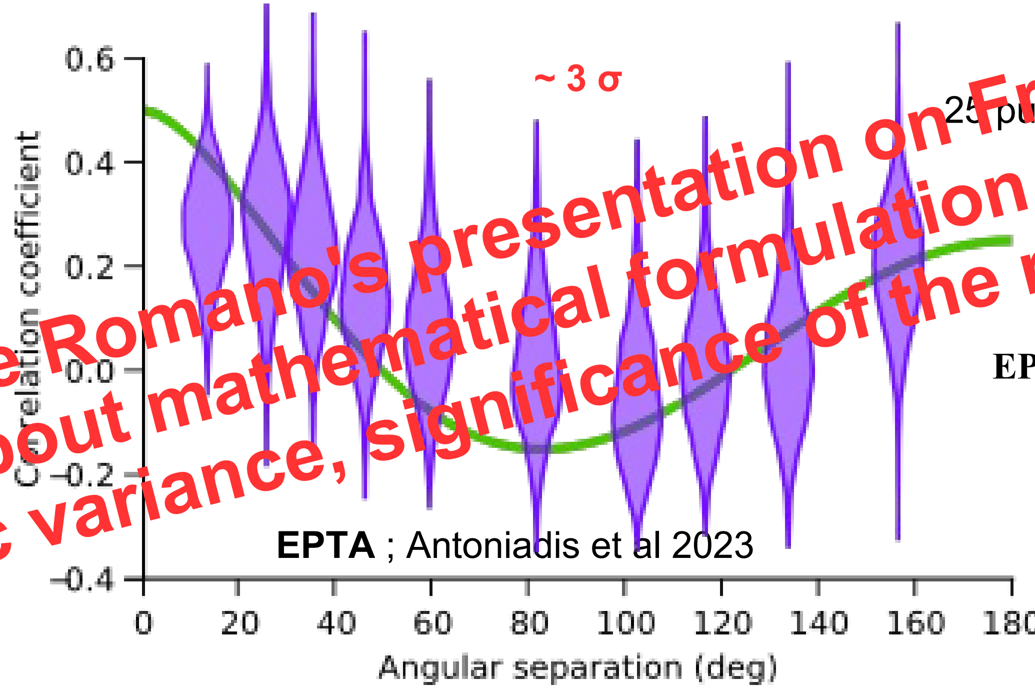

29th June 2023
EPTA, NANOGrav and PPTA show coherent results

30 pulsars

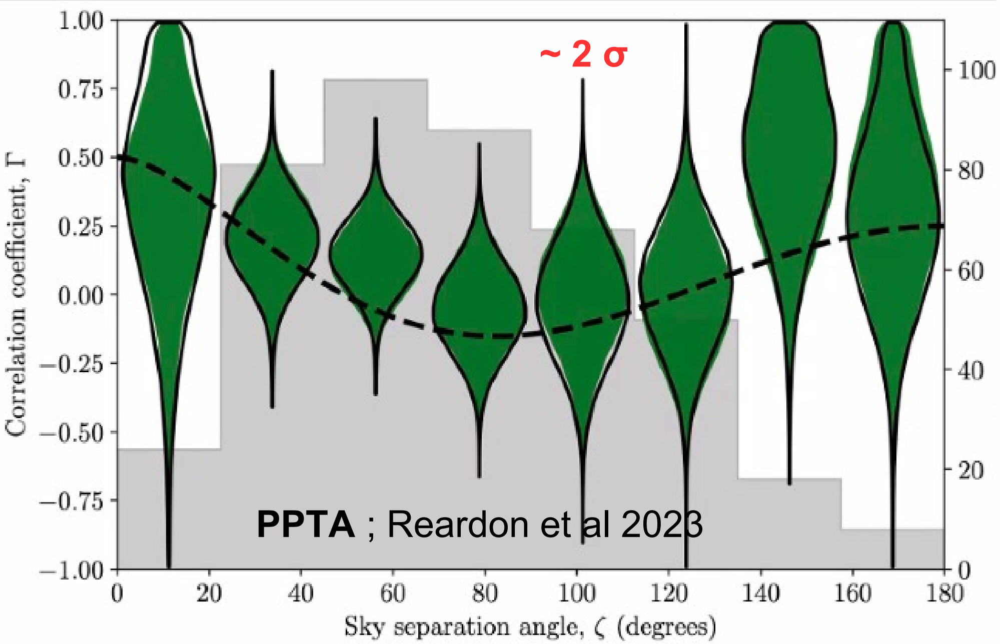

67 pulsars

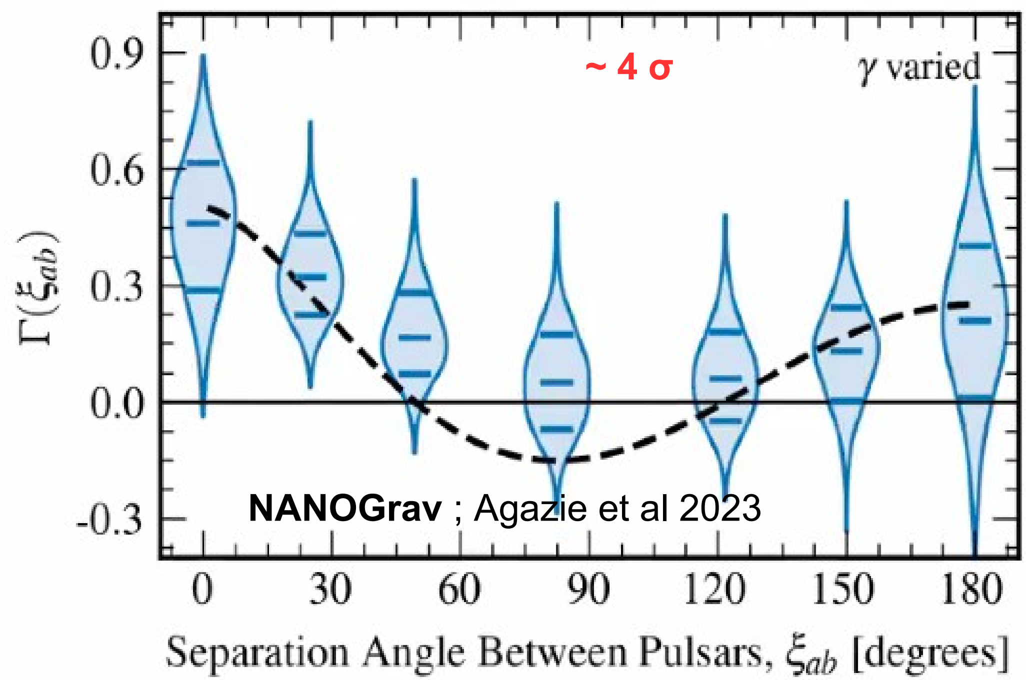

How interpreting such a common signal in terms of astrophysics ?

The life cycle of Super Massive Black Hole Binaries:

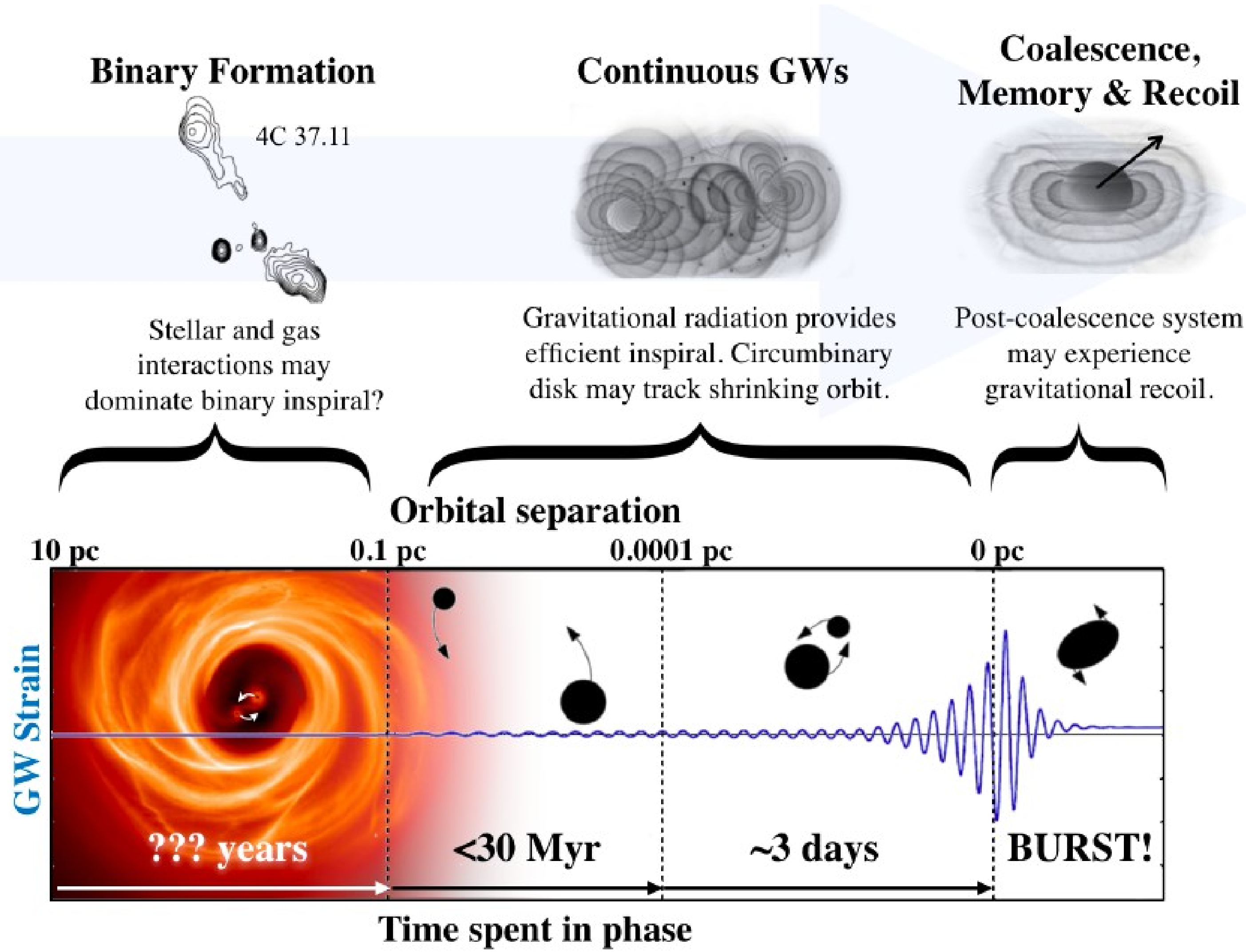

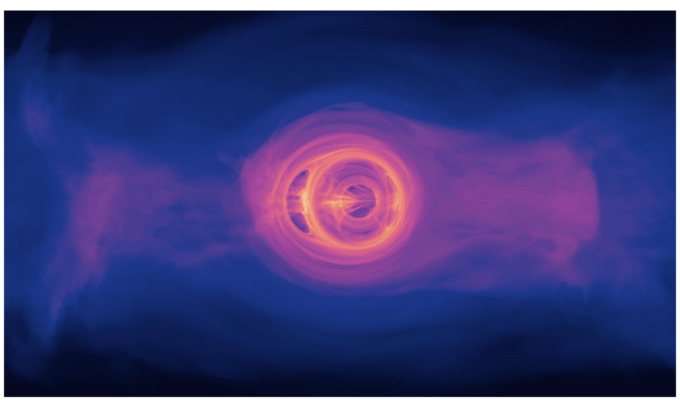

monochromatic
PTA regime

Burke-Spolaor 2018

Population synthesis ingredients

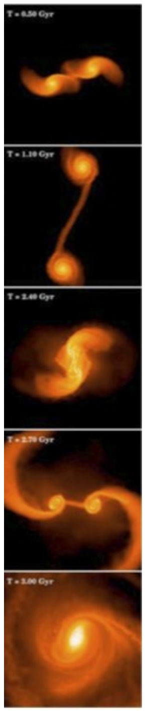

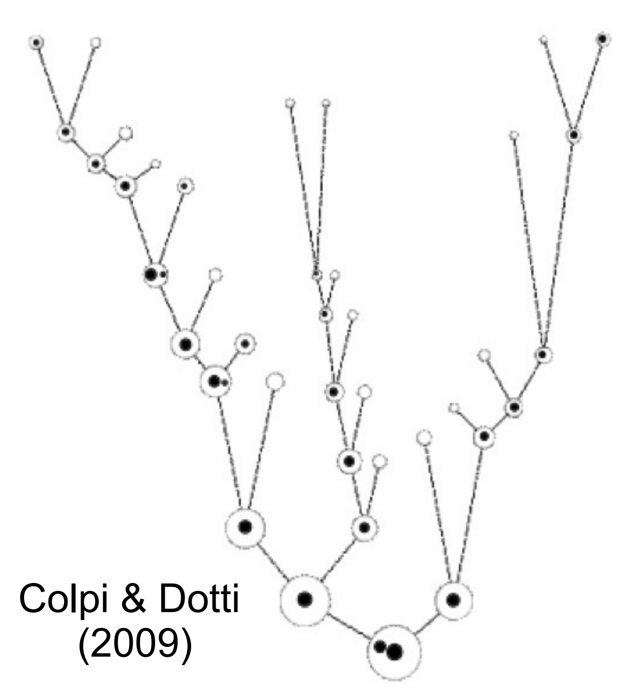

Colpi & Dotti (2009)

Reines & Volonteri (2015)

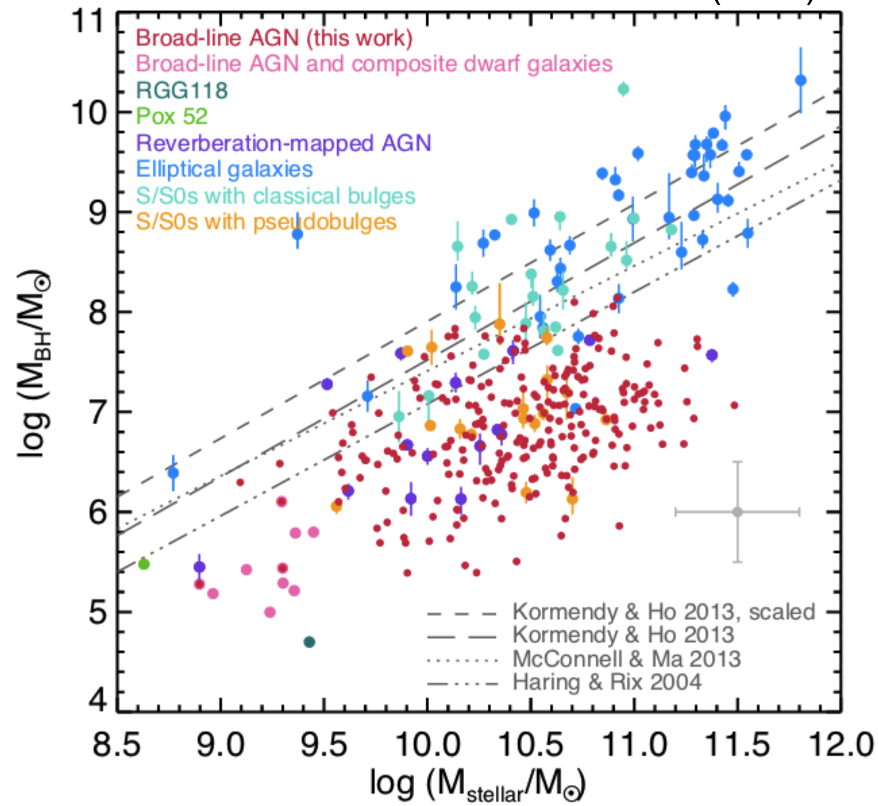

Merger trees from cosmological N-body simulations (Illustris, TNG, EAGLE, Horizon-AGN, SIMBA ...)

Bulge to BH mass ratio from galaxies dynamical studies

Add dynamical friction with stars and gas to migrate the BHs towards the center

Three body interaction with stars from the loss cone region (when binary orbital velocity > stars)

Population of SMBBH : contribution from background & individual sources

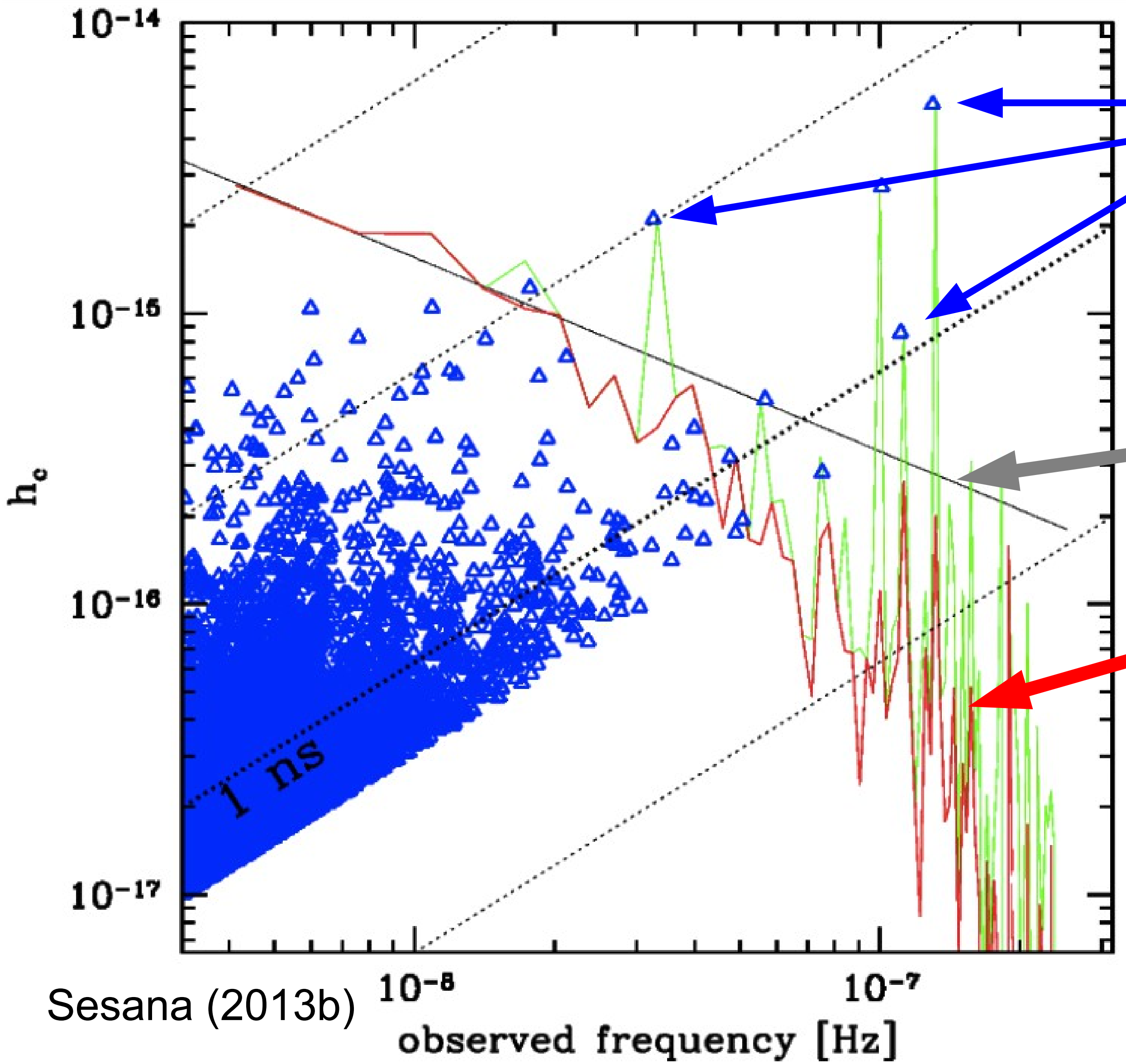

Sesana (2013b)

Hypothesis :

- circular orbits
- all the population reaches the sub-pc GW emission regime

+ uncertainties about :
fusion rate
BH – host galaxy mass relation
time to coalescence

stochastic background ~ f $^{-2/3}$

$$h_c^2(f) = \int_0^\infty dz \int_0^\infty d\mathcal{M} \, \frac{d^3 N}{dz d\mathcal{M} d\ln f_r} h^2(f_r) \longrightarrow h_c(f) = A \left(\frac{f}{\mathrm{yr}^{-1}} \right)^{-2/3}$$

(Phinney 2001)

Pulsar Timing Arrays : principles

GW induced timing residuals (simulated data) from Burke-Spolaor (2015)

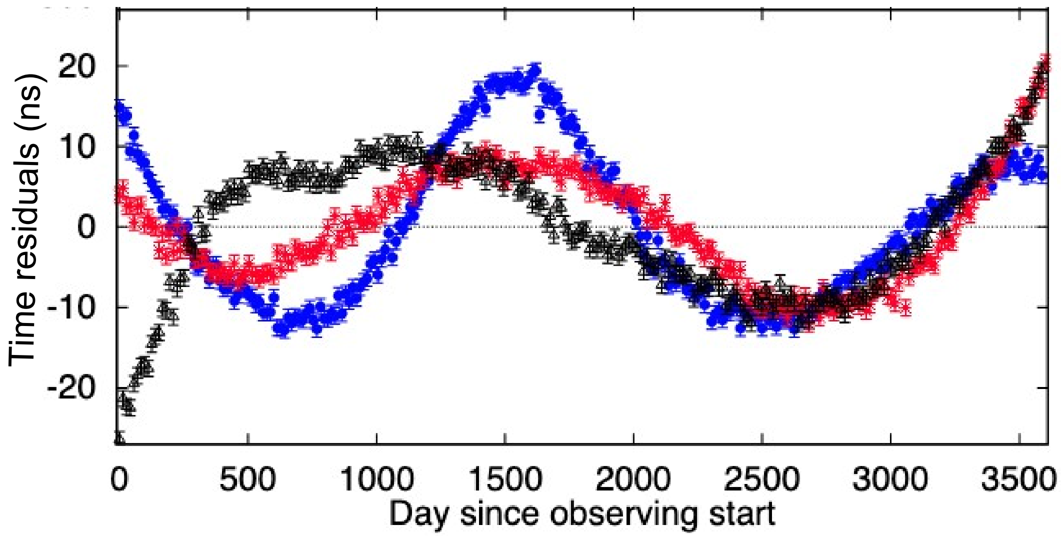

(a) Gravitational Wave Background

PSR J0437–4715
PSR J1012+5307
PSR J1713+0747

(a) a GWB with $h_c = 10^{-15}$ and $\alpha = -2/3$

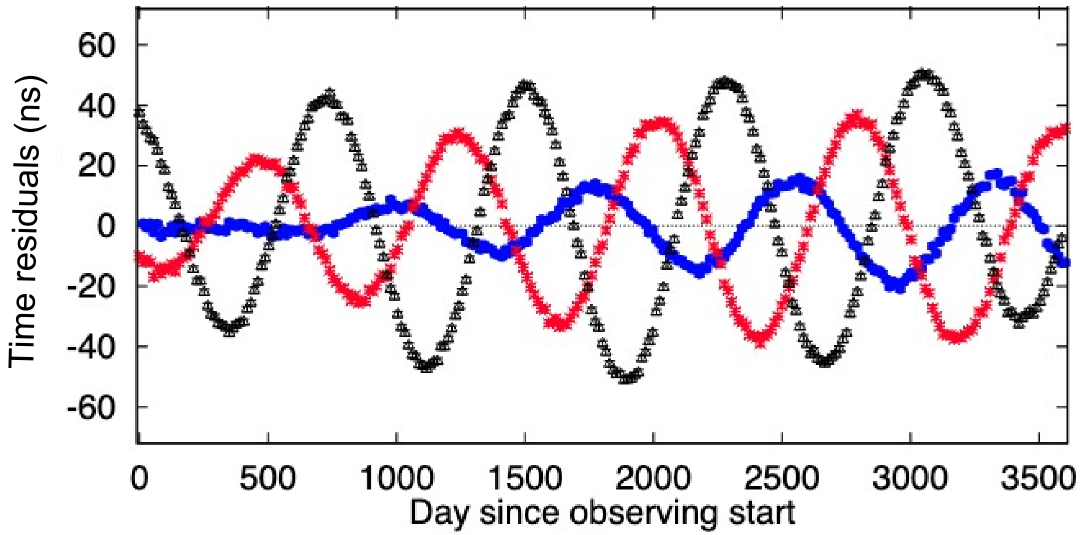

(b) Continuous Wave

(b) a continuous wave
(injected in the same sky location)
from an equal-mass 10^9 M BSMBH
at redshift z = 0.01.

distortion from a perfect sinusoid is caused by the lower-frequency pulsar term

The PTA signal vs SMBHB population models

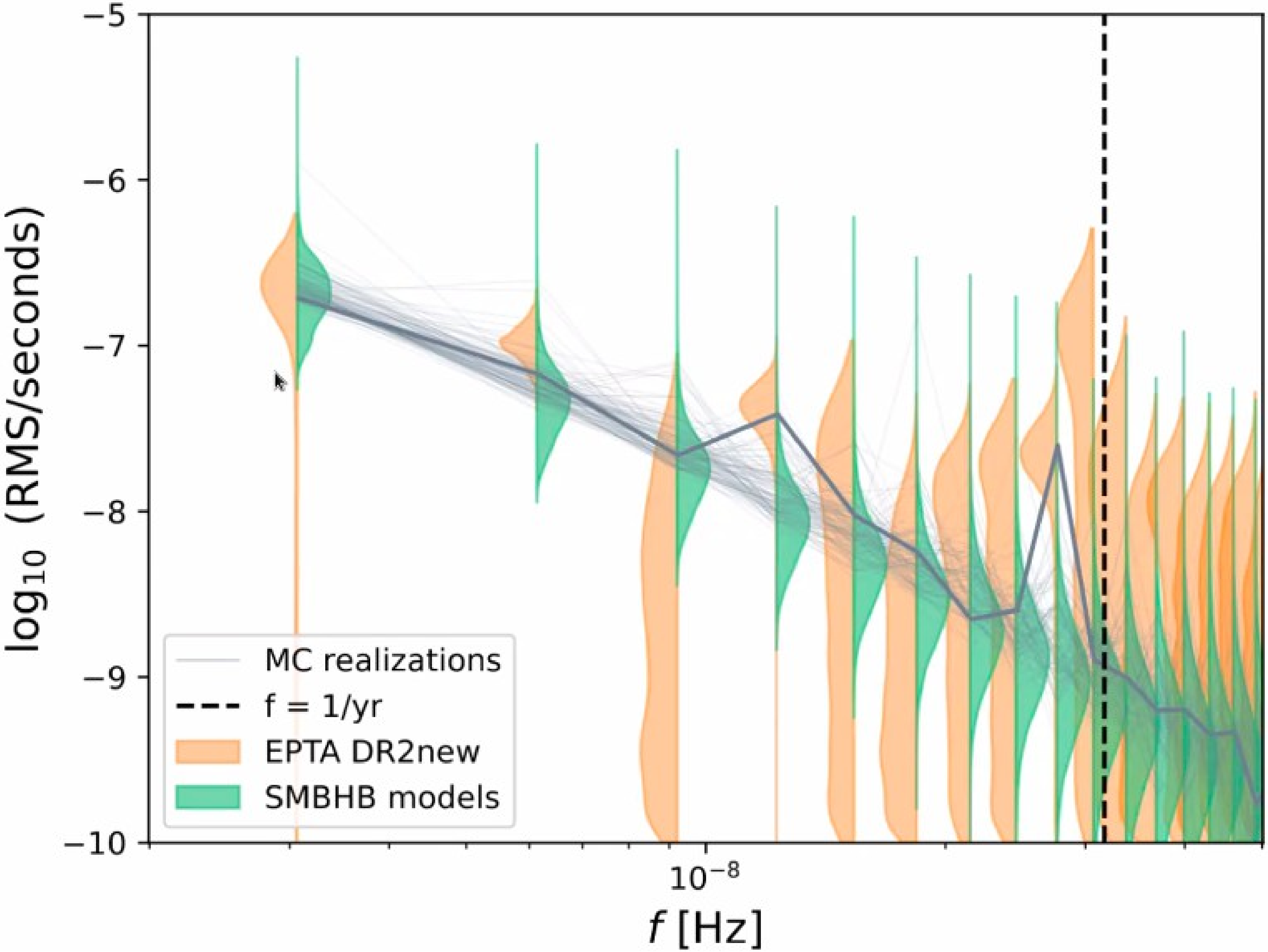

EPTA 10.3 yrs

Comparing with the predictions of astrophysical models (EPTA paper V)

$$h_c(f) = A\left(\frac{f}{\mathrm{yr}^{-1}}\right)^{-2/3}$$

The PTA signal vs SMBHB population models

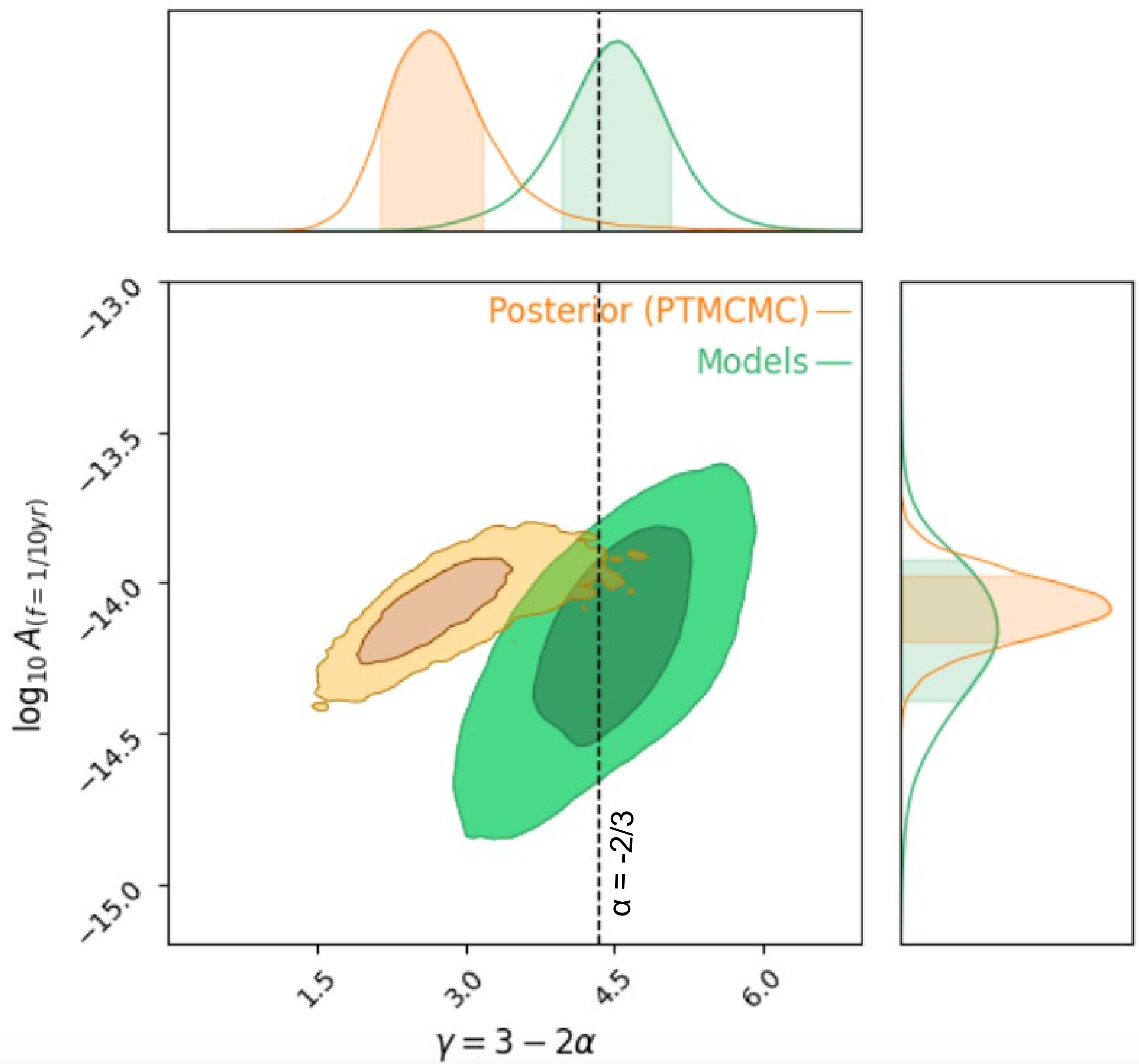

EPTA 10.3 yrs

Comparing with the predictions of astrophysical models (EPTA paper V)

$$h_c(f) = A\left(\frac{f}{\mathrm{yr}^{-1}}\right)^{-2/3}$$

The PTA signal vs SMBHB population models

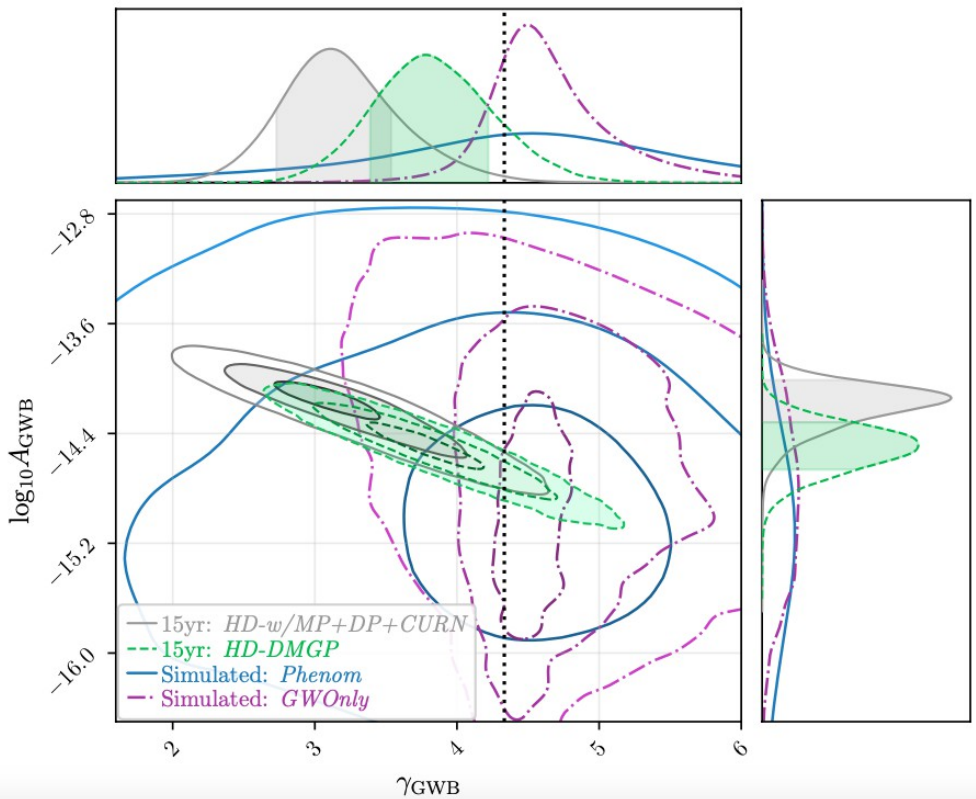

NANOGrav 15-yrs
Agazie et al 2023e

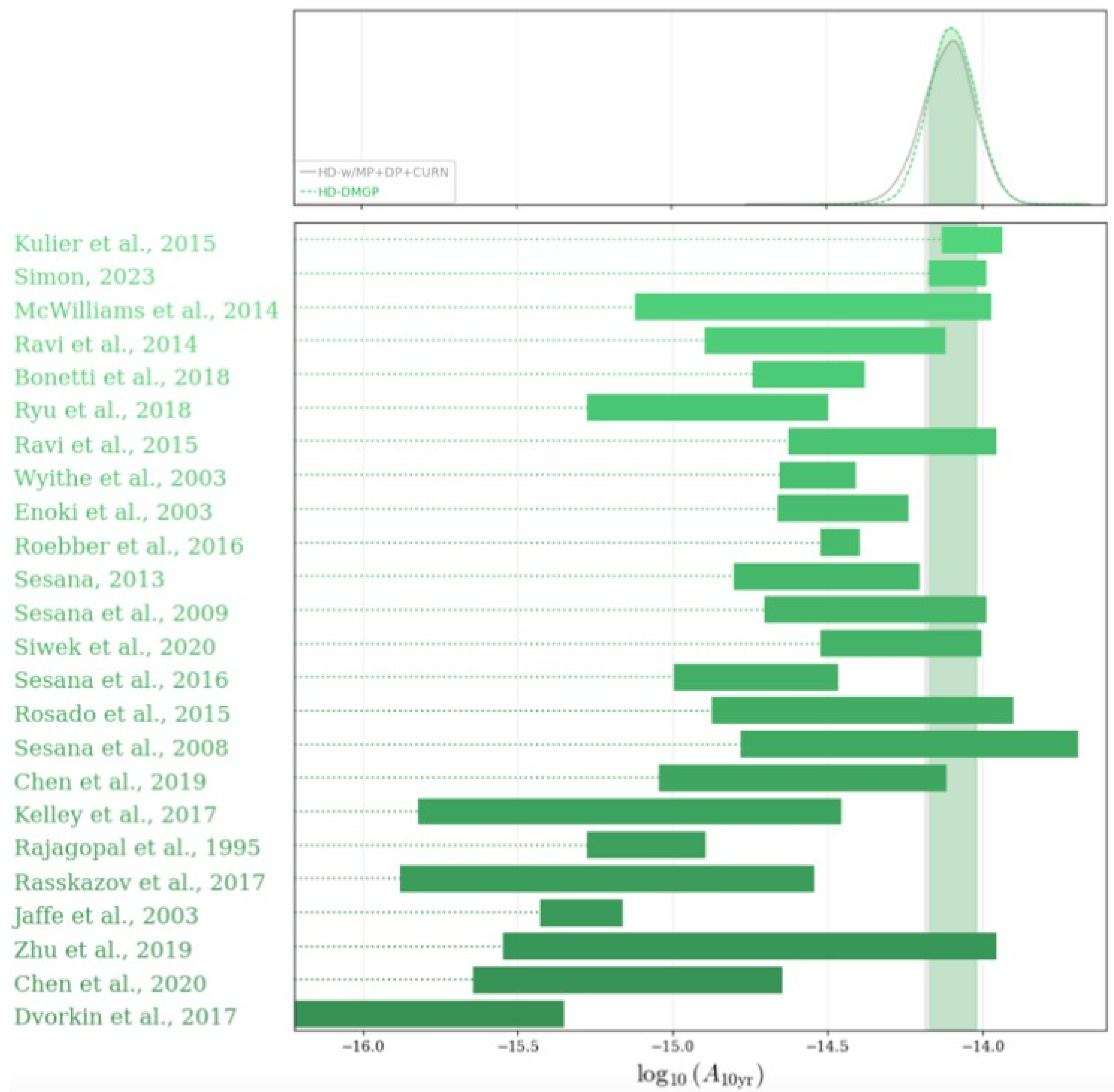

The PTA signal vs SMBHB population models

cosmic merger rate

$$h_c^2(f) = \int_0^\infty dz \int_0^\infty dM_1 \int_0^1 dq \frac{d^4N}{dz dM_1 dq dt_r} \frac{dt_r}{d\ln f_{K,r}} \times h^2(f_{K,r}) \sum_{n=1}^{\infty} \frac{g[n, e(f_{K,r})]}{(n/2)^2} \delta\left[f - \frac{n f_{K,r}}{1+z}\right].$$

physical processes driving BH pair

harmonics of gravitational wave signal from the various pairs

(Courtesy of Alberto Sesana IPTA meeting 2023)

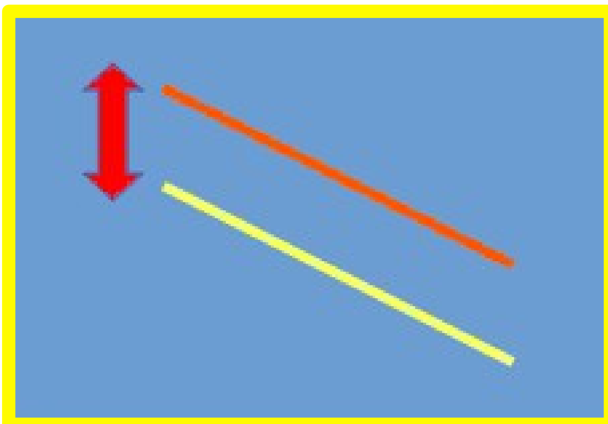

The PTA signal vs SMBHB population models

cosmic merger rate

$$h_c^2(f) = \int_0^\infty dz \int_0^\infty dM_1 \int_0^1 dq \frac{d^4N}{dz\,dM_1\,dq\,dt_r} \frac{dt_r}{d\ln f_{K,r}} \times h^2(f_{K,r}) \sum_{n=1}^{\infty} \frac{g[n, e(f_{K,r})]}{(n/2)^2} \delta\left[f - \frac{n f_{K,r}}{1+z}\right].$$

physical processes driving BH pair

harmonics of gravitational wave signal from the various pairs

(Courtesy of Alberto Sesana IPTA meeting 2023)

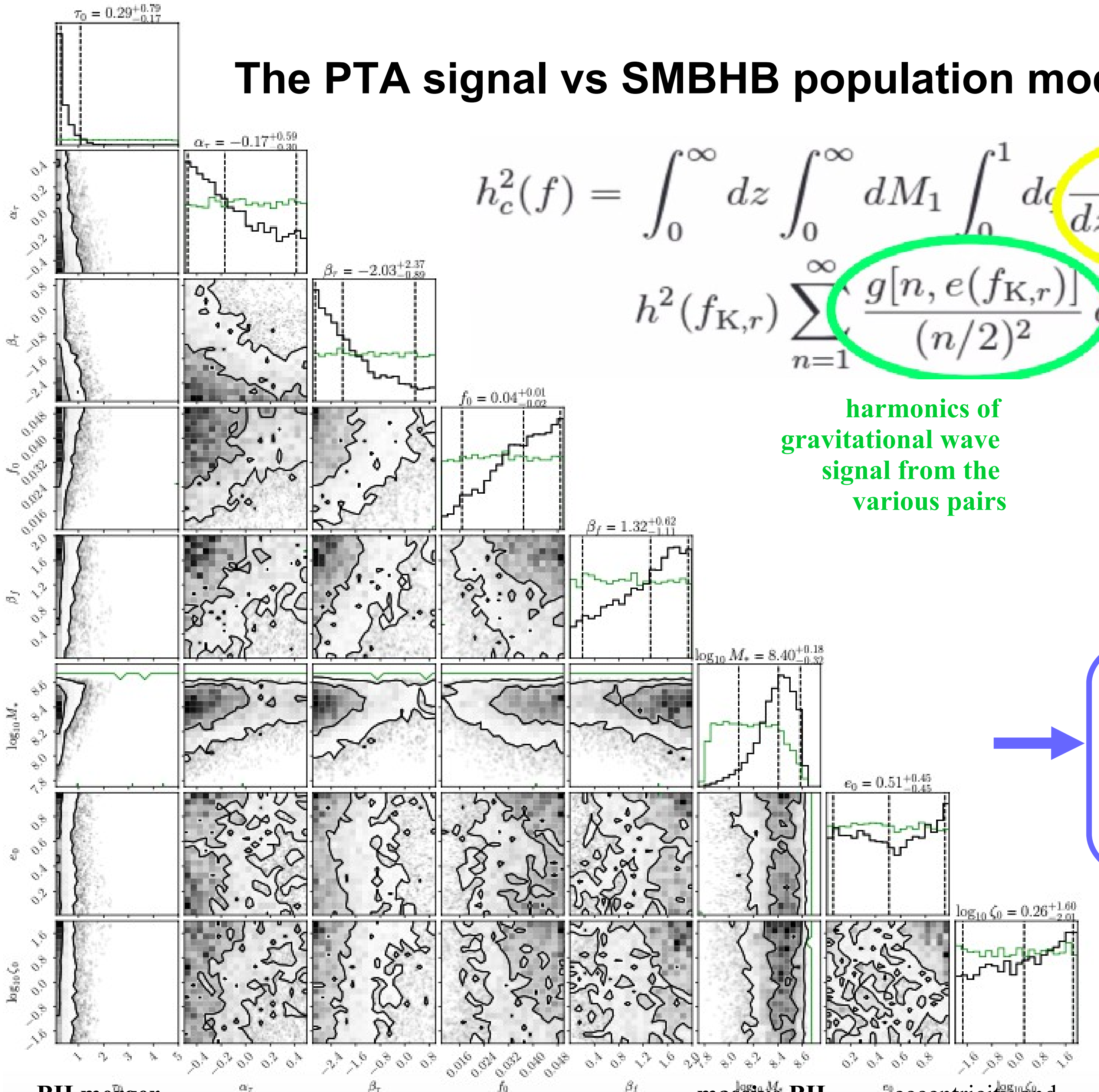

BH merger timescale < 1Gyr

shorter merger times for massive galaxies

high normalisation of pair fraction

massive BH compared to bulge mass

eccentricity and environment effects poorly constrained

high merger rate densities

short merger timescales

high normalization for BH-bulge mass relation

(EPTA paper V)

Distance limit skymap

(e.g. NANOGrav, Agazie et al 2023c)

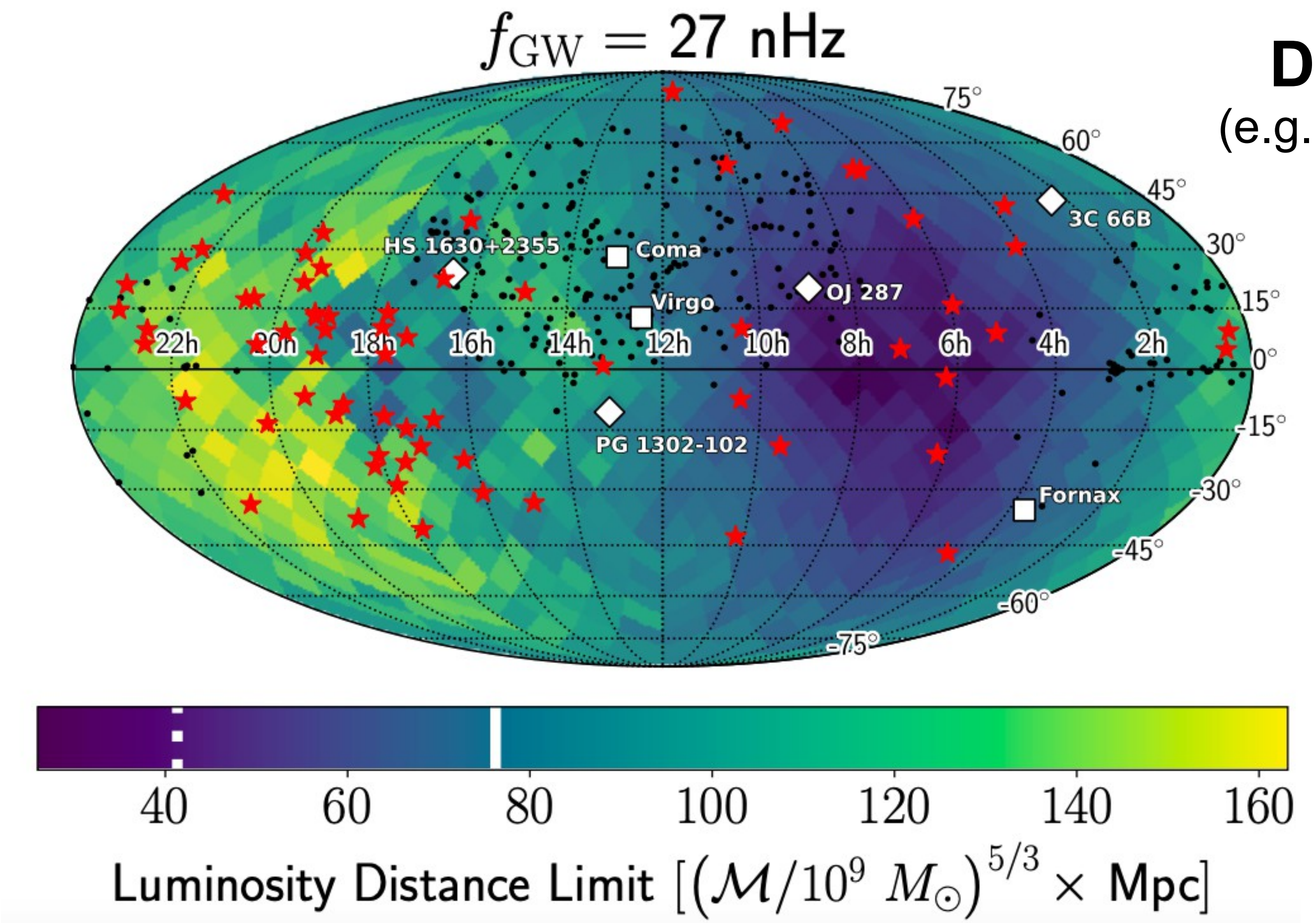

continuous wave search,
single source candidates

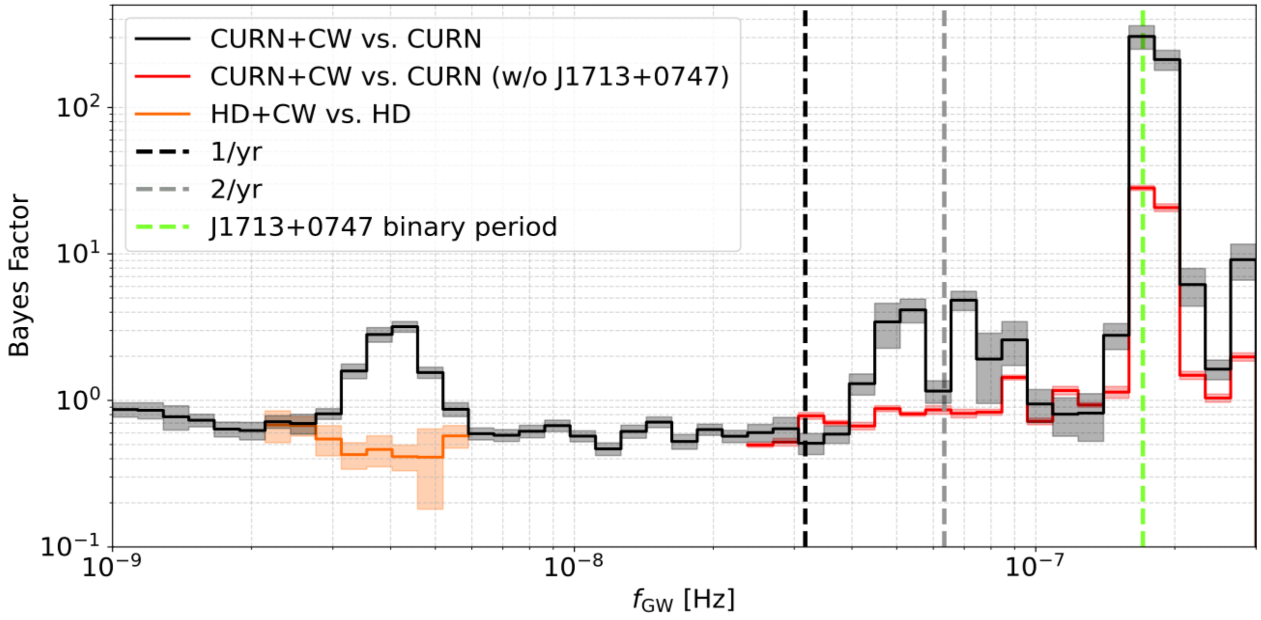

« detection map » @ 4.6 nHz (EPTA, Antoniadis et al 2023d)

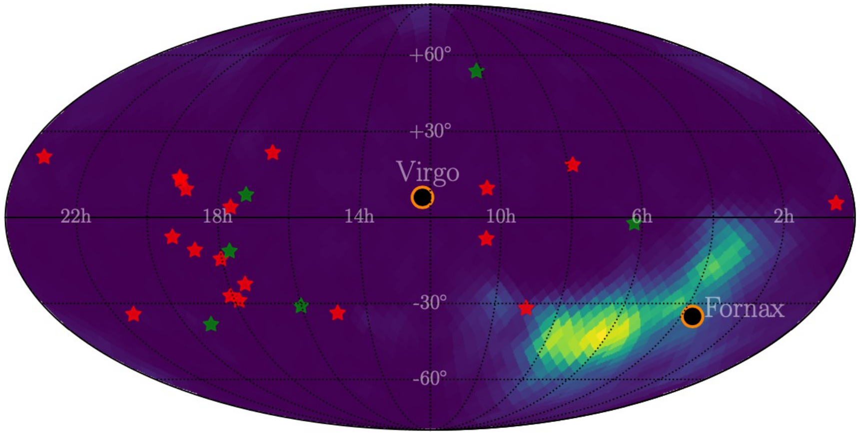

Bayesian

A stochatic background
or
a unique source
or
both ?

A signal at 4.6 nHz

poor sky position determination

very high Bayes factor

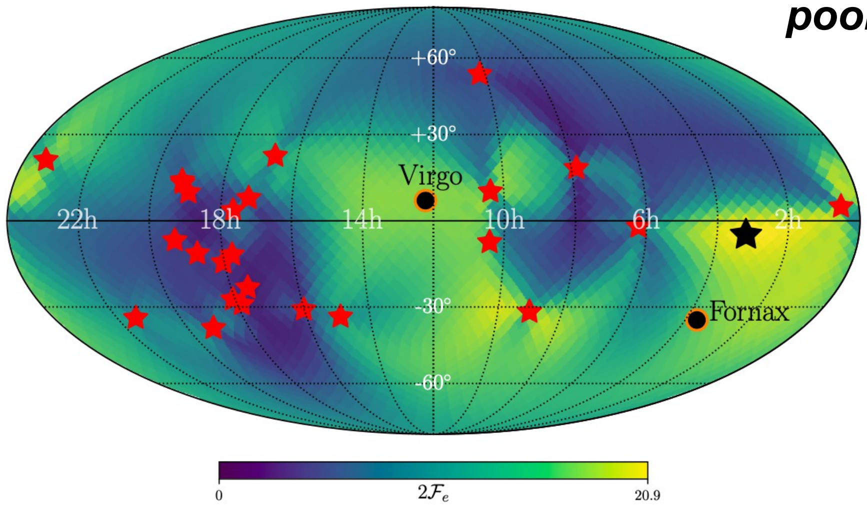

Frequentist

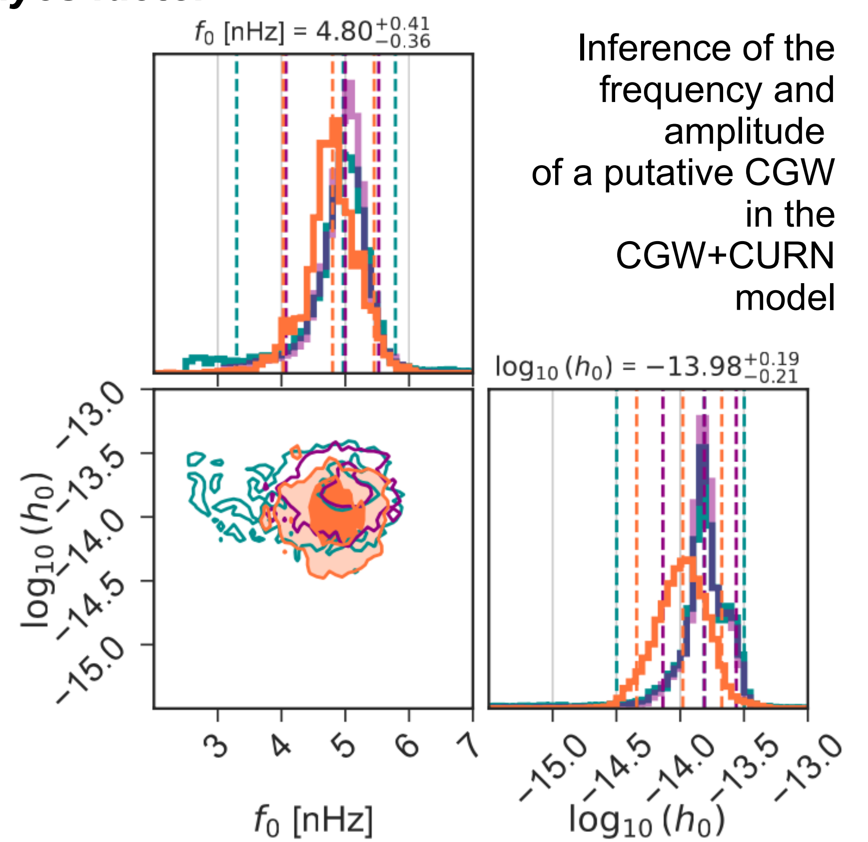

Inference of the frequency and amplitude of a putative CGW in the CGW+CURN model

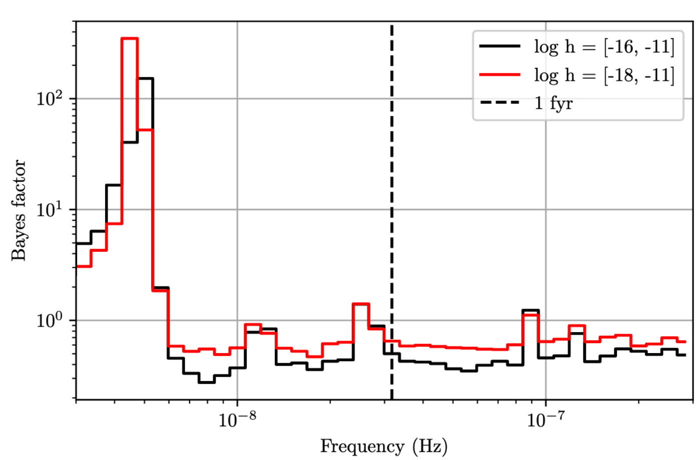

Bayes Factor spectral distribution CGW+CURN model

Cosmological models (e.g. from EPTA - paperV)

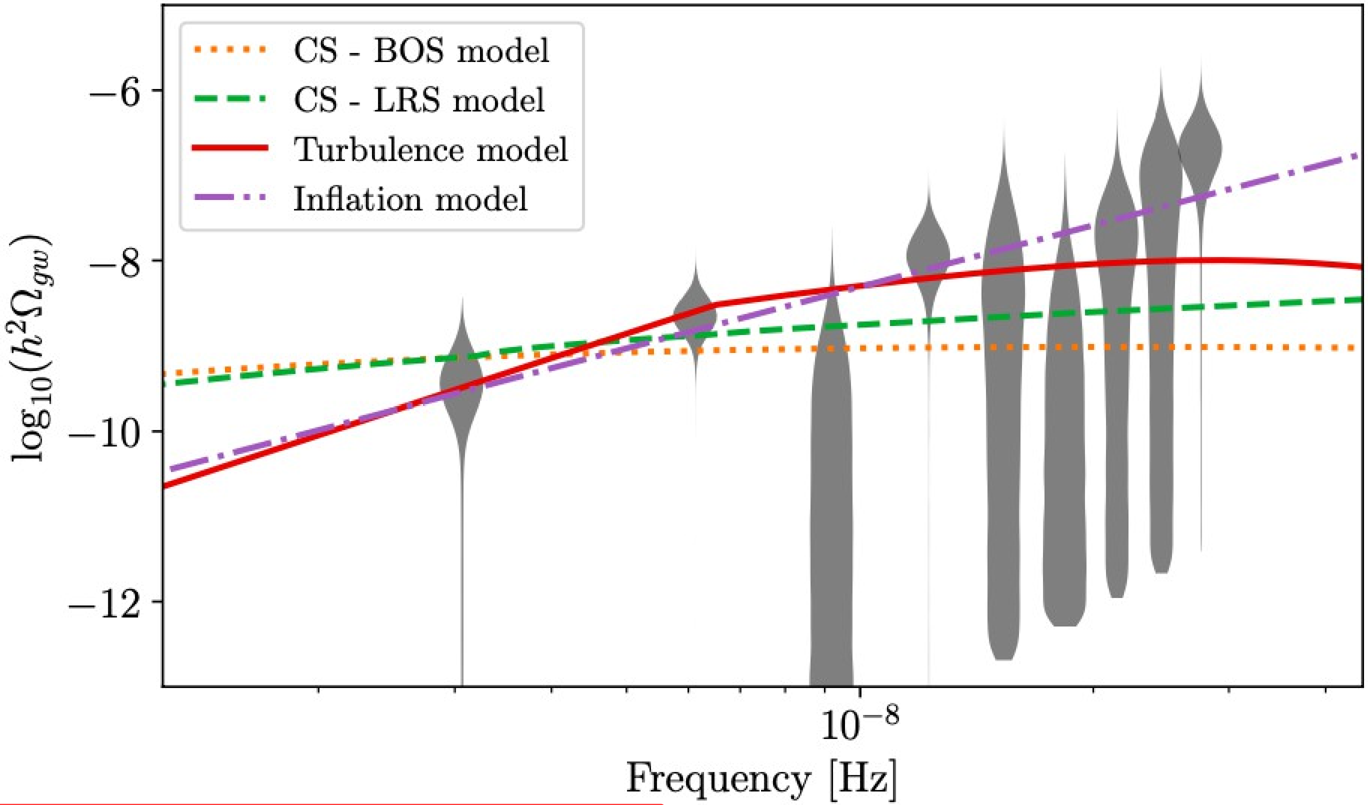

GWB produced from vortical (M)HD turbulence around QCD energy scale:

temperature scale T* → 140 MeV
turbulence strenght Ω* → 0.3
turbulence characteristic lenght scale λ*H* → 1

Inflation model : i.e. tensor quantum fluctuation of metric amplified by accelerated expansion :

tensor/scalar perturbation ratio → $\log_{10}$ r = -13.1
spectral index of tensor perturbation → n_T = 2.4

Cosmic string background :

string tension → $\log_{10}$ Gμ = -10.1/-10.6
features → Ncusp = 2 ; Nkinks = 0

For more details, please read :

arXiv:2306.16227v1

The second data release from the European Pulsar Timing Array

V. Implications for massive black holes, dark matter and the early Universe

J. Antoniadis[1,2,I], P. Arumugam[3,II], S. Arumugam[4,II], P. Auclair[5], S. Babak[6,I], M. Bagchi[7,8,II],
A.-S. Bak Nielsen[2,9,I], E. Barausse[10], C. G. Bassa[11,I], A. Bathula[12,II], A. Berthereau[13,14,I]
M. Bonetti[15,16,17,I], E. Bortolas[15,16,17,I], P. R. Brook[18,I], M. Burgay[19,I], R. N. Caball...
A. Chalumeau[15,I], D. J. Champion[2,I], S. Chanlaridis[1,I], S. Chen...

arXiv:16220v1

The NANOGrav 15-year Data Set:
Constraints on Supermassive Black Hole Binaries from the Gravitational Wave Background

...briella Agazie[1], Akash Anumarlapudi[1], Anne M. Archibald[2], Paul T. Baker[3], Bence Bécsy[4], Laura Blecha[5],
...[6,7] Adam Brazier[8,9] Paul R. Brook[10] Sarah Burke-Spolaor[11,12] Rand Burnette,[4] Robin Case,[4]
...[13] Maria Charisi[14] Shami Chatterjee[8] Katerina Chatziioannou,[15] Belinda D. Cheeseboro,[11,12]

arXiv:16219v1

The NANOGrav 15-year Data Set: Search for Signals from New Physics

Adeela Afzal,[1,2] Gabriella Agazie,[3] Akash Anumarlapudi,[3] Anne M. Archibald,[4] Zaven Arzoumanian,[5]
Paul T. Baker,[6] Bence Bécsy,[7] Jose Juan Blanco-Pillado,[8,9,10] Laura Blecha,[11] Kimberly K. Boddy,[12]
Adam Brazier,[13,14] Paul R. Brook,[15] Sarah Burke-Spolaor,[16,17] Rand Burnette,[7] Robin Case,[7] Maria Charisi,[18]

More interpretation papers :

17+ preprints published since last week on arXiv

Work in progress...

Expect interesting results in the coming year using world wide combined IPTA data

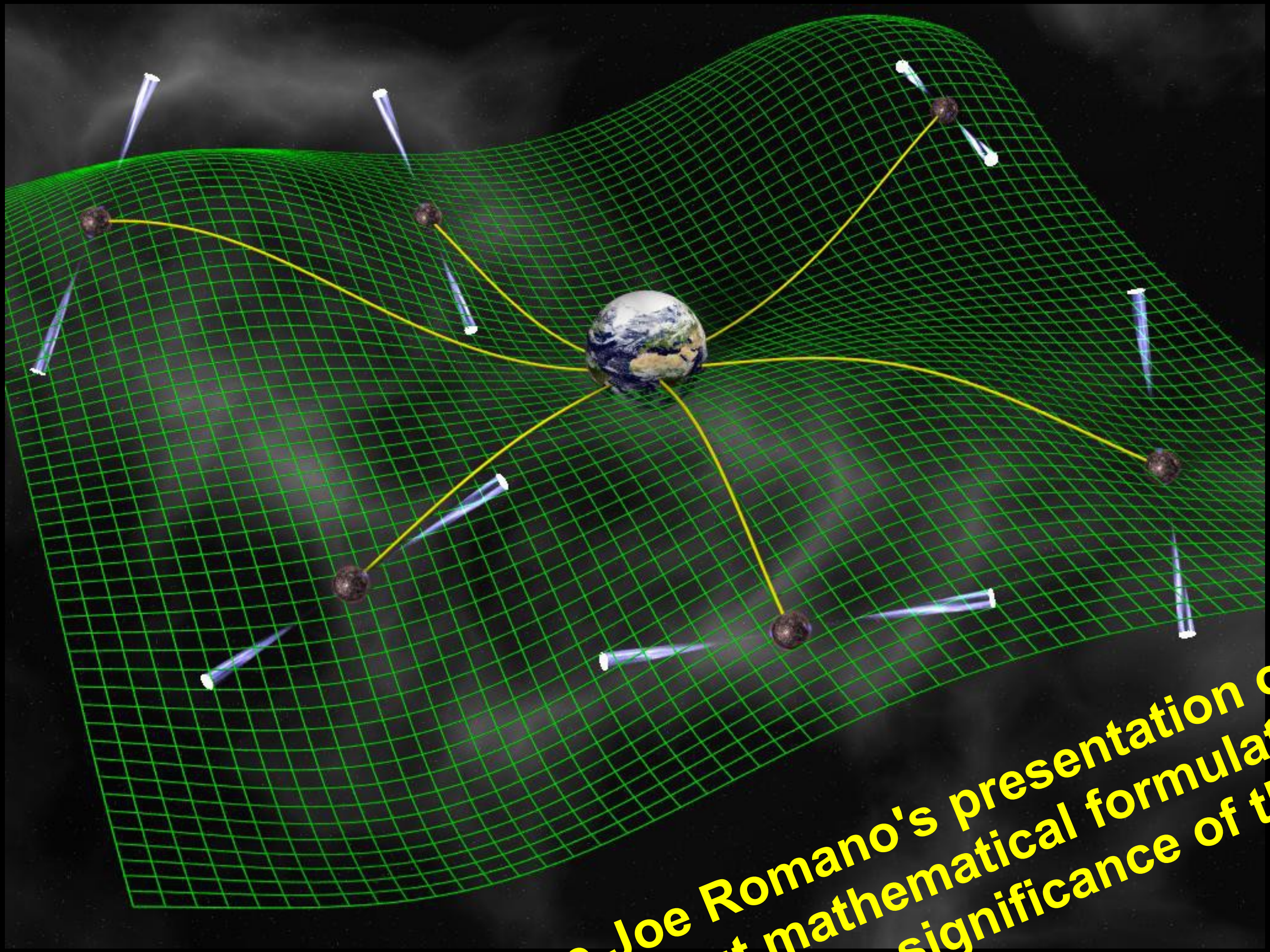

+ see Joe Romano's presentation on Friday
about mathematical formulation,
cosmic variance, significance of the results...